

Understanding the role of Maurer's clefts in virulence protein trafficking

Emma McHugh

Submitted in total fulfilment of the requirements of the degree of
Doctor of Philosophy

December 2017

Department of Biochemistry and Molecular Biology
The University of Melbourne

Abstract

The malaria parasite *Plasmodium falciparum* modifies the host red blood cell to establish virulence protein-trafficking pathways. The major virulence protein, *P. falciparum* erythrocyte membrane protein 1 (PfEMP1) is exported from the parasite to the red blood cell surface, where it mediates attachment of the infected cell to ligands on the host vascular endothelium. This process of sequestration enables infected red blood cells to avoid immune detection in the spleen and contributes to the development of severe malaria. The Maurer's clefts are organelles formed by the parasite and are present in the red blood cell cytoplasm. The primary function of Maurer's clefts is thought to be the transport of PfEMP1 to the red blood cell membrane.

We investigate a Maurer's clefts protein, ring-exported protein-1 (REX1) and its role in PfEMP1 trafficking. We show that Maurer's clefts morphology is disrupted by knocking down REX1 and that PfEMP1 surface display is decreased. Using transfectant parasites expressing truncated forms of the protein, we identify a repeat region of REX1 that mediates Maurer's clefts morphology and is required for efficient PfEMP1 trafficking.

We have developed a method to enrich the Maurer's clefts from infected red blood cells and define their protein composition by tandem mass spectrometry. We epitope-tag a number of putative and established Maurer's clefts proteins and confirm the location of several novel Maurer's clefts proteins. Using super-resolution microscopy, we localise Maurer's clefts proteins to subcompartments within these organelles. Finally, we use co-precipitation to describe a protein interaction network at the Maurer's clefts.

Declaration

This is to certify that:

- (i) This thesis comprises only my original work towards the Doctor of Philosophy except where indicated in the Preface.
- (ii) Due acknowledgement has been made in the text to all other material used.
- (iii) The thesis is fewer than 100,000 words in length exclusive of tables, bibliographies and appendices.

A handwritten signature in black ink that reads "EMcHugh". The letters are cursive and connected, with a prominent loop on the 'H'.

Emma McHugh

Preface

1) Chapter 3 of this thesis contains an analysis of the Maurer's clefts protein the ring-exported protein-1. Some of the data presented were generated as part of my Honours project at the University of Melbourne in 2013. Specifically, Figure 3.4A & B, Figure 3.6A and Figure 3.12B and D were generated during my Honours project.

2) Chapter 3 of this thesis is comprised of a part of the multi-author paper entitled:

A repeat sequence domain of the ring-exported protein-1 of *Plasmodium falciparum* controls machinery architecture and virulence protein trafficking

Emma McHugh, Steven Batinovic, Eric Hanssen, Paul J. McMillan, Shannon Kenny, Michael D. W. Griffin, Simon Crawford, Katharine R. Trenholme, Donald L. Gardiner, Matthew W. A. Dixon and Leann Tilley (2015). *Molecular Microbiology*. 98(6): 1101–1114.

The contributions of other authors are acknowledged below.

Steven Batinovic performed growth analysis of parasite lines presented in Figure 3.2.

Paul McMillan performed the OMX 3D-SIM imaging in Figure 3.7.

Donald Gardiner and **Katharine Trenholme** generated the REX1¹⁻⁵⁷⁹ and REX1^(Δ371-579)-GFP transfectant parasite lines.

Shannon Kenny assisted with sample preparation for Figure 3.7B.

Eric Hanssen performed scanning transmission electron microscopy and subsequent analysis and rendering presented in Figure 3.10B.

Matthew Dixon generated the REX1-GFP and REX1-HA-glmS parasite lines. He co-supervised the project with Leann Tilley and contributed to writing the manuscript and final editing for publication.

Leann Tilley co-supervised the project with Matthew Dixon and contributed to writing the manuscript and final editing for publication.

3) Chapters 4 and 5 contain results of mass spectrometry experiments. Samples were run on the mass spectrometers by **Nicholas Williamson** and **Ching-Seng Ang**.

4) 3D-SIM imaging in Chapter 4 was performed with the assistance of **Paul McMillan**

Acknowledgements

Firstly, I would like to thank my supervisors Leann and Matt. Leann, thank you for taking me into your lab and giving me the opportunity to do my PhD. It is thanks to you that I have had the chance to get involved in collaborations, attend conferences and develop my skills as a researcher. Thank you! Matt, you've patiently taught me so many lab techniques, going back to my Honours year when I barely knew how to use a pipette. Thank you for being so generous with your time and your enthusiasm for my project. You have been a fantastic supervisor to me and I am very grateful.

Thank you to my committee members Diana Stojanovski, Malcolm McConville and Michael Duffy for steering me in the right direction.

Steven, I owe you big time. Thank you for answering countless questions and sharing your skills. You have been a great mentor. The advice you have given me over the years has been invaluable and I feel extremely lucky to have worked with you. It is so great to see you loving life as a post-doc!

Laure, thanks for all our little coffee and chat sessions! Best of luck for your own project ... you are so close! Also thanks to the lab's more recent additions Natalie and Emily - you guys are awesome. And a special thanks to Tuo (for all the dumplings) and to Shannon for patiently helping me out time and again. Congratulations on your exciting new project - motherhood!

Olly, Jess, Dean, Kit and David - as you know, lunch time was always my favourite part of the work day. Thanks for all those (probably hundreds) of hours of food and fun, it is part of the reason why I loved going to the lab every day.

Thank you to all the other past and present Tilley lab members.

Thank you to my family especially Mum, Steph and Kate for the constant support. Most importantly, thank you to Sarah. Your daily encouragement has kept me going. I can't thank you enough.

Publications resulting from candidature

Disrupting assembly of the inner membrane complex blocks *Plasmodium falciparum* sexual stage development

Molly Parkyn Schneider*, Boyin Liu*, Philipp Glock*, Annika Suttie*, Emma McHugh, Dean Andrew, Steven Batinovic, Nicholas Williamson, Eric Hanssen, Paul McMillan, Marion Hliscs, Leann Tilley†, Matthew W.A. Dixon†

*† These authors contributed equally to this work

2017 Oct 6; 13(10): e1006659. PLOS Pathogens.

An exported Protein-Interacting Complex involved in the trafficking of virulence determinants in *Plasmodium*-infected erythrocytes

Steven Batinovic, Emma McHugh*, Scott A. Chisholm*, Sarah C. Charnaud, Laure Dumont, Paul R. Gilson, Tania F. de Koning-Ward, Matthew W. A. Dixon and Leann Tilley

* These authors contributed equally to this work

2017 Jul 10; 8: 16044. Nature Communications.

Contrasting Inducible Knockdown of the Auxiliary PTEX Component PTEX88 in *P. falciparum* and *P. berghei* Unmasks a Role in Parasite Virulence

Scott A. Chisholm, Emma McHugh, Rachel Lundie, Matthew W. A. Dixon, Sreejoyee Ghosh, Meredith O'Keefe, Leann Tilley, Ming Kalanon, Tania F. de Koning-Ward

2016 Feb 17; 11(2): e0149296. PLOS ONE.

A repeat sequence domain of the ring-exported protein-1 of *Plasmodium falciparum* controls machinery architecture and virulence protein trafficking

Emma McHugh, Steven Batinovic, Eric Hanssen, Paul J. McMillan, Shannon Kenny, Michael D. W. Griffin, Simon Crawford, Katharine R. Trenholme, Donald L. Gardiner, Matthew W. A. Dixon and Leann Tilley

2015 Dec; 98(6): 1101-14. Molecular Microbiology.

Conference presentations

Oral presentations

- 2016 27th Woods Hole Molecular Parasitology Meeting**
Woods Hole, MA, USA
- 2016 VIIN Young Investigator Symposium**
Parkville, VIC, Australia
- 2015 Malaria Seminar Series**
Melbourne, VIC, Australia
- 2015 Malaria in Melbourne Symposium**
Caulfield, VIC, Australia

Poster presentations

- 2017 Malaria in Melbourne Symposium**
Parkville, VIC, Australia
- 2016 Molecular Approaches to Malaria**
Lorne, VIC, Australia
- 2016 Melbourne Protein Group Student Symposium**
Bundoora, VIC, Australia
- 2014 ComBio**
Canberra, ACT, Australia
- 2014 Melbourne Protein Group Student Symposium**
Bundoora, VIC, Australia
- 2014 Biological Optical Microscopy Platform Symposium**
Parkville, VIC, Australia

Table of Contents

Chapter 1	: Introduction.....	1
1.1	Malaria - the disease.....	1
1.1.1	Malaria pathology and mechanism of cytoadherence	4
1.2	<i>Plasmodium falciparum</i> biology.....	5
1.2.1	Lifecycle of the parasite.....	5
1.3	Export of parasite proteins by <i>Plasmodium falciparum</i>	8
1.3.1	The secretory pathway during the blood stages of <i>P. falciparum</i>	8
1.3.2	Transit of exported proteins across the parasitophorous vacuole.....	11
1.3.3	The role of exported co-chaperones/chaperones	12
1.4	The Maurer's clefts of <i>Plasmodium falciparum</i>	13
1.4.1	Morphology and motion of the Maurer's clefts	13
1.4.2	Targeting of proteins to the Maurer's clefts.....	15
1.4.3	Maurer's clefts proteins involved in trafficking of PfEMP1	15
1.4.4	Transport of PfEMP1 from the Maurer's clefts to the red blood cell membrane	16
1.4.5	Parasite-induced structures in other <i>Plasmodium spp.</i>	20
1.5	The virulence complex and red blood cell membrane modifications	20
1.6	Exported proteins that are not trafficked via the Maurer's clefts	21
1.7	The role of ring exported protein 1 in virulence protein trafficking	23
1.8	Scope and aims of this study.....	25
Chapter 2	: Materials and Methods.....	27
2.1	Parasite culture.....	27
2.1.1	Parasite lines used in this study.....	Error! Bookmark not defined.
2.1.2	Sorbitol synchronisation	28
2.1.3	Gelatine selection of knob-positive infected red blood cells	28
2.1.4	Percoll enrichment of trophozoite stage parasite-infected red blood cells	28
2.1.5	Magnetic separation of haemozoin-containing trophozoites from parasite cultures	29
2.1.6	Tight synchronisation of parasite cultures	29

2.1.7	Transfection of <i>P. falciparum</i> parasites.....	31
2.1.8	Knockdown of proteins using the <i>glmS</i> ribozyme.....	31
2.2	Analysis of infected RBC binding to recombinant human CD36 under constant flow conditions	31
2.3	Molecular biology	31
2.3.1	Genomic DNA extraction from infected RBCs	31
2.3.2	Polymerase chain reaction (PCR) and PCR product preparation and analysis	32
2.3.3	Subcloning.....	35
2.3.4	Ligation of DNA fragments into vectors	35
2.3.5	Restriction enzyme digestion of DNA.....	35
2.3.6	DNA analysis and purification after PCR and restriction enzyme digestion	35
2.4	Microscopy	35
2.4.1	Acetone and acetone/methanol fixation of infected red blood cells.....	35
2.4.2	Glutaraldehyde/paraformaldehyde fixation of infected red blood cells	36
2.4.3	Addition of antibodies and microscopy of immunofluorescence assays (IFAs)	36
2.4.4	Live-cell fluorescence microscopy	38
2.4.5	Immunolabelling of samples for electron microscopy	38
2.4.6	Sample embedding, microtome sectioning and electron microscopy analysis	38
2.5	Analysis of protein samples from <i>P. falciparum</i>	39
2.5.1	Preparation of saponin-lysed infected RBCs for SDS-PAGE.....	39
2.5.2	SDS-PAGE, immunoblotting and membrane stripping.....	40
2.5.3	Trypsin digestion of surface-exposed PfEMP1	42
2.5.4	Protease treatment of enriched Maurer's clefts.....	42
2.5.5	Co-immunoprecipitation	42
2.5.6	Mass spectrometric analysis of Maurer's clefts and co-immunoprecipitations.....	43
2.6	Enrichment of Maurer's clefts from ring-stage parasites	39

Chapter 3	: A repeat sequence domain of the ring-export protein-1 of <i>Plasmodium falciparum</i> controls export machinery architecture and virulence protein trafficking.....	44
3.1	Foreword.....	44
3.2	Introduction.....	44
3.2.1	Plasmid constructs and <i>P. falciparum</i> transfection.....	47
3.2.2	Fluorescence microscopy.....	47
3.2.3	Immunoblotting.....	48
3.2.4	CD36 binding assays and PfEMP1 variant up-selection.....	48
3.3	Results.....	50
3.3.1	Knockdown of REX1 expression is associated with Maurer's cleft reorganization without loss of KAHRP.....	50
3.3.2	The repeat region of REX1 is involved in Maurer's cleft sculpting.....	58
3.3.3	Tether-like structures accumulate on the stacked Maurer's clefts.....	64
3.3.4	The repeat region of REX 1 is needed for efficient trafficking of PfEMP1 to the RBC surface.....	68
3.4	Discussion.....	73
Chapter 4	: Enrichment and analysis of the Maurer's clefts.....	76
4.1	Introduction.....	76
4.2	Results.....	78
4.2.1	Validation of the method to enrich the Maurer's clefts.....	78
4.2.2	Mass spectrometric analysis of enriched Maurer's clefts.....	82
4.2.3	The Maurer's clefts are enriched in human proteins involved in membrane trafficking and lipid biogenesis.....	87
4.2.4	Annexin A4 and protein VAC14 homolog partially co-localise with REX1 at the Maurer's clefts.....	89
4.2.5	Epitope-tagging of established and putative Maurer's clefts proteins....	91
4.2.6	Super-resolution analysis of protein localisation within the Maurer's clefts	97
4.3	Discussion.....	103
Chapter 5	: Investigation of protein interaction networks at the Maurer's clefts	107

5.1	Introduction.....	107
5.2	Results	109
5.2.1	A network of protein-protein interactions in the centre of the Maurer's clefts	109
5.2.2	Generation of an inducible knockdown transfectant parasite line.....	116
5.2.3	Partial knockdown of GEXP07 does not affect other exported proteins	118
5.2.4	Two Maurer's clefts edge proteins co-immunoprecipitate and share similarities	122
5.2.5	Networks of exported protein interactions at the Maurer's clefts	127
5.2.6	Analysis of the Maurer's clefts protein interaction network.....	132
5.3	Discussion.....	135
Chapter 6 : Summary and conclusion		140
6.1	New understanding of the function of ring-exported protein-1	140
6.2	A more complete picture of Maurer's clefts.....	141
6.3	Conclusions.....	144

List of Tables and Figures

Figures

Figure 1.1 Countries endemic for malaria in 2000 and 2016.....	3
Figure 1.2 The adhesin PfEMP1 is responsible for the severe pathology of <i>P. falciparum</i> -malaria.....	6
Figure 1.3 The lifecycle of <i>Plasmodium falciparum</i>	7
Figure 1.4 Parasite-induced modifications to the host red blood cell.....	10
Figure 1.5 Remodelling of the host red blood cell by <i>P. falciparum</i>	19
Figure 3.1 Schematic representation of strategy used to generate transfected parasites	51
Figure 3.2 Analysis of the growth of 3D7 and REX1-KD parasites in the presence and absence of GlcN.....	54
Figure 3.3 Schematics of REX1 and REX1 mutants.....	53
Figure 3.4 Immunofluorescence microscopy of KAHRP, PfEMP3 and PfEMP1.....	56
Figure 3.5 Inducible knockdown of REX1 using the glmS ribozyme system decreases the number of Maurer's cleft puncta	57
Figure 3.6 Deletion of the repeat region of REX1 decreases the number of Maurer's cleft puncta	59
Figure 3.7 REX1($\Delta^{371-579}$)-GFP parasites exhibit giant Maurer's clefts.....	61
Figure 3.8 Transmission electron microscopy analysis of REX1-GFP and REX1($\Delta^{371-579}$)-GFP Maurer's clefts.....	63
Figure 3.9 Live cell imaging of REX1-GFP and REX1($\Delta^{371-579}$)-GFP ring- and trophozoite- infected RBCs.	65
Figure 3.10 Analysis of the Maurer's clefts ultrastructure and distribution of tethers of REX1($\Delta^{371-579}$)-GFP parasites.....	67
Figure 3.11 Control to monitor integrity of infected RBCs during trypsin digestion. ...	71
Figure 3.12 PfEMP1 surface-exposure and cytoadherence of REX1 transfectants	70
Figure 3.13 Binding of 3D7 parent parasites to CD36 under flow conditions.....	72
Figure 4.1 Enrichment and analysis of Maurer's clefts.....	79
Figure 4.2 Analysis of the enriched Maurer's clefts fragments	81
Figure 4.3 Annexin A4 and protein VAC14 homolog co-locate with REX1	90
Figure 4.4 Schema and validation of exported proteins that were GFP-tagged.....	92
Figure 4.5 Live-cell fluorescence microscopy of GFP-tagged transfectant parasites	94
Figure 4.6 Immunofluorescence analysis of transfectant parasites.....	96
Figure 4.7 3D-SIM analysis GEXP07-GFP- and GEXP10-GFP-infected red blood cells.	98
Figure 4.8 3D-SIM analysis of PTP5-GFP- and PTP6-GFP-infected red blood cells.	100

Figure 4.9 3D-SIM analysis of REX1-GFP, REX2-GFP and Pf13_0275-GFP localisation.....	102
Figure 5.1 Immunoprecipitation analysis of GEXP10-GFP, GEXP07-GFP and MAHRP1-GFP.....	110
Figure 5.2 Diagrams of exported protein interactions identified by immunoprecipitation of MAHRP1-GFP, GEXP07-GFP and GEXP10-GFP.....	112
Figure 5.3 Characterisation of a GEXP07-HA-glmS conditional knockdown parasite line.....	117
Figure 5.4 Immunofluorescence analysis of glucosamine-treated 3D7 and GEX07-HA-glmS parasites.....	119
Figure 5.5 Analysis of the effect of GEXP07 knockdown on exported proteins.....	121
Figure 5.6 Immunoprecipitation of wild-type 3D7, REX1-GFP and PTP5-GFP parasite lines.....	123
Figure 5.7 Immunoprecipitation with REX2-GFP, PTP6-GFP and Pf13_0275-GFP..	128
Figure 5.8 Network map and analysis of co-precipitating proteins.....	133
Figure 6.1 Schematic representing protein locations within the Maurer's clefts.....	143

Tables

Table 1 Transfectant parasite lines used in study.....	30
Table 2 Thermal cycler conditions used for PCR.....	33
Table 3 List of primers used in this study.....	34
Table 4 List of antibodies used for immunofluorescence microscopy.....	37
Table 5 List of antibodies used for immunoblotting.....	41
Table 6 Mass spectrometry analysis of enriched Maurer's clefts.....	83
Table 7 PfEMP1 variants detected in enriched Maurer's clefts.....	85
Table 8 Overview of proteins identified in the enriched Maurer's cleft.....	86
Table 9 <i>Homo sapiens</i> proteins enriched in the Maurer's clefts.....	88
Table 10 Mass spectrometry analysis of MAHRP1-GFP co-precipitated proteins.....	113
Table 11 Mass spectrometry analysis of GEXP07-GFP co-precipitated proteins.....	114
Table 12 Mass spectrometry analysis of GEXP10-GFP co-precipitated proteins.....	115
Table 13 Mass spectrometry analysis of REX1-GFP co-precipitated proteins.....	125
Table 14 Mass spectrometry analysis of PTP5-GFP co-precipitated proteins.....	126
Table 15 Mass spectrometry analysis of PTP6-GFP co-precipitated proteins.....	129
Table 16 Mass spectrometry analysis of Pf13_0275-GFP co-precipitated proteins....	130
Table 17 Mass spectrometry analysis of REX2-GFP co-precipitated proteins.....	131
Table S1 Human proteins enriched in PTP5-GFP LC-MS/MS.....	145

Table S2 Human proteins enriched in PTP6-GFP LC-MS/MS	146
Table S3 Human proteins enriched in REX1-GFP LC-MS/MS	147
Table S4 Human proteins enriched in REX2-GFP LC-MS/MS	148
Table S5 Human proteins enriched in MAHRP1-GFP LC-MS/MS	149
Table S6 Human proteins enriched in GEXP07-GFP LC-MS/MS	150
Table S7 Human proteins enriched in GEXP10-GFP LC-MS/MS	151
Table S8 Human proteins enriched in PF13_0275-GFP LC-MS/MS	152

Abbreviations

ATS	Acidic terminal segment
BODIPY	boron dipyrromethene difluoride
BSA	Bovine serum albumin
CD36	cluster of differentiation 36
CCM	Complete culture medium
CRMP	Cysteine repeat modular protein
CSA	Chondroitin sulphate A
DAPI	4', 6-diamidino-2-phenylindole
DNA	Deoxyribonucleic acid
DSP	Dithiobis(succinimidyl proprionate)
ECL	Electrochemiluminescence
EDTA	Ethylenediaminetetraacetic acid
EDV	Electron-dense vesicle
EM	Electron microscopy
EPF	Exported protein family
EPIC	Exported protein-interacting complex
EqII	Equinatoxin II
EPCR	Endothelial protein C receptor
ESCRT	Endosomal sorting complexes required for transport
EXP1	Exported protein-1
EXP2	Exported protein-2
EXP3	Exported protein-3
GAPDH	Glyceraldehyde 3-phosphate dehydrogenase
GEXP07	Gametocyte-exported protein 7
GEXP10	Gametocyte-exported protein 10
GFP	Green fluorescent protein
GlcN	Glucosamine
HA	Haemagglutinin
HCl	Hydrochloric acid
HEPES	4-(2-hydroxyethyl)-1-piperazineethanesulfonic acid
HRP	Horseradish peroxidase

HSP70x	Heat shock protein-70x
HSP101	Heat shock protein-101
ICAM-1	Intracellular adhesion molecule 1
IFA	Indirect immunofluorescence assay
KAHRP	Knob-associated histidine-rich protein
kDa	Kilodalton
LC-MS/MS	Liquid chromatography - tandem mass spectrometry
LDS	Lithium dodecyl sulphate
MAHRP1	Membrane-associated histidine-rich protein-1
MAHRP2	Membrane-associated histidine-rich protein-2
MESA	Mature parasite-infected erythrocyte surface antigen
MOPS	3-(N-morpholino)propanesulfonic acid
MW	Molecular weight
NaCl	Sodium chloride
Na ₂ CO ₃	Sodium carbonate
NPP	New permeability pathway
PAGE	Polyacrylamide gel electrophoresis
PBS	Phosphate buffered saline
PEST	Proline, glutamic acid, serine, threonine
PEXEL	Protein export element
PFA	Paraformaldehyde
PfEMP1	<i>Plasmodium falciparum</i> erythrocyte membrane protein 1
PfEMP3	<i>Plasmodium falciparum</i> erythrocyte membrane protein 3
PfMC-2TM	<i>Plasmodium falciparum</i> Maurer's clefts two transmembrane protein
PIESP2	Parasite-infected erythrocyte surface protein-2
PLA	Proximity ligation assay
PNEP	PEXEL-negative exported protein
PPD	P-phenylenediamine
PTEX	<i>Plasmodium</i> translocon of exported proteins
PTEX88	PTEX protein-88
PTEX150	PTEX protein-150
PTP	PfEMP1 trafficking protein
PV1	Parasitophorous vacuolar protein-1
PV2	Parasitophorous vacuolar protein-2

PVM	Parasitophorous vacuole membrane
RBC	Red blood cell
REX1	Ring-exported protein-1
REX2	Ring-exported protein-2
REX3	Ring-exported protein-3
RNA	Ribonucleic acid
SBP1	Skeleton-binding protein-1
SEMP1	Small exported membrane protein 1
SDS	Sodium dodecyl sulphate
SDS-PAGE	SDS polyacrylamide gel electrophoresis
STARP	Sporozoite threonine and asparagine-rich protein
STEM	Scanning transmission electron microscopy
TCA	Trichloroacetic acid
TCEP	Tris(2-carboxyethyl(phosphine))
TEAB	Tetraethylammonium bromide
TFE	Tetrafluoroethylene
TM	Transmembrane domain
TRiC	T-complex protein-1 ring complex
TRX2	Thioredoxin-2
TSG101	Tumour suppressor gene 101
TX-100	Triton X-100
VPS28	Vacuolar protein sorting-associated protein 28 homologue

Chapter 1 : Introduction

1.1 Malaria - the disease

In the distant past, it is suggested that the malaria parasite *Plasmodium falciparum* was transmitted from a gorilla to a human for the first time (Liu et al., 2010). Since this transmission event, *P. falciparum* has plagued our species. The symptoms of malaria were recorded as early as 2700 BCE in ancient Chinese medical writings. The lethality of *P. falciparum* has influenced the course of human evolution and caused the emergence of compensatory genetic diseases such as thalassaemia and sickle-cell disease (Taylor and Fairhurst, 2014).

There are five species of *Plasmodium* that infect humans: *P. falciparum*, *P. knowlesi*, *P. malariae*, *P. vivax* and *P. ovale*. Of these species, *P. falciparum* causes the most mortality and is the most prevalent globally (WHO 2016). In 2015, there were an estimated 212 million new cases of malaria. In the same year, malaria caused the deaths of 429,000 people. Of the deaths due to malaria, 92% occurred in Africa, 6% in South-East Asia and 2% in the Eastern Mediterranean (WHO 2016). Of those who died, an estimated 71% were children under the age of five.

Malaria continues to have a devastating impact in low-income countries. However, important progress is being made towards reducing malaria prevalence and mortality. A number of countries have eliminated malaria between 2000-2016 (Figure 1.1). These include Sri Lanka, Argentina, Egypt, Morocco, Syria, Iraq, Turkey and nine other countries. Since 2000, malaria mortality has decreased by 62%. This is due to the implementation of vector control measures, and an increasing proportion of suspected malaria cases receiving a rapid diagnostic test and effective antimalarial treatment (WHO 2016). Interventions such as the use of insecticide-treated bed nets in sub-Saharan Africa has reduced childhood malaria mortality by 55% (WHO 2016).

Artemisinin derivatives are the first-line drugs used to treat malaria. They are fast-acting drugs that have a ~1 h half-life *in vivo*, and are typically given with a partner drug (called artemisinin combination therapies) such as mefloquine, sulfadoxine-pyrimethamine, amodiaquine and piperaquine (Tilley et al., 2016). In 2009, partial resistance to artesunate (an artemisinin derivative) was reported in patients from Pailin in Cambodia (Htut, 2009).

The resistance manifests as delayed parasite clearance following drug treatment and has been experimentally linked to SNPs within the kelch 13 gene (PF3D7_1343700) (Ariey et al., 2014). Resistance to artemisinin combination therapies (including resistance to the partner drug) has been detected for four different drug combinations (WHO 2016). Stopping the spread of such parasites to Africa, as well as developing new drugs to treat malaria are important future challenges.

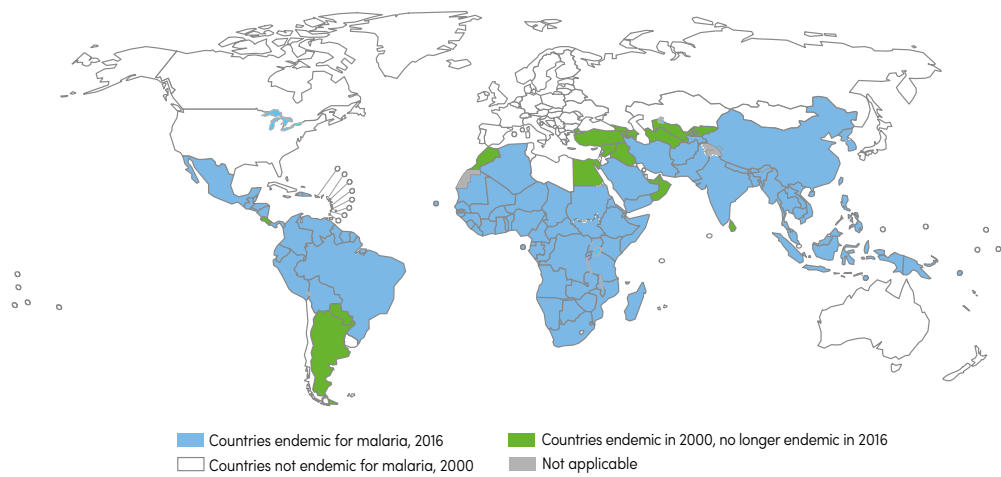


Figure 1.1 Countries endemic for malaria in 2000 and 2016.

Countries were considered to have eliminated malaria after 3 consecutive years with no indigenous cases. Reprinted with permission from the World Health Organisation: World Malaria Report 2016, WHO, Copyright (2016)

1.1.1 Malaria pathology and mechanism of cytoadherence

Infection with *P. falciparum* can cause symptoms such as fever, chills, headache and nausea. Severe malaria is a life-threatening condition with symptoms such as metabolic acidosis, severe anaemia, cerebral malaria, and coma. *P. falciparum* expresses antigens on the host red blood cell surface that enable the parasitised cell to bind to receptors on the host endothelium, such as CD36 and endothelial protein C receptor (EPCR). The adhesin *P. falciparum* erythrocyte membrane protein 1 (PfEMP1) is responsible for the binding of infected RBCs to endothelial cells. The PfEMP1 is a variant protein encoded by up to ~60 genes in the parasite genome. Despite the significance of PfEMP1 to the pathogenesis of *P. falciparum*-malaria, there are no drugs that prevent its trafficking or assembly. Naturally-acquired protective antibodies to malaria infection often bind to PfEMP1, but the extensive antigenic variation of PfEMP1 makes vaccine development to this protein a challenge (Beeson and Brown, 2002, Beeson et al., 2013).

Expression of PfEMP1 is regulated epigenetically by the heterochromatic silencing of *var* promoters and mono-allelic expression of a single *var* gene in transcriptionally competent regions of the parasite nucleus (Ralph et al., 2005, Voss et al., 2006). This regulation results in the expression of a single PfEMP1 variant at the infected red blood cell surface. Each PfEMP1 variant binds to one or more specific host ligands such as cluster of differentiation 36 (CD36), intracellular adhesion molecule 1 (ICAM1), endothelial protein C receptor (EPCR) or chondroitin sulphate A (CSA), with the majority of PfEMP1 variants binding to CD36, a ligand present throughout the vascular endothelium. The EPCR is expressed on cells in most tissues, including in the brain, and the binding of infected red blood cells to this receptor is associated with severe malaria (Turner et al., 2013). The varied binding phenotypes of the PfEMP1 protein is a result of variation of extracellular adhesion domains: the Duffy binding-like (DBL) and cysteine-rich interdomain region (CIDR) (Figure 1.2A).

Primigravid women in endemic areas are also at high risk of severe *P. falciparum* malaria, even if they were previously clinically immune. This is because parasitised RBCs express an adhesin on the RBC surface that specifically binds to chondroitin sulphate A (CSA) in the placental intervillous space. The PfEMP1 variant responsible for adhesion to CSA in

the placenta is var2csa, a gene conserved between parasite strains (Rogerson et al., 2007). In addition to causing maternal morbidity and mortality, *P. falciparum* infection of the placenta is associated with premature birth, low birth weight and stillbirths (de Moraes et al., 2013) (Figure 1.2B).

1.2 *Plasmodium falciparum* biology

1.2.1 Lifecycle of the parasite

The definitive host of *P. falciparum* is the *Anopheles* mosquito (Figure 1.3a). A feeding mosquito ingests male and female forms of the parasite when it takes a blood meal. The male and female gametocytes activate within the mosquito midgut forming male microgametes and female microgametes. The male and female gametes fuse to form a zygote, which develops into the motile ookinete, which then crosses the midgut wall and develops into an oocyst on the mosquito stomach. A population of a motile form of the parasite, the sporozoite, is formed within the oocyst and eventually ruptures from the cyst and migrates to the mosquito salivary glands, where the sporozoites remain until injected into a human host during the course of a blood meal. In the human host, sporozoites invade hepatocytes and replicate into thousands of merozoites over the course of 1-2 weeks. After the rupture of the infected hepatocyte, the merozoites enter the bloodstream and invade red blood cells (RBCs). Inside the red blood cell, the parasite develops inside the parasitophorous vacuole developing through the ring, trophozoite and schizont stages. During this development the parasite remodels the red blood cell and feeds on haemoglobin within the red blood cell cytoplasm (Figure 1.3b) until undergoing schizogony. The blood stage asexual cycle repeats approximately every ~48 h, with the rupture of schizonts and release of merozoites triggering the symptoms of malaria. A small proportion of parasites will develop into gametocytes that can be taken up by a feeding mosquito completing the lifecycle.

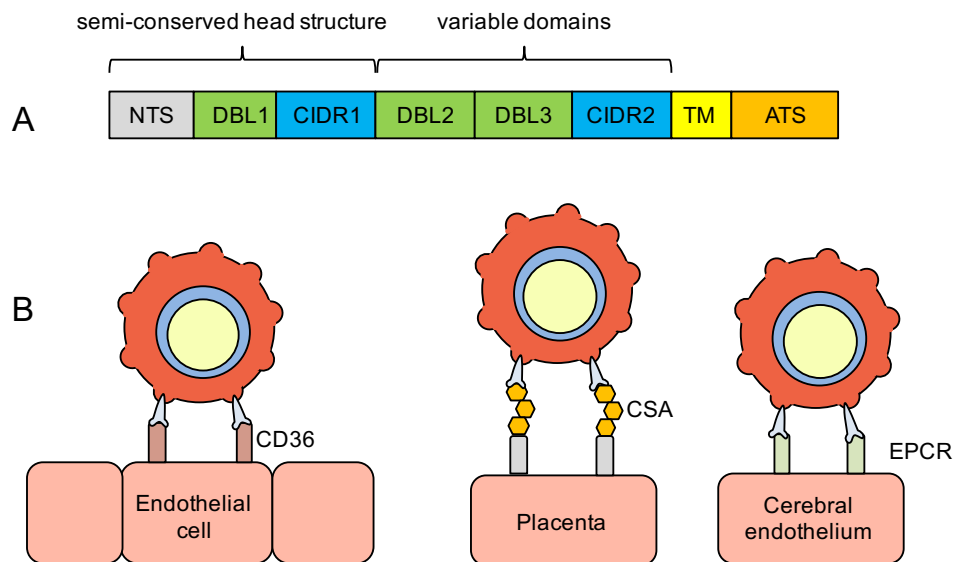


Figure 1.2 The adhesin PfEMP1 is responsible for the severe pathology of *P. falciparum*-malaria

(A) The general structure of a PfEMP1 protein. The extracellular portion of the protein comprises the N-terminal segment (NTS) and a variable number of DBL and CIDR domains. A transmembrane domain (TM) inserts into the red blood cell membrane, followed by the acidic terminal segment (ATS) which interacts with knob-associated histidine rich protein (KAHRP) on the intracellular side of the red blood cell membrane, anchoring PfEMP1 and forming the virulence complex

(B) Adhesion of infected red blood cells via PfEMP1 to ligands expressed on the surface of the vascular endothelium (CD36); in the placental intervillous space (CSA); and on cerebral endothelium (EPCR)

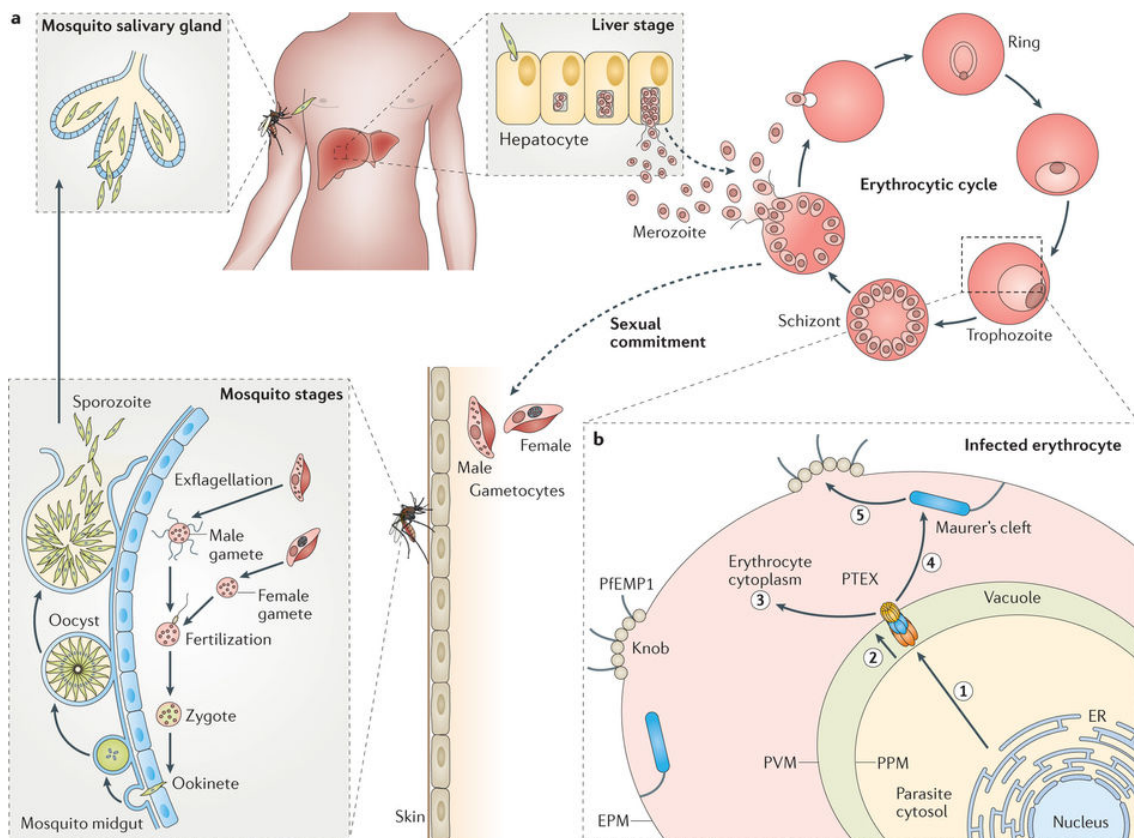


Figure 1.3 The lifecycle of *Plasmodium falciparum*

(A) The parasite undergoes asexual reproduction within the *Anopheles* mosquito, then commences asexual reproduction in hepatocytes within the human host.

(B) After egress from hepatocytes, the merozoites invade red blood cells. The parasite remodels the host red blood cell by exporting the adhesin PfEMP1 (*P. falciparum* erythrocyte membrane protein-1) to the membrane surface, allowing the infected cell to bind to the host endothelium. PTEX = *Plasmodium* translocon of exported proteins; PVM = parasitophorous vacuole membrane; PPM = parasite plasma membrane; EPM = erythrocyte plasma membrane; ER = endoplasmic reticulum.

Reprinted with permission from MacMillan Publishers Ltd: Nature Reviews Microbiology, de Koning-Ward, T., et al. Copyright (2016).

1.3 Export of parasite proteins by *Plasmodium falciparum*

The malaria parasite *P. falciparum* remodels the host red blood cell throughout the course of its asexual development (for a review, see (de Koning-Ward et al., 2016)). The parasite is surrounded by a parasitophorous vacuole membrane across which proteins destined for export must transit (Figure 1.3B). A translocon spanning the parasitophorous vacuole membrane is responsible for exporting proteins to the red blood cell cytoplasm. Exported proteins have diverse functions within the host cell. Some remain soluble in the red blood cell cytoplasm, others localise to mobile structures such as J-dots (thought to be protein chaperone complexes) and Maurer's clefts (organelles involved in virulence protein trafficking). Other exported proteins are targeted directly to the red blood cell skeleton and membrane. The major virulence protein, PfEMP1, is exported in a soluble state and becomes membrane-embedded once it reaches the Maurer's clefts (Batinovic et al., 2017). From the Maurer's clefts, PfEMP1 is transported to the red blood cell membrane where it mediates cytoadherence (described in Sections 1.4.3 and 1.4.4). This section describes generic export pathways from the parasite to the red blood cell cytoplasm. Additionally, exported proteins that reach their target locations independently of Maurer's clefts are discussed.

1.3.1 The secretory pathway during the blood stages of *P. falciparum*

The parasite exports proteins into the host red blood cell (by a pathway involving the secretory system and a translocon) to destinations such as the red blood cell cytoskeleton and Maurer's clefts - discoid parasite-derived organelles (Figure 1.4). The exported proteins can be grouped into two broad categories: those with a *Plasmodium* export element (PEXEL), and PEXEL-negative exported proteins (PNEPs). The PEXEL motif (also called vacuolar targeting signal) was identified by multiple sequence alignment of known exported proteins and has the consensus sequence RxLxE/Q/D (Marti et al., 2004, Hiller et al., 2004). Around 400 proteins contain a PEXEL and are predicted to be exported. However, predicting the total number of exported proteins is still unknown due to the difficulty in identifying PNEPs. Although PNEPs have no obvious unifying feature that has enabled their identification such as a PEXEL motif, they tend to have a two-exon structure and a non-canonical signal peptide (typically recessed from the N-terminus) (Haase et al., 2009, Heiber et al., 2013). The most successful PNEP identified study found more than 10 novel PNEPs by transcriptional profile similarity, chromosomal location and sequence similarity to other PNEPs (Heiber et al., 2013). Some of the most well-

characterised PNEPs are Maurer's clefts proteins, such as ring exported protein 1 (REX1), membrane-associated histidine-rich protein 1 (MAHRP1) and skeleton binding protein 1 (SBP1). These three proteins are critical for efficient PfEMP1 trafficking and parasite virulence (Dixon et al., 2011, Spycher et al., 2008, Maier et al., 2007).

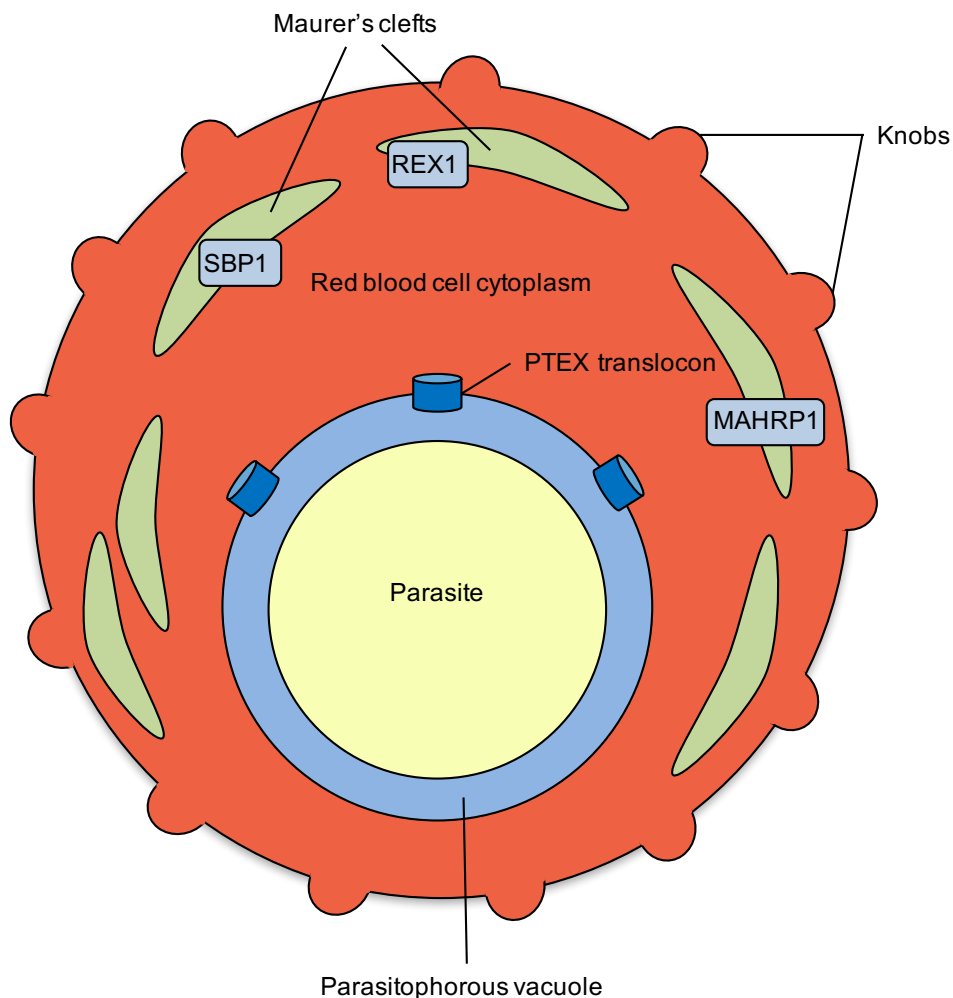


Figure 1.4 Parasite-induced modifications to the host red blood cell

The *Plasmodium falciparum* parasite (yellow) secretes proteins into the parasitophorous vacuole surrounding it (blue) where some proteins are targeted for export via the PTEX translocon. Exported proteins can reside at the Maurer's clefts (green), or the red blood cell cytoplasm or cytoskeleton. The Maurer's clefts proteins REX1, SBP1 and MAHRP1 are depicted in light blue.

Both PEXEL proteins and PNEPs are directed into the endoplasmic reticulum during translation. During translation into the endoplasmic reticulum, PEXEL proteins are cleaved by the aspartyl protease plasmepsin V after the lysine residue of the PEXEL motif, and the new N-terminus is acetylated (Boddey et al., 2010, Boddey et al., 2016, Russo et al., 2010, Chang et al., 2008). One study suggested that targeting of exported proteins to the red blood cell was independent of cleavage by plasmepsin V and was instead due to binding of the PEXEL motif to phosphatidylinositol-3-phosphate (PI(3)P) on the inner leaflet of the endoplasmic reticulum (Bhattacharjee et al., 2012). However, the findings that the PEXEL motif bound PI(3)P, and that PI(3)P was located on the luminal side of the endoplasmic reticulum membrane could not be reproduced (Boddey et al., 2016).

The PNEPs are not cleaved by plasmepsin V. Both PNEPs and PEXELs (with a mature N-terminus) leave the endoplasmic reticulum and are thought to transit through the Golgi before being secreted into the parasitophorous vacuole (Saridaki et al., 2008).

1.3.2 Transit of exported proteins across the parasitophorous vacuole

It has been suggested that after secretion, membrane-bound PNEPs are extracted from the parasite plasma membrane (Mesen-Ramirez et al., 2016), although this process is not currently well understood. Inside the parasitophorous vacuole, proteins may be directed to certain sub-compartments, for example certain sites that are enriched in translocation machinery or cargo (Bullen et al., 2012, McMillan et al., 2013, Batinovic et al., 2017). Blocking of protein translocation or protein unfolding leads to the accumulation of exported reporter proteins in puncta at the parasitophorous vacuole in association with PTEX (Mesen-Ramirez et al., 2016, Riglar et al., 2013). These puncta may represent sub-compartments in the parasitophorous vacuole that have been previously observed by electron microscopy and have been shown to contain PfEMP1 destined for export (Aikawa et al., 1986, McMillan et al., 2013).

The export pathways of both PEXEL and PNEPs converge at the parasitophorous vacuole where all exported proteins are unfolded and then translocated into the red blood cell by the *Plasmodium* translocon of exported proteins (PTEX) (Beck et al., 2014, Elsworth et

al., 2014, Gruring et al., 2012, Mesen-Ramirez et al., 2016, Gehde et al., 2009, Batinovic et al., 2017).

The PTEX is comprised of five core subunits: heat shock protein 101, an ATPase involved in translocation; PTEX150; exported protein 2 (EXP2), units of which are thought to oligomerise to form a pore in the parasitophorous vacuole membrane; PTEX88 and thioredoxin 2 (de Koning-Ward et al., 2009). The protein components of the translocon are synthesised in the schizont stage, stored within the dense granules of merozoites and delivered to the host red blood cell during invasion (Bullen et al., 2012). Functional PTEX is essential for parasite survival (Beck et al., 2014, Elsworth et al., 2014). An exported protein interacting complex (EPIC) associates with PTEX and may be involved in transferring exported cargo to the translocon for export (Batinovic et al., 2017).

1.3.3 The role of exported co-chaperones/chaperones

Proteins must be refolded after they are translocated to the red blood cell cytoplasm. Exported *Plasmodium* chaperone proteins are presumed to play a role in this process and a number of likely candidates have been identified. Folding of proteins by heat shock protein 70s (HSP70s) is an ATP-dependent process that is regulated by HSP-40 proteins (for a review, see (Hartl et al., 2011)). Of the 43 HSP40s encoded in the *P. falciparum* genome, 19 are predicted to be exported (Sargeant et al., 2006). Two type II HSP40s (PFA0660w and PFE0055c) have been localised to J-dots: mobile, cholesterol-rich puncta in the red blood cell cytoplasm (named for the J domain within these HSP40s) (Kulzer et al., 2010). In addition, an exported *Plasmodium* HSP70 (HSP70-x) is present in J-dots where it forms chaperone/co-chaperone complexes with the HSP40s PFA0660w and PFE0055c (Kulzer et al., 2012, Daniyan et al., 2016). One report suggested that the group II chaperonin TCP-1 ring complex (*Pf*TRiC) was exported to the red blood cell cytoplasm where it was suggested to interact with exported proteins and play a role in protein trafficking within the host cell (Mbengue et al., 2015). However, epitope-tagging of *Pf*TRiC subunits showed that *Pf*TRiC is not exported, and knockdown of functional *Pf*TRiC did not affect protein export, arguing against *Pf*TRiC as an exported molecular chaperone (Spillman et al., 2017).

1.4 The Maurer's clefts of *Plasmodium falciparum*

The Maurer's clefts were first described by the German physician Georg Maurer in 1902, after he observed stippling in the cytoplasm of Giemsa-stained infected red blood cells. Similar structures had already been observed in *Plasmodium vivax*-infected red blood cells, termed Schüffner's dots (Schüffner, 1899, Maurer, 1900). The membrane-bound clefts were eventually observed by electron microscopy and connected to the stippling originally observed by Maurer (Trager et al., 1966). The virulence protein PfEMP1 transits through the Maurer's clefts before being transferred to the red blood cell membrane. Due to the Maurer's clefts' involvement in virulence protein trafficking and the uniqueness of their biology, these organelles have been studied for over a century.

1.4.1 Morphology and motion of the Maurer's clefts

Maurer's clefts are formed shortly after parasite invasion into the red blood cell, with early Maurer's clefts resident proteins arriving at the clefts within 2 – 6 hours post-invasion (Gruring et al., 2011, McMillan et al., 2013). Maurer's clefts may be formed from the parasitophorous vacuole membrane, however other possibilities have not been ruled out (McHugh et al., 2015, Hanssen et al., 2008b). They are surrounded by a single membrane bilayer and are typically unilamellar in 3D7, CS2 and other laboratory parasite strains, though reportedly multi-lamellar in others eg K1 (Hanssen et al., 2008b, Trager et al., 1966).

During the ring stage of the parasite lifecycle, the Maurer's clefts move by Brownian motion within the red blood cell cytoplasm (Kilian et al., 2013, Gruring et al., 2011, McMillan et al., 2013). As the parasite transitions from a ring form to the trophozoite stage, the parasite position becomes fixed and the Maurer's clefts immobilise at the periphery of the host cell within a 1-2 hour timeframe, at around 20 - 24 h post-invasion (Gruring et al., 2011, McMillan et al., 2013). The immobilisation of the Maurer's clefts may partly occur through actin filaments formed by rearrangement of actin from the host cytoskeleton (Cyrklaff et al., 2011, Rug et al., 2014). However, the immobilisation of Maurer's clefts is not sensitive to treatment with the actin polymerisation inhibitor cytochalasin D (McMillan et al., 2013) so it is possible that additional structures called tethers may be involved in Maurer's clefts arrest (Hanssen et al., 2008b, Pachlatko et al., 2010).

During the trophozoite stage, Maurer's clefts lamellae adopt a cisternal shape and have an electron-dense coat and electron-lucent lumen after chemical fixation, however cryo-preparations have shown that the lumen of the Maurer's clefts has a similar density and appearance to the red blood cell cytoplasm (Hanssen et al., 2008b, Henrich et al., 2009). Ultrastructural studies of the Maurer's clefts tend to describe two broad lamellar arrangements: mostly single lamellae dispersed within the red blood cell cytoplasm, or stacked and whorled lamellae. It is interesting to consider whether any of these morphologies predominate in samples from the field and are representative of 'wild-type' Maurer's clefts. Some early electron microscopy studies of infected red blood cells from field samples often identified single lamellar Maurer's clefts, i.e. single lamellae (Ladda et al., 1966, Trager et al., 1966). Many studies of wild-type 3D7, A4, CS2 and other parasite strains also find primarily single Maurer's clefts lamellae (Hanssen et al., 2010, Rug et al., 2014, Hanssen et al., 2008b, Kriek et al., 2003, Elford et al., 1995). Maurer's clefts with stacked lamellae and other convoluted forms have been extensively studied by serial sectioning and three-dimensional rendered reconstructions (Wickert et al., 2004, Wickert et al., 2003b). It is possible that the stacked and convoluted Maurer's clefts reported in the literature could be due to truncation of the region of chromosome 9 encoding REX1 (and other cytoadherence-related genes). This portion of chromosome 9 is frequently lost during long term culturing of *P. falciparum*. The D10 parasite strain (which has a truncation in chromosome 9 including the gene encoding REX1) exhibits stacked Maurer's clefts. A study of the Maurer's clefts protein REX1 showed that this protein is required for the single-lamella phenotype (Hanssen et al., 2008a). The D10 parasite strain was shown to revert from stacked to single clefts when complemented with REX1 (Hanssen et al., 2008a). The role of REX1 in maintaining single Maurer's clefts has since been further characterised (Chapter 3) (Dixon et al., 2011, McHugh et al., 2015).

Some earlier work suggested that exported proteins may be loaded into the Maurer's clefts during their formation from the parasitophorous vacuole, or that the clefts shared a continuous lumen with this compartment (Spycher et al., 2006, Wickert et al., 2003b, Wickert et al., 2004, Bhattacharjee et al., 2008). Yet others found that the Maurer's clefts and other compartments were not interconnected (Henrich et al., 2009). It has now been shown that proteins are trafficked to existing clefts in the red blood cell cytoplasm throughout the parasite lifecycle (Gruring et al., 2011, Gruring et al., 2012).

In the schizont stage of asexual development, the amount of remaining host cell cytoplasm is reduced and the Maurer's clefts appear to aggregate around 2 - 4 h prior to host cell rupture (Gruring et al., 2011). Dismantling the Maurer's clefts at the schizont life cycle stage may assist in successful merozoite egress.

1.4.2 Targeting of proteins to the Maurer's clefts

The Maurer's clefts are a repository for a number of exported proteins and are essential for trafficking the major virulence protein PfEMP1 to the red blood cell surface. Exactly how exported proteins are targeted to the Maurer's clefts is largely unknown. However, truncation studies with the REX1 protein have shown that the predicted coiled-coil region is required for localisation of REX1 to the Maurer's clefts (Dixon et al., 2008). Investigation of another PNEP, ring exported protein 2 (REX2), found that a short N-terminal region as well as a particular transmembrane region were required for REX2 localisation to the Maurer's clefts, and were able to target other reporter proteins to the clefts (Haase et al., 2009).

1.4.3 Maurer's clefts proteins involved in trafficking of PfEMP1

Once proteins have been translocated to the red blood cell cytoplasm, a number become sequestered at the Maurer's clefts. For example, the major virulence protein PfEMP1 is initially transported to the Maurer's clefts where it is membrane-embedded with the ATS facing the red blood cell cytoplasm (Kriek et al., 2003).

Three proteins have been identified that are required for trafficking of PfEMP1 past the parasitophorous vacuole membrane to the Maurer's clefts. Disruption of the Maurer's clefts protein SBP1 led to retention of PfEMP1 within the parasite and parasitophorous vacuole (Maier et al., 2007). Similarly, knockout of the resident Maurer's clefts protein MAHRP1 prevented export of PfEMP1 from the parasitophorous vacuole and completely ablated surface-exposed PfEMP1 (Spycher et al., 2008, Maier et al., 2008). There is still no congruent explanation for why knockout of Maurer's clefts proteins that are exported before PfEMP1 causes PfEMP1 to become trapped in the parasite or parasitophorous

vacuole (McMillan et al., 2013). A second study of SBP1-deleted parasites found that PfEMP1 was exported to the Maurer's clefts but not transferred to the red blood cell surface (Cooke et al., 2006). Deletion of SBP1 does not seem to affect Maurer's clefts morphology, although MAHRP1 deletion lead to longer clefts. Exported proteins other than PfEMP1 that were analysed for both SBP1 and MAHRP1 knockouts did not appear to be affected (Maier et al., 2007, Spycher et al., 2008).

The biggest advance in the understanding of exported proteins in *P. falciparum* came with a large-scale protein knockout study (Maier et al., 2008). This group targeted 46 PEXEL and 5 PNEPs for genetic disruption and assessed each for defects in PfEMP1 transport. This led to the identification of 6 novel PEXEL proteins which are required for efficient PfEMP1 transport, PfEMP1 trafficking proteins (PTPs) 1-6 (Maier et al., 2008). Knockout of one of these proteins, PTP1, has a striking effect on Maurer's clefts morphology. In these parasites, membranous globular structures that label with Maurer's clefts markers REX1 and SBP1 are distributed throughout the host cytoplasm (Rug et al., 2014). The PTP1 knockout parasite line also had disrupted actin filaments that usually link the Maurer's clefts to the red blood cell cytoskeleton (Rug et al., 2014).

Other Maurer's clefts proteins, REX1, PTP2, virulence associated protein 1 (VAP1) and PTP5 play roles in the transport of PfEMP1 to the red blood cell surface (Maier et al., 2008, Nacer et al., 2015, Dixon et al., 2011). Knockout of each of these proteins leads to decreased surface expression of but does not affect transfer to the Maurer's clefts. Of these, the most severe phenotype is displayed by PTP2 and REX1 knockout parasites that show no surface exposed PfEMP1 at the infected red blood cell surface (Maier et al., 2008, Dixon et al., 2011).

1.4.4 Transport of PfEMP1 from the Maurer's clefts to the red blood cell membrane

Electron microscopy analysis of *P. falciparum*-infected red blood cells has identified a number of parasite-induced structures associated with the Maurer's clefts (Figure 1.5A), such as tethers, electron dense vesicles and actin filaments. Tethers are tubular, electron-dense structures that protrude from the edges of Maurer's clefts and contain the protein membrane-associated histidine-rich protein 2 (MAHRP2) (Pachlatko et al., 2010,

Hanssen et al., 2008b). They often appear to connect the Maurer's clefts to the red blood cell membrane, however, because MAHRP2 is associated with the Maurer's clefts from ~ 4 h post-invasion, additional processes are likely involved in Maurer's clefts immobilisation (Hanssen et al., 2008b). While MAHRP2 is localised exclusively to tethers, the Maurer's clefts protein REX1 and PfEMP1 have also been observed at the tethers (Pachlatko et al., 2010, Hanssen et al., 2008b, Hanssen et al., 2008a, McMillan et al., 2013). The role of tethers, if any, in PfEMP1 trafficking is unclear.

Actin filaments have been visualised connecting the Maurer's clefts to the red blood cell membrane (Figure 1.5B; orange lines). It is suggested that in the trophozoite stage, host actin is remodelled from the red blood cell cytoskeleton and incorporated into branching filaments that connect the Maurer's clefts with the red blood cell membrane (Cyrklaff et al., 2011). Electron tomography showed that vesicles (with sizes ranging from 20 nm - 200 nm) are associated with these actin filaments, and some contained PfEMP1 (Cyrklaff et al., 2011). Actin remodelling has been investigated in the context of haemoglobinopathies, as humans with haemoglobins S and C are protected against severe malaria compared to those with wild-type haemoglobin A (Cserti and Dzik, 2007). Parasitised red blood cells with haemoglobins S and C had altered Maurer's clefts morphology and disrupted actin filaments around the aberrant clefts, suggesting that the protective haemoglobinopathies interfere with the remodelling of actin to Maurer's clefts (Cyrklaff et al., 2011).

Electron dense vesicles (EDVs) containing PfEMP1 have been observed in red blood cells infected with trophozoite stage parasites (McMillan et al., 2013, Trelka et al., 2000). These vesicles are ~80 nm in diameter, have an electron-dense coat, and have been imaged in the apparent process of fusion with the red blood cell membrane (Trelka et al., 2000, McMillan et al., 2013). Electron dense vesicles are considered a possible vehicle for PfEMP1 transport from the Maurer's clefts to the red blood cell membrane. Interestingly, PTP2 has been associated with electron-dense vesicles budding from the Maurer's clefts as knockout of PTP2 leads to loss of these vesicles (Regev-Rudzki et al., 2013). The PTP2 knockout parasites do not display PfEMP1 on the surface of the infected red blood cell and PfEMP1 remains trapped at the Maurer's clefts (Maier et al., 2008). Smaller uncoated vesicles of ~25 nm diameter termed 'vesicle-like structures' have also been observed around the Maurer's clefts and around electron dense vesicles, but the

protein cargo of these (if any) is still unknown (McMillan et al., 2013, Hanssen et al., 2010).

Two studies have identified exosomes (or microvesicles) that are released from *P. falciparum*-infected red blood cells and suggest that parasites communicate by exosome budding and fusion from the host cell membrane (Regev-Rudzki et al., 2013, Mantel et al., 2013). One report has implicated PTP2 in the formation of these vesicles (Regev-Rudzki et al., 2013).

In red blood cells infected with trophozoites, PTP2 was localised to the Maurer's clefts (co-located with SBP1), but localises to distinct vesicles in the schizont stage (Maier et al., 2008, Regev-Rudzki et al., 2013). It was suggested that PTP2 is present in vesicles budding from the Maurer's clefts, and that these may be the same vesicles described as EDVs that contain PfEMP1 (Regev-Rudzki et al., 2013, Hanssen et al., 2010, McMillan et al., 2013). Yet Regev-Rudzki et al. (2013) describe the PTP2-labelled vesicles as 'exosome-like', despite not being enclosed within a membrane such as a multivesicular body and thus having no obvious way to exit the red blood cell (Regev-Rudzki et al., 2013). The microvesicles described by Mantel et al. (2013) were analysed by mass spectroscopy and were not found to contain PTP2, but were enriched in other Maurer's clefts proteins such as SBP1, Pf332, MAHRP2, MAHRP1, PfMC-2TMs, SEMP1, REX1, REX2, PIESP2 and PF07_0008 (Mantel et al., 2013). The microvesicles were also enriched in parasite proteins associated with the red blood cell cytoskeleton and membrane, such as RhopH2, RhopH3, Clag 3.1, MESA, RESA and PFD1170c (Mantel et al., 2013). The relationship between exosomes/microvesicles, the Maurer's clefts and inter-cellular communication warrants further investigation.

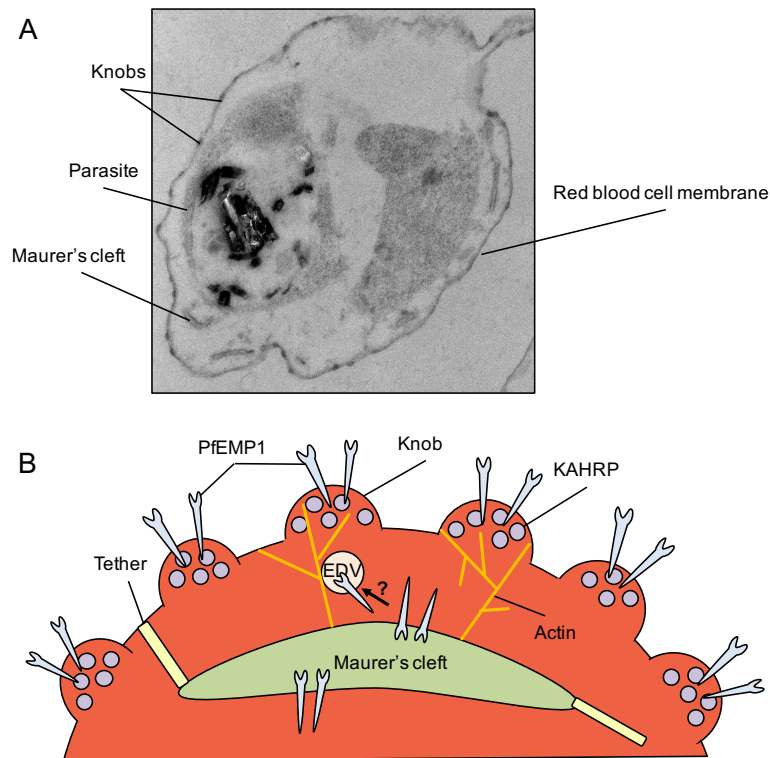


Figure 1.5 Remodelling of the host red blood cell by *P. falciparum*

(A) Transmission electron microscopy of a *P. falciparum*-infected red blood cell. The sample was treated with Equinatoxin II to remove haemoglobin in order to better observe structures within the red blood cell. Knobs appear as electron-dense protrusions on the red blood cell surface. Maurer's clefts are dispersed throughout the red blood cell. A trophozoite-stage parasite with a large digestive vacuole fills the centre of the host red blood cell.

(B) The Maurer's clefts are membranous structures that attach to the red blood cell membrane via remodelled host actin (orange) and parasite-induced tethers (yellow). Electron dense vesicles (EDVs; beige) may function as trafficking vesicles between the Maurer's clefts and the red blood cell membrane. Protrusions on the red blood cell membrane (knobs) form as a result of deposition of KAHRP (mauve) and other parasite proteins at the cytoskeleton. These structures serve to present PfEMP1 (blue) which binds to ligands in the host microvasculature, sequestering the infected red blood cell from circulation.

1.4.5 Parasite-induced structures in other *Plasmodium* spp.

The ‘Schüffner’s dots’ of *P. vivax* were discovered around the same time as Maurer’s clefts, appearing as red stippling on Romanowsky-stained infected reticulocytes/red blood cells (Schüffner, 1899). Electron microscopy revealed that in *P. vivax* and *P. cynomolgi*, the stained Schüffner’s dots corresponded to caveola-vesicle complexes along the red blood cell membrane (Aikawa et al., 1975). These caveolae are open to the extracellular space, and have tubules and vesicles associated with the intracellular face (Akinyi et al., 2012, Aikawa, 1988). They have been linked to the trafficking of parasite proteins, in particular a 95 kDa *Plasmodium* helical interspersed subtelomeric (PHIST) protein that may be essential for parasite survival (Matsumoto et al., 1988, Akinyi et al., 2012, Udagama et al., 1988). Clefts are also present in the cytoplasm of *P. vivax*- and *P. cynomolgi*-infected red blood cells and tend to be longer than the Maurer’s clefts of *P. falciparum* (Aikawa et al., 1975, Udagama et al., 1988). The function of the clefts in *P. vivax* and *P. cynomolgi* and their relationship to the caveola-vesicles complexes is not currently understood.

The rodent malaria *P. berghei* also produces structures in the red blood cell, termed intra-erythrocytic *P. berghei*-induced structures (IBIS) (Ingmundson et al., 2012). The first IBIS protein identified (termed IBIS1) is a membrane bound protein associated with mobile structures in the red blood cell cytoplasm, hypothesised to be similar to Maurer’s clefts (Ingmundson et al., 2012). *P. falciparum* Maurer’s clefts markers expressed in *P. berghei* label the IBIS (Ingmundson et al., 2012). Electron microscopy showed that IBIS are vesicular-tubular structures in the red blood cell cytoplasm (Ingmundson et al., 2012, Haase et al., 2013). Recently, *P. berghei* orthologues of two *P. falciparum* Maurer’s clefts markers SBP1 and MAHRP1 have been localised to IBIS, where they perform an equivalent function in enabling cytoadherence (De Niz et al., 2016). These orthologues had very low sequence similarity to the *P. falciparum* equivalents, suggesting that proteins with very divergent primary sequences can perform the same function at IBIS, and that bioinformatics approaches (particularly hidden Markov modelling) could be a good way to identify virulence-associated proteins in other *Plasmodium* spp.

1.5 The virulence complex and red blood cell membrane modifications

Many exported parasite proteins are targeted to the red blood cell membrane where they mediate cytoadherence and/or alter cell shape and rigidity. A key feature of *P. falciparum*-infection is the appearance of knobs on the red blood cell membrane, first observed by transmission electron microscopy as protrusions of electron dense material under the membrane (Trager et al., 1966). Knobs are formed by the knob-associated histidine-rich protein (KAHRP), which is required for cytoadherence under physiological blood flow conditions (Crabb et al., 1997, Taylor et al., 1987). Other proteins essential for knob formation are the PHIST protein PFD1170c and the DnaJ-containing protein PF10_0381 (Maier et al., 2008). The main function of knobs appears to be the presentation of PfEMP1 on the surface of the red blood cell, enhancing cytoadherence (Baruch et al., 1995). Additionally, knobs contribute to the increased rigidity of the infected red blood cell (Glenister et al., 2002, Zhang et al., 2015). Other proteins reported to be associated with knobs include PfEMP3, Pf332 and the PHIST protein PFE1605w (Oberli et al., 2016, Waterkeyn et al., 2000, Hinterberg et al., 1994). Recently, a comprehensive ultrastructural analysis of knobs showed that there is a spiral scaffold within the knob which is underpinned by KAHRP, and that there is a ‘discontinuity’ at the knobs apex in which membrane proteins (likely PfEMP1) are inserted (Watermeyer et al., 2016). The identification of the spiral-forming protein will advance the understanding of virulence complex formation.

1.6 Exported proteins that are not trafficked via the Maurer’s clefts

After export through PTEX, the major virulence protein PfEMP1 is transported via the Maurer’s clefts to the red blood cell membrane, however many other exported proteins do not follow this route. These proteins fall under two broad categories: those that remain soluble in the red blood cell cytoplasm, and proteins that localise to the red blood cell membrane. Exported proteins that are soluble in the red blood cell cytoplasm include ring exported proteins 3 and 4 (REX3 and REX4), histidine-rich protein II (HRPII) and PTP3 (Spielmann et al., 2006, Maier et al., 2008, Iqbal et al., 2004). In addition, a part of the population of exported HSP40 proteins and HSP70x is soluble whilst the rest exists in structures known as J-dots (Kulzer et al., 2010). Similarly, FIKK4.2 localises to undefined structures termed “K-dots” in the red blood cell cytoplasm although other

FIKK kinases localise to the Maurer's clefts (i.e. FIKK4.1, FIKK9.3, FIKK 9.6 and FIKK12) (Kats et al., 2014, Nunes et al., 2007).

The knob protein KAHRP was thought to transit via the Maurer's clefts (based on fluorescence microscopy of a GFP-tagged chimera) however subsequent studies have not observed KAHRP at the clefts (Wickham et al., 2001, Rug et al., 2006, McHugh et al., 2015). Instead, KAHRP appears to be directly targeted to the red blood cell membrane skeleton where it forms knobs and anchors the cytoplasmic segment of PfEMP1 to the red blood cell membrane skeleton (Rug et al., 2006, Watermeyer et al., 2016, Crabb et al., 1997).

The RESA protein is released from dense granules into the parasitophorous vacuole during invasion and is then exported to the red blood cell cytoskeleton, where it associates with spectrin and modulates the host cell deformability properties (Silva et al., 2005, Mills et al., 2007). A similar route of entry to the host cell is taken by the RhopH2 and RhopH3 proteins, which are discharged from the rhoptries, then associate with the red blood cell cytoskeleton and are essential for generation of new permeability pathways (Counihan et al., 2017, Sherling et al., 2017). The MESA and PfEMP3 proteins are exported during the trophozoite stage of parasite development and bind to the cytoskeleton without (apparently) passing through the Maurer's clefts (Coppel et al., 1988, Pei et al., 2007).

The *Plasmodium* helical interspersed subtelomeric (PHIST) protein family consists of 89 proteins that are divided into the PHISTa, PHISTb and PHISTc subfamilies (Sargeant et al., 2006). Of this large protein family, only a few PHIST proteins have been studied in detail. A PHISTc protein (PF3D7_0936800) may interact with PfEMP1 at the parasite periphery although its export pathway has not yet been characterised (Mayer et al., 2012). The gametocyte-expressed protein GEXP05 is a member of the PHISTc family and is exported to the red blood cell cytoplasm where it remains as a predominately soluble protein (Tiburcio et al., 2015). At least one PHIST protein transits through the Maurer's clefts (PFE1605w, also known as LyMP) (Moreira et al., 2016, Oberli et al., 2014). The export of other PHIST proteins may follow a different pathway to the red blood cell cytoplasm or cytoskeleton, as is the case for the PHIST protein RESA.

1.7 The role of ring exported protein 1 in virulence protein trafficking

The ring exported protein 1 (REX1) is an 83 kDa protein expressed during the ring stage of the parasite (PlasmoDB: PF3D7_0935900) (Hawthorne et al., 2004, Hanssen et al., 2008a). The gene encoding REX1 has two exons separated by a short intron. In 3D7 parasites, the full length REX1 protein consists of 712 amino acids and has several features: a hydrophobic stretch, a predicted coiled-coil region and a variable repeat region.

A coiled-coil refers to a protein fold where two (or more) alpha helices are wound around each other, with non-polar residues populating the core of the coil (Burkhard et al., 2001). Coiled-coils have diverse functions, mediated by their roles in protein-protein interactions (Burkhard et al., 2001). The coiled-coil domain of REX1 is followed by the repeat region which contains two types of repeats. These repeating sequences in the 3D7 strain of *P. falciparum* are PQA EK DASKL TTTYDQTKEVK and PQA EK DALAKTENQNGELL. These sequences confer a high overall charge and net negative charge to the repeat region of REX1 (pI = 4.88). Different strains of *P. falciparum* have differing patterns, numbers and types of REX1 repeats.

After synthesis, the hydrophobic stretch of REX1 presumably functions as a recessed signal sequence and mediates entry of the protein into the lumen of the endoplasmic reticulum (Hawthorne et al., 2004). It is likely trafficked through the parasite endomembrane into the parasitophorous vacuole, presumably through a classical vesicle-mediated pathway (Heiber et al., 2013, Wickham et al., 2001). Interestingly, REX1 does not contain the PEXEL motif present in many exported proteins. Nonetheless, it was recently shown that disruption of the PTEX component HSP101 blocks export of REX1 from the PVM, suggesting that REX1 is exported through the PTEX translocon (Beck et al., 2014).

REX1 is first observed at the Maurer's clefts at around 2 hours post-invasion (Gruring et al., 2011, McMillan et al., 2013). The coiled-coil region of REX1 is thought to associate with the cytosolic surface of the Maurer's clefts, either directly through lipid-protein interactions, or indirectly via a protein-protein association with another Maurer's cleft resident (Dixon et al., 2008). The newly identified Maurer's clefts protein small exported membrane protein 1 (SEMP1) has been shown to be a potential interacting partner of

REX1, however a SEMP1 knockout had no observable phenotypic change including no change in REX1 localisation (Dietz et al., 2014).

Electron tomography of immunogold labelled REX1 in 3D7-infected RBCs permeabilised with equinatoxin II has shown that REX1 is more likely to be found on the edges of Maurer's clefts as opposed to the flattened regions (Hanssen et al., 2008a). Knockout studies of REX1 have shown that it plays a role in determining the morphology of Maurer's clefts; deletion of the gene leads to a stacked Maurer's cleft appearance (Hanssen et al., 2008a). In addition to regulating Maurer's cleft architecture, REX1 is also involved in the trafficking of PfEMP1 from the Maurer's clefts to the RBC surface. Deletion of the REX1 gene is associated with accumulation of PfEMP1 at stacked Maurer's clefts, and no surface PfEMP1 expression is detectable using a trypsin accessibility assay (Dixon et al., 2011). Complementation of the REX1 deletion parasites with an episomally maintained vector encoding REX1-cherry fluorescent protein resulted in partial restoration of PfEMP1 surface expression and CD36 binding (Dixon et al., 2011). The precise role that REX1 plays in the maintenance of the Maurer's clefts structure and the reason for its localisation to the edges of the Maurer's clefts is unclear, however, it is possible that the highly charged, low pI repeat region plays a role in shaping Maurer's cleft architecture through charge repulsion effects.

Ablation of the gene encoding REX1 was concomitant with loss of the region of chromosome 2 distal to and including the *kahrp* gene – a region predicted to contain ~20 genes (Dixon et al., 2011). Parasites expressing a REX1 construct that lacks the C-terminal half of the protein ($\Delta\text{Cterm}^{1-259}$) also underwent this concomitant truncation of chromosome 2 (Dixon et al., 2011). When a KAHRP-GFP fusion protein was expressed in ΔREX1 -infected parasites, the KAHRP-GFP was trafficked to the RBC cytoplasm where it formed large puncta, with no knob formation on the RBC membrane. However, in RBCs infected with $\Delta\text{Cterm}^{1-362}$ parasites, the KAHRP-GFP was trafficked to the erythrocyte membrane (Dixon et al., 2011).

Initial investigation of the roles of the C-terminal and repeat domains of REX1 in PfEMP1 trafficking have been undertaken using reverse genetics approaches (Dixon et al., 2011). The $\Delta\text{Cterm}^{1-362}$ parasites exhibited a stacked Maurer's cleft phenotype, despite localisation of the truncated protein at the Maurer's clefts. These parasites, where both

the REX1 repeat region and C-terminal was absent, showed decreased PfEMP1 surface expression and decreased ability to bind to CD36 (Dixon et al., 2011). Furthermore, RBCs infected with the $\Delta\text{Cterm}^{1-362}$ truncation line showed decreased recognition by serum from hyperimmune individuals. This suggests that REX1 plays a role in PfEMP1 trafficking, possibly release from the Maurer's clefts, loading into transport vesicles or trafficking of another protein important for the correct transport and display of PfEMP1 (Dixon et al., 2011).

1.8 Scope and aims of this study

The modifications that asexual stage *P. falciparum* parasites make to the host red blood cell are crucial for its survival *in vivo*. In particular, the Maurer's clefts are critical for delivery of parasite proteins such as PfEMP1 to the red blood cell membrane. The adhesin PfEMP1 is directly responsible for the relative virulence of *P. falciparum*, enabling parasitized red blood cells to bind to ligands in the brain (ICAM-1 and EPCR), placenta (CSA) and vascular endothelium throughout the body (CD36). By sequestering away from circulation, infected red blood cells avoid passage through and destruction in the spleen. Because of the significance of PfEMP1-mediated sequestration in malaria pathology, it is important to investigate the mechanisms of virulence protein trafficking in *P. falciparum*. The Maurer's clefts protein REX1 is required for efficient transport of PfEMP1 to the red blood cell membrane (Dixon et al., 2011). Previous work has shown that REX1 has a coiled-coil region that targets the protein to the Maurer's clefts, and that truncations at the beginning of the repeat region decrease PfEMP1 transport to the red blood cell surface (Dixon et al., 2008). In this study, we dissect the role of the repeat region of REX1 and define a section of the protein that controls Maurer's clefts architecture and influences PfEMP1 trafficking efficiency. A conditional knockdown of REX1 is generated and analysed to study the effect of decreased REX1 in knob-positive parasites.

Despite their central role in the virulence of *P. falciparum*, the Maurer's clefts and their resident proteins remain inadequately studied. A previous study has used mass spectrometry analysis of infected red blood cell ghosts to analyse the protein composition of the Maurer's clefts (Vincensini et al., 2005). Now more than 12 years later, we revisit the Maurer's clefts protein composition with improved enrichment and mass

spectrometry methods. In the present study, we develop a method to enrich the Maurer's clefts from 14 - 18 h post-invasion ring-stage infected red blood cells. In addition to the parasite-derived proteins, we identify a number of human proteins recruited to the Maurer's clefts. By epitope-tagging a number of Maurer's clefts proteins (both novel and established), we further define the composition of the sub-compartments within these organelles. Using epitope-tagged Maurer's clefts proteins, we investigate protein interaction networks at the Maurer's clefts and place this information within the context of the existing literature. We identify proteins that interact with PfEMP1 and describe these findings in the spatial environment of the Maurer's clefts. This study improves the current understanding of Maurer's clefts and the proteins that reside there. The data presented here provide a list of putative Maurer's clefts proteins as well as the protein-protein interactions and sub-compartmental location for several Maurer's clefts proteins.

Chapter 2 : Materials and Methods

2.1 Parasite culture

P. falciparum cultures were maintained according to previously described methods (Trager and Jensen, 1976). Parasites were cultured in type O+ blood (Australian Red Cross Blood Service) in RPMI 1640 with GlutaMAX and HEPES (Thermo Scientific) supplemented with 0.25% (w/v) AlbuMAX II (Gibco), 5% (v/v) pooled human serum (Australian Red Cross Blood Service), 10 mM glucose, 0.5 mM hypoxanthine and 42 μ M gentamicin. Wash media composed of RPMI 1640 with 10 mM glucose, 0.5 mM hypoxanthine and 42 μ M gentamicin was used for some applications. Cultures were maintained in a low-oxygen environment (1% O₂, 5% CO₂, 94% N₂) at 37°C. Parasitaemia was maintained between 1-7% and cultures were kept at 5% haematocrit. Parasitaemia was assessed by 10% (v/v) Giemsa-stained thin blood smears observed under a 100X oil immersion objective.

The wild type parasites used in this study are the 3D7 clonal line, originally cloned from the NF54 isolate obtained from a patient in the Netherlands (Ponnudurai et al., 1981, McLean et al., 1987). Transgenic parasites expressing the human dihydrofolate reductase (hDHFR) drug resistance cassette were maintained on 5 nM WR99210. A list of transfectant parasites used in this study is presented in

Table 1. For transfectant parasites also containing a skip peptide and Neomycin resistance cassette, integrants were selected by the addition of 400 µg/mL Geneticin® (Thermo Fisher Scientific).

2.1.1 Sorbitol synchronisation

Late stage asexual parasites can be selectively lysed by D-sorbitol, which is taken into the infected RBCs through new permeation pathways (NPPs). Ring stage parasites lack NPPs and are not affected by sorbitol treatment (Lambros and Vanderberg, 1979). Parasite cultures containing at least 2% rings were centrifuged at 400 g for 5 min. The supernatant was removed and the infected RBCs were resuspended in 5 times the pellet volume of 5% (w/v) D-sorbitol for 10 min at room temperature. The suspension was then centrifuged at 400 g for 5 min and the lysate was removed. The pellet, containing the uninfected and ring stage-infected RBCs, was returned to culture.

2.1.2 Gelatine selection of knob-positive infected red blood cells

Red blood cells infected with trophozoite stage parasites with knobs on the RBC surface can be enriched from culture by floatation in a solution gelatine (Pasvol et al., 1978). Parasite cultures were pelleted by centrifugation at 400 g for 5 min, and then resuspended in 20 times the pellet volume of 70% (v/v) Gelofusine® (Braun) in wash media in a 10 mL tube. The gelatine parasite suspension was incubated at 37°C for 45 min in a low oxygen environment. During incubation, the uninfected RBCs, ring stage and knob-negative infected RBCs settle to the bottom whilst knob-positive infected RBCs remain in the supernatant. The supernatant containing the knob-positive parasites was removed and centrifuged at 400 g for 5 min. The resulting parasite pellet was then returned to culture or used for experimentation.

2.1.3 Percoll enrichment of trophozoite stage parasite-infected red blood cells

Red blood cells infected with schizont and trophozoite stage parasites can be purified by density centrifugation on a Percoll cushion (Kramer et al., 1982). Parasite cultures were centrifuged at 400 g for 5 min and the pellet was resuspended in 3 mL wash media. The infected RBC suspension was layered onto a of 65% (v/v) Percoll® (GE Healthcare) cushion in PBS and centrifuged at 1870 g for 10 min. After centrifugation, the schizont and trophozoite-infected RBCs remained on top of the Percoll layer and the uninfected RBCs, ring- and early trophozoite-infected RBCs were in the pellet. The schizont- and trophozoite-infected RBCs were removed and washed in wash media before use in downstream applications.

2.1.4 Magnetic separation of haemozoin-containing trophozoites from parasite cultures

Red blood cells infected with trophozoites older than ~24 h post-invasion can be separated from uninfected RBCs and ring-stage-infected red blood cells by application of a magnetic field, due to the paramagnetism of the haemozoin crystal formed in the parasite digestive vacuole. Parasite cultures were centrifuged at 400 g for 5 min and the infected RBC pellet was resuspended in wash media. The infected RBCs were passed through a CS column (Miltenyi Biotec) in a VarioMACS™ magnet. A 21-gauge needle was affixed to the column to slow the passage of cells through the column. The haemozoin-containing trophozoite-infected red blood cells remained in a column in the presence of the magnetic field, whilst the uninfected and ring stage-infected RBCs flowed through. The column was washed with 20 mL wash media, then removed from the magnetic field and the trophozoite-infected red blood cells were eluted with 15 mL wash media. The purified trophozoites were then used for experimentation.

2.1.5 Tight synchronisation of parasite cultures

To obtain tightly synchronised parasites, parasite-infected red blood cells were first synchronised by Percoll purification (as previously described) of 60 mL of parasite culture containing schizonts (5% haematocrit and ~5% parasitaemia). The purified schizont-infected red blood cells were added to a petri dish containing 250 µL uninfected RBCs and 5 mL complete culture media. This dish was incubated for the desired synchronisation window on an orbital shaker at 37°C. The culture was then treated with sorbitol (as previously described) and returned to culture. For most applications, parasites were synchronised to within a 2 or 4 h window.

Table 1 Transfectant parasite lines used in study

Strain	Transfectant parasite line	Reference
3D7	REX1-GFP	(Hanssen et al., 2008a)
3D7	REX1 ¹⁻⁵⁷⁹	(McHugh et al., 2015)
3D7	REX1 ^{Δ371-579} -GFP	(McHugh et al., 2015)
3D7	REX1-HA-glmS	(McHugh et al., 2015)
3D7	MAHRP1-GFP	(Batinovic et al., 2017)
3D7	REX2-GFP	Emma McHugh
3D7	PTP5-GFP	(Batinovic et al., 2017)
3D7	PTP6-GFP	Emma McHugh
3D7	GEXP07-GFP	Emma McHugh
3D7	GEXP10-GFP	Emma McHugh
3D7	Pf11_0505-GFP	Emma McHugh
3D7	Pf13_0275-GFP	Emma McHugh
3D7	GEXP07-HA-glmS	Paul Gilson and Emma McHugh

2.1.6 Transfection of *P. falciparum* parasites

Parasite-infected RBCs were transfected as previously described (Deitsch et al., 2001) with 50-100 µg of plasmid DNA. Ring stage parasites were electroporated at 310V, 950 µF. After electroporation, parasites were returned to culture media in the presence of 5 nM WR99210. For parasites transfected with plasmids designed for single-crossover homologous recombination, parasites were cycled off (21 days) and on drug (14 days) to select for integrated parasites.

2.1.7 Knockdown of proteins using the *glmS* ribozyme

In this study, we made use of the *glmS* ribozyme/riboswitch protein knockdown system that has been previously used in *P. falciparum* (Prommana et al., 2013, McHugh et al., 2015). In this system, a *glmS* sequence is incorporated prior to the 3' UTR of the gene of interest. The *glmS* riboswitch is activated by the addition of glucosamine, which binds to the *glmS* riboswitch on the gene of interest mRNA and causes self-cleavage of the *glmS* ribozyme. The transcript is destabilised upon the removal of the poly-A tail and is degraded, causing a decrease in protein expression.

2.2 Analysis of infected RBC binding to recombinant human CD36 under constant flow conditions

Synchronised trophozoite stage parasites (2 - 4 h window) were resuspended in bicarbonate-free RPMI-HEPES (Thermo Fisher Scientific) at 3% parasitaemia and 1% haematocrit. A µ-Slide I flow chamber (ibidi) was coated with 125 µg/mL recombinant human CD36 (R&D Systems) in PBS and incubated overnight at 4°C. The chamber was blocked for 1 h at 37°C with 1% BSA (CSL Limited) in PBS then washed with bicarbonate-free RPMI-HEPES. The chamber was then placed in the DeltaVision DV Elite Restorative Widefield Deconvolution Imaging System (GE Healthcare). The parasite suspension was flowed through the chamber at 37°C at a rate of 190 µL/min for 5 min using a programmable syringe pump (Harvard Apparatus). The chamber was then washed for 10 min with bicarbonate-free RPMI-HEPES. The number of bound infected RBCs was counted for 10 pre-programmed fields of view using the 60X oil immersion objective (1.42 NA). Counts were performed under flow conditions.

2.3 Molecular biology

2.3.1 Genomic DNA extraction from infected RBCs

Genomic DNA was extracted from wild-type 3D7 parasites for use as a template for PCR. Parasite culture was centrifuged at 400 g for 5 min and the pellet was resuspended in 10 times pellet volume 0.03% (w/v) saponin on ice for 20 min. The saponin lysate was

centrifuged at 3000 g for 10 min at 4°C. The pellet containing the parasites was then washed twice in PBS. Genomic DNA was extracted from the parasite pellet using the Wizard SV genomic DNA purification system (Promega). The concentration of the genomic DNA was determined using a NanoDrop 2000 (Thermo Scientific).

2.3.2 Polymerase chain reaction (PCR) and PCR product preparation and analysis

Genes or gene fragments were amplified from purified 3D7 gDNA using Q5® High Fidelity DNA polymerase (New England BioLabs) or Phusion® High Fidelity DNA polymerase (New England BioLabs). Colony screens were performed using GoTaq® Green 2X Master Mix (Promega) or OneTaq® 2X Master Mix (New England BioLabs). Reactions were performed using a Veriti® Thermal Cycler (Applied Biosystems). Thermal cycler programs used for each polymerase are presented in Table 2. A full list of oligonucleotides used in this study is presented in Table 3. All PCR products were subjected to analysis as described in Section 2.3.6. Prior to subcloning, the PCR products from Phusion® or Q5® high-fidelity polymerases were poly-A-tailed by incubation with GoTaq® Green 2X Master Mix (Promega) for 15 min at 70°C.

Table 2 Thermal cycler conditions used for PCR

DNA Polymerase	Step	Temperature	Time
Q5®	Denaturation	98°C	3 min
	30 cycles	98°C	15 s
		45-65°C	30 s
		60-72°C	1-3 min
	Final extension	60-72°C	10 min
	Hold	10°C	∞
Phusion®	Denaturation	98°C	3 min
	30 cycles	98°C	15 s
		45-65°C	30 s
		60-72°C	1-3 min
	Final extension	60-72°C	10 min
	Hold	10°C	∞
OneTaq®	Denaturation	94°C	3 min
	30 cycles	94°C	15 s
		40-60°C	30 s
		60°C	1-3 min
	Final extension	60°C	10 min
	Hold	10°C	∞
GoTaq®	Denaturation	94°C	3 min
	30 cycles	94°C	15 s
		40-60°C	30 s
		60°C	1-3 min
	Final extension	60°C	10 min
	Hold	10°C	∞

Table 3 List of primers used in this study

Primer name	Cut site	Sequence
PTP6-FOR	Xho	5'-CTCGAGATGGTAGTGCTATATAATAATAAGG-3'
PTP6-REV	KpnI	5'-GGTACCGGACGTTTTAGTAACATTTG-3'
PTP5-FOR	Xho	5'-CTCGAGATGGAAAACATAATAAACAAG-3'
PTP5-REV	KpnI	5'-GGTACCTTTTAATTTCTTTTGAGATCTAC-3'
MAHRP1-FOR	XhoI	5'-CTCGAGATGGCAGAGCAAGCAG-3'
MAHRP1-REV	KpnI	5'-GGTACCATTATCTTTTTTTTCTTGTTCTAA-3'
GEXP07-FOR	Xho	5'-CTCGAGATGTCCTTTTGTTACGTTAGAAC-3'
GEXP07-REV	KpnI	5'-GGTACCAAATTAGAACTTGTTTAATGATTC-3'
GEXP10-FOR	Xho	5'-CTCGAGATGAACATTTATATTAGGACC-3'
GEXP10-REV	KpnI	5'-GGTACCTTGAAAATGTAATATTTGTCTTAAT-3'
PF11_0505-FOR	Xho	5'-CTCGAGATGGAAGCTGAGAAAAAG-3'
PF11_0505-REV	KpnI	5'-GGTACCTTTAAAGAACGTTACATAAAATG-3'
PF13_0275-FOR	Xho	5'-CTCGAGATGAAGACATAACAATTCTT-3'
PF13_0275-REV	KpnI	5'-GGTACCAGCTTCAACTACTTCTTC-3'

2.3.3 Subcloning

The A-tailed product was then ligated into pGEM®-Teasy vector (Promega) as described below. Ligated products were transformed into competent DH5α *E. coli* (Biolone) by heat shock at 42°C for 40 s, followed by 2 min incubation on ice. The transformed cells were then incubated at 37°C for 1 h in SOC media, before being spread on a 2YT agarose plate containing 100 µg/mL carbenicillin and incubated overnight at 37°C.

2.3.4 Ligation of DNA fragments into vectors

Ligation of DNA fragments into vectors was performed using T4 DNA ligase (Invitrogen) and T4 DNA ligase buffer (Invitrogen) according to the manufacturer's instructions. DNA ligation reactions contained 25 ng plasmid DNA and 3 molar equivalents of insert DNA. Reactions were incubated for 1-2 h at room temperature.

2.3.5 Restriction enzyme digestion of DNA

Restriction enzyme digestion of DNA was performed in 30 µL reactions. Plasmid DBA (1 µg) was digested for 2 h at 37°C with restriction enzymes listed in Table 3 with the appropriate buffer according to the manufacturer's instructions.

2.3.6 DNA analysis and purification after PCR and restriction enzyme digestion

DNA was run on 0.5-2% agarose gels containing SYBR® Safe DNA gel stain (Thermo Fisher Scientific) in TAE buffer at 100V for 30 min. The DNA fragments were then visualised using a LAS-3000 Imaging System (Fuji). A 1 kb DNA ladder (New England BioLabs) was used to determine digested DNA fragment size. For excision of enzyme-cleaved DNA fragments, gels were placed on a UV transilluminator and the required DNA digestion products were removed with a razor blade. Gel fragments were purified using the Wizard® SV Gel and PCR Clean-Up System (Promega) according to the manufacturer's instructions. The purity and concentration of the gel-extracted digestion products was determined using NanoDrop 2000 (Thermo Scientific).

2.4 Microscopy

2.4.1 Acetone and acetone/methanol fixation of infected red blood cells

Infected RBCs were washed in PBS and resuspended at 50% haematocrit in PBS. This suspension was smeared on a glass slide and allowed to air dry for a minimum of 2 h. The slide was then incubated in a solution of 90% acetone and 10% methanol at -20°C for 5 min, or in 100% acetone at room temperature for 10 min. Slides were dried for at least 1 h before a hydrophobic PAP pen (Sigma) was used to demarcate wells on the slide.

2.4.2 Glutaraldehyde/paraformaldehyde fixation of infected red blood cells

A coverslip was divided into 4 wells with a PAP pen and each well was coated with *Phaseolus vulgaris* agglutinin erythroagglutinin (PHA-E) (Sigma). Wells were washed in PBS and a suspension of infected RBCs (1% haematocrit) was added to each well and incubated for 15 min at room temperature. Excess cells were washed from the wells with PBS. A mixture of 4% formaldehyde and 0.0065% glutaraldehyde was added to each well for 20 min. The fixed cells were then washed three times in PBS, permeabilised with 0.1% Triton-X-100 for 10 min, then washed a further three times in PBS.

2.4.3 Addition of antibodies and microscopy of immunofluorescence assays (IFAs)

Infected red blood cell were prepared on slides as described in Sections 2.4.1 and 2.4.2. Primary antibodies were diluted in 3% (v/v) BSA in PBS and added to wells for 1 h at room temperature. A full list of antibodies used in this study can be found in Table 4. Primary antibodies were washed from the samples three times with PBS before the addition of the secondary antibody in 3% (v/v) BSA in PBS for 1 h. Samples were again washed three times in PBS, stained with DAPI (2 µg/mL) to visualise nuclei, then mounted with 5 mM PPD anti-fade (Sigma) in 90% glycerol. Coverslips were sealed to slides using nail polish and were stored at 4°C prior to imaging.

Imaging of IFAs was performed on a DeltaVision DV Elite Restorative Widefield Deconvolution Imaging System (GE Healthcare) using the 100X oil immersion objective (1.4NA). The fluorescent samples were excited by 390, 475, 542 or 632 nm LEDs and were imaged using band pass filters at 435, 523, 994 or 676 nm. Microscopy data was processed using Image J software (version 2.0.0). Z-stacks were imaged at 0.2 µm intervals and are presented as maximum projections. Images were cropped and adjustments were made to brightness and contrast. We used 3D structured illumination microscopy (3D-SIM), a super-resolution microscopy technique that enables an 8-fold increase in three dimensional resolution (Schermelleh et al., 2010). To achieve this, samples are illuminated with striped patterns in different orientations, and the resulting images are amalgamated by computer algorithms (Schermelleh et al., 2010). A DeltaVision OMX V4 Blaze (GE Healthcare) was used for 3D-SIM analysis.

Table 4 List of antibodies used for immunofluorescence microscopy

Antigen	Species	Dilution	Reference
REX1 (N-terminus)	rabbit	1:1000	(Dixon et al., 2008)
REX1 (repeat region)	rabbit	1:1000	(Hawthorne et al., 2004)
REX1 (C-terminus)	mouse	1:1000	(Dixon et al., 2008)
SBP1	rabbit	1:1000	(Cooke et al., 2006)
MAHRP1	mouse	1:300	(Spycher et al., 2003)
MAHRP2	rabbit	1:300	(Pachlatko et al., 2010)
PfEMP1 (ATS region)	mouse	1:100	(Maier et al., 2007)
PfEMP3	mouse	1:300	(Waterkeyn et al., 2000)
EXP2	rabbit	1:1000	(de Koning-Ward et al., 2009)
GFP	mouse	1:300	Roche
GFP	rabbit	1:300	(Humphries et al., 2005)
HA	mouse	1:300	Sigma
HA	rabbit	1:300	Sigma
KAHRP	rabbit	1:300	(Rug et al., 2006)

2.4.4 Live-cell fluorescence microscopy

For imaging of live parasites, 5 μ l of parasite culture was mounted on a coverslip and sealed on a slide using nail polish. Samples were imaged using the DeltaVision DV Elite Restorative Widefield Deconvolution Imaging System (GE Healthcare) using the 100X oil immersion objective (1.4NA). Longer-term live cell imaging was performed at 37°C in 8 well μ Slides (ibidi) with a thin layer of infected RBCs in RPMI coating the bottom of each well.

2.4.5 Immunolabelling of samples for electron microscopy

For electron microscopy, red blood cells infected with trophozoite stage parasites were purified from culture using Percoll (as described above) or magnetic separation (as described above) and washed twice in PBS. The purified infected RBCs were fixed in 1X pellet volume 2% formaldehyde, 0.0065% glutaraldehyde in PBS for 20 min at room temperature. The fixed cells were washed in PBS and permeabilised with 4 haemolytic units of equinatoxin II (EqII) for 6 min. After equinatoxin treatment, the cells were fixed again 2% formaldehyde, 0.0065% glutaraldehyde in PBS for 5 min at room temperature, then washed in PBS. The primary antibody, mouse anti-GFP (Roche), was diluted in 3% BSA (v/v) in PBS and 1X pellet volume was added to the sample for 2 h at room temperature. The sample was washed once in 3% BSA (v/v) PBS, then 1:20 Protein A 6 nm gold (Aurion) in PBS was added for 1 h. The sample was washed in 3% BSA (v/v) in PBS, then in PBS, then stored in 2% formaldehyde, 0.0065% glutaraldehyde in PBS.

2.4.6 Sample embedding, microtome sectioning and electron microscopy analysis

Prior to dehydration, cells were suspended in 1X pellet volume warmed 1% (w/v) agarose in PBS. The agarose block was divided in 1x1x1 mm cubes with a razor blade and the cubes were washed 5 times in PBS, waiting 10 min between each washing step. The samples were then stained with 2% (v/v) OsO₄ in H₂O for 1 h at room temperature. The samples were washed twice for 2 min in H₂O and were then dehydrated for 10 min each in an ethanol series of increasing concentrations in H₂O: 30%, 50%, 70%, 80%, 90%, then three times in 100% ethanol. Samples were then dehydrated in 50% ethanol and 50% acetone for 10 min, then transferred to 100% acetone for 10 min. An epoxy resin mixture containing 58% (v/v) dodecyl succinic anhydride (DDSA; ProSciTech), 26% (v/v) Procure (ProSciTech), and 16% (v/v) Araldite (ProSciTech) was prepared and was mixed on a rotating wheel for 2 h at room temperature, then incubated for 1 h at 60°C before use. The samples were infiltrated with 50% acetone and 50% epoxy resin mixture for 30

min at room temperature, then transferred to 100% resin for 1 h at 60°C. The resin was replaced twice at 12 h intervals and incubated at 60°C. A mixture of 2.74% benzyldimethylamine (BDMA) in the epoxy resin was prepared and incubated on a rotating wheel for 2 h at room temperature, then stood for 1 h at room temperature before use. The samples were transferred to the resin containing BDMA and were polymerised at 60°C for 48 h. The resin blocks were trimmed with a razor blade, and thin (70 nm) and thick (200 nm) sections were cut using a Leica UC7 ultramicrotome and placed on Formvar-coated 200h copper grids. Sections were stained with uranyl acetate and lead citrate before observation on a Tecnai Spirit or Tecnai F20 transmission electron microscope.

2.5 Enrichment of Maurer's clefts from ring-stage parasites

Parasites expressing REX1-GFP were synchronised to a 4 h window by Percoll purification and sorbitol lysis (Section 2.1.5). At 14-18 h post-invasion, a culture containing parasites at ~15% parasitaemia was harvested by centrifugation at 1800 g and washed in PBS. Infected red blood cells were lysed on ice with chilled hypotonic buffer (1 mM HEPES.NaOH, 1X Roche cOmplete EDTA-free protease inhibitor, pH 7.4). The lysed infected red blood cells were passaged through a 27-gauge needle 10 times and the solution was then made isotonic by the addition of a 4X assay buffer (200 mM HEPES-NaOH, 200mM NaCl, 8 mM EDTA, pH 7.4). The solution was centrifuged at 2500 g for 10 min at 4 °C, the supernatant was collected and centrifuged again at 2500 g for 10 min at 4 °C. The supernatant (containing the Maurer's clefts) was then pre-cleared with Pierce (TM) Protein A agarose beads (Thermo Scientific) for 30 min at 4 °C on a mixing wheel. The Protein A agarose beads were pelleted by centrifugation at 6000 g and the supernatant was transferred to a tube containing a 15 µL slurry (50:50) of GFP-Trap agarose beads (Chromotek) in PBS. The sample was incubated for 4 h at 4 °C on a mixing wheel. The beads were then collected and used for downstream applications.

2.6 Analysis of protein samples from *P. falciparum*

2.6.1 Preparation of saponin-lysed infected RBCs for SDS-PAGE

Infected RBCs were pelleted by centrifugation at 400 g for 5 min. Cell pellets were resuspended in 10 times pellet volume of 0.03% (w/v) saponin in PBS on ice for 20 min. The saponin lysate was centrifuged at 16,000 g for 10 min at 4°C and the resulting parasite

pellet was washed twice in PBS. The pellet was then resuspended in LDS Sample Buffer (Thermo Fisher Scientific) and 50 mM DTT and heated to 90°C for 10 min prior to gel electrophoresis.

2.6.2 SDS-PAGE, immunoblotting and membrane stripping

Samples were loaded on a 4-12% Bis-Tris polyacrylamide gels (Life Technologies) and were run in 3-(N-morpholino)propanesulfonic acid (MOPS) running buffer in water at 200V for 32 min. The SeeBlue Plus2® protein standard (Thermo Fisher Scientific) was used to estimate protein molecular weight. For separation of higher molecular weight proteins (>150 kDa), samples were run on 3-8% Tris-Acetate polyacrylamide gels (Life Technologies) in NuPAGE® Tris-Acetate SDS Running Buffer. The HiMark™ prestained protein standard was used for molecular weight estimation.

After SDS-PAGE, proteins were transferred from the gel to a nitrocellulose membrane using an iBlot® Transfer Stack (Novex) and the iBlot® Dry Blotting System (Novex). The nitrocellulose membranes were blocked in 3% (w/v) skim milk in PBS for 1 h at room temperature and then incubated with primary antibody diluted in 3% (w/v) skim milk in PBS overnight at 4°C. A complete list of antibodies used for immunoblotting is presented in Table 5. The membrane was washed three times for 10 min with 0.05% Tween-20 in PBS. The membrane was then incubated for 1 h at room temperature with the secondary antibody diluted in 3% (w/v) skim milk in PBS. The membrane was washed again three times with 0.05% Tween-20 in PBS and then in PBS before the addition of Clarity™ ECL western blotting substrate (BioRad). The membrane chemiluminescence was visualised using a LAS-3000 Imaging System (Fuji).

Western blotting membranes were stripped of antibodies prior to being reprobed with a different primary antibody. Nitrocellulose membranes were incubated in a hot (>90°C) 100 mM glycine (pH = 2) on an orbital shaker. The glycine solution was replaced every 10 min a total of 4 times. The membrane was then washed in 0.05% Tween20 in PBS for 10 min, then blocked in 3.5% (w/v) skim milk in PBS before the addition of primary antibody.

Table 5 List of antibodies used for immunoblotting

	Antigen	Species	Dilution	Reference
	REX1 (N-terminus)	rabbit	1:1000	(Dixon et al., 2008)
	GADPH	rabbit	1:1000	
	GFP	mouse	1:1000	Roche
	HA	mouse	1:1000	Sigma
	HA	rabbit	1:1000	Sigma
	Spectrin (human)	mouse	1:1000	
	EXP1	mouse	1:1000	
	MAHRP1	mouse	1:1000	(Spycher et al., 2003)
	PfEMP1 (ATS)	mouse	1:200	(Maier et al., 2007)
HRP-conjugated secondaries	mouse IgG (H+L)	goat	1:25,000	Promega
	rabbit IgG (H+L)	goat	1:25,000	Promega

2.6.3 Trypsin digestion of surface-exposed PfEMP1

Trypsin cleavage of PfEMP1 exposed on the surface of infected RBCs was used to assess relative efficiency of PfEMP1 trafficking across transfectant parasite lines. Red blood cells infected with trophozoite stage parasites were harvested by Percoll or magnet purification as described above. Three tubes were prepared to a volume of 200 μ L: PBS alone (P), 1 mg/mL TPCK-treated trypsin (Sigma) in PBS, and 1 mg/mL TPCK-treated trypsin in PBS with 4 mg/mL soybean trypsin inhibitor (Sigma) (I). The intact parasite-infected red blood cells (10 μ L) were added to each of the P, T and I reactions and were incubated at 37°C for 1 h. Soybean trypsin inhibitor was added to the P and T tubes to a final concentration of 4 mg/mL and incubated at room temperature for 15 min. Samples were centrifuged for 5 min and the resulting pellets were resuspended in 1% Triton X-100 with protease inhibitor (Roche) in PBS and incubated on ice for 20 min. Lysates were centrifuged at 16,000 g at 4°C for 10 min. The pellet was washed in 1% Triton X-100 with 1X protease inhibitor (Roche) in PBS. The Triton X-100-insoluble pellet was then resuspended in 2% SDS in PBS with protease inhibitor and incubated on a mixing wheel at room temperature for 20 min. The sample was centrifuged for 10 min at 16,000 g and the supernatant was subjected to SDS-PAGE and immunoblotting as described in Section 2.6.2.

2.6.4 Protease treatment of enriched Maurer's clefts

Enriched Maurer's clefts from REX1-GFP-infected red blood cells (Section 2.5) and a 3D7 control sample were treated with either PBS, PBS and proteinase K (1 mg/mL) or saponin in PBS (0.03% w/v) and proteinase K (1 mg/mL) for 15 min. Samples were subjected to SDS-PAGE and immunoblotting (Section 2.6.2). When the Maurer's clefts membrane integrity is compromised, protease digestion will result in the production characteristic SBP1 fragment (Blisnick et al., 2000). Membranes were probed with α BR5, an antibody recognising this SBP1 fragment.

2.6.5 Co-immunoprecipitation

Trophozoite-infected red blood cells (24 - 30 h post-invasion) were purified from 60 mL of parasite culture (~8% parasitaemia, 5% haematocrit) by either magnetic separation or Percoll purification (Section 2.1.3 or 2.1.4). Purified trophozoite-infected RBCs were washed twice in PBS, then solubilised on ice for 30 min with immunoprecipitation buffer

containing 1% Triton X-100 in 50 mM Tris-HCl, 150 mM NaCl, 2 mM EDTA and cOmplete™ EDTA-free Protease Inhibitor Cocktail (Roche). The lysate was centrifuged at 13000 16,000g for 10 min at 4°C. The supernatant was removed and placed in a clean tube and centrifuged again at 16,000 g for 5 min at 4°C to pellet any remaining Triton X-100-insoluble material. A 50 µL slurry (50:50) of Pierce™ Protein A Agarose (Thermo Fisher Scientific) was washed twice in PBS. The supernatant, containing the Triton X-100 soluble fraction, was incubated with washed Protein A agarose beads for 30 min at 4°C on a rotating wheel. A 25 µL slurry of GFP-Trap® agarose beads was washed twice in PBS and added to the pre-cleared Triton X-100 soluble material for 4 h or overnight at 4°C on a rotating wheel. The GFP-Trap® beads were pelleted by centrifugation at 6000 g for 2 min at 4°C and were washed 5 times in immunoprecipitation buffer. For western blotting, the beads were resuspended in LDS Sample Buffer (Thermo Fisher Scientific) containing 50 mM DTT and heated to 90°C for 10 min prior to SDS-PAGE. For mass spectrometry, the beads were washed a further two times in 1 mM Tris-HCl.

2.6.6 Mass spectrometric analysis of Maurer's clefts and co-immunoprecipitations

Samples were prepared for mass spectrometric analysis as previously described (Batinovic et al., 2017). Proteins were eluted from GFP-Trap beads by the addition of 20% (v/v) trifluoroethanol in formic acid (0.1%, pH 2.4) and incubation at 50 °C for 5 min. The eluate was reduced with 5 mM TCEP (Thermo Fischer Scientific) and neutralised with TEAB (tetraethylammonium bicarbonate). Samples were digested with trypsin (Sigma) overnight at 37 °C.

Samples were analysed by ESI LC-MS/MS on a Orbitrap Elite (purified Maurer's clefts) or a Q Exactive (co-immunoprecipitations) mass spectrometer. Mass spectra (ProteoWizard) were searched against a custom database containing the *Plasmodium falciparum* 3D7 and UniProt human proteomes. Searches were performed on MASCOT (Matrix Science), with the following parameters: precursor ion mass tolerance of 10 ppm, fragment ion mass tolerance of 0.2 Da, trypsin as the cleavage enzyme, three allowed missed cleavages and allowing for oxidation.

Chapter 3 : A repeat sequence domain of the ring-export protein-1 of *Plasmodium falciparum* controls export machinery architecture and virulence protein trafficking

3.1 Foreword

This chapter is an edited, reformatted replication of the manuscript entitled: **A repeat sequence domain of the ring-export protein-1 of *Plasmodium falciparum* controls export machinery architecture and virulence protein trafficking.**

Emma McHugh, Steven Batinovic, Eric Hanssen, Paul J. McMillan, Shannon Kenny, Michael D. W. Griffin, Simon Crawford, Katharine R. Trenholme, Donald L. Gardiner, Matthew W. A. Dixon and Leann Tilley

Molecular Microbiology. (2015) 98(6): 1101-14.

All contributions made by the authors of this manuscript have been duly acknowledged in the Preface of this thesis.

3.2 Introduction

Despite enormous efforts, malaria remains a disease of global significance. Annually about 600,000 deaths are attributed to infection with *Plasmodium falciparum* (WHO, 2014, Murray et al., 2012). The particular virulence of *P. falciparum* is due, in part, to the cytoadherence of infected red blood cells (RBCs) to the walls of post-venule capillaries. Mediated by a protein called *P. falciparum* erythrocyte membrane protein-1 (PfEMP1) (Scherf et al., 2008, Baruch et al., 1995), cytoadherence enables *P. falciparum* to avoid splenic clearance, thus permitting a more rapid multiplication rate. An exacerbated inflammatory response to the sequestered parasites is involved in precipitating severe complications, such as coma and under-weight births (White et al., 2013, Beeson et al., 2001, Turner et al., 2013).

Because mature human RBCs lack the machinery for protein synthesis and trafficking, export of Plasmodium virulence proteins requires the assembly of a parasite-derived exomembrane system in the host RBC cytoplasm. For example, PfEMP1, an integral membrane protein, is secreted through the parasite's endomembrane system, and exported across the parasitophorous vacuole membrane (PVM) in which the parasite resides (Maier et al., 2009). It is trafficked to compartments known as the Maurer's clefts, and then transferred to the RBC membrane, where it is assembled into knobs (Voigt et al., 2000). Despite its importance, much remains unclear about the trafficking, sorting and fusion machinery that mediates delivery of PfEMP1 to the RBC surface.

The term Maurer's *cleft* is, in fact, a misnomer as these parasite-derived structures are flattened cisternae, with no direct opening onto the RBC surface. In the 3D7 strain, they number ~15 per cell, and are roughly disc-shaped, with a diameter of ~500 nm and a thickness of ~40 nm (Hanssen et al., 2008b). They are connected to the RBC membrane via direct cytoskeletal interactions (Cyrklaff et al., 2011) and via distinct tether-like structures (tubes of about ~25 nm by ~200 nm) (Pachlatko et al., 2010, Hanssen et al., 2010). The Maurer's clefts are thought to function as a sorting compartment; some exported proteins transiently associate with the Maurer's clefts *en route* to the RBC cytoskeleton or membrane, while some remain as resident proteins. Resident proteins play important roles in the PfEMP1 trafficking process; and proteins such as the ring exported protein-1 (REX1) (Dixon et al., 2011), the skeleton-binding protein-1 (SBP1) (Maier et al., 2007, Cooke et al., 2006), the membrane-associated histidine-rich protein-1 (MAHRP1) (Spycher et al., 2008), PfEMP1 trafficking protein 1 (PfPTP1) (Rug et al., 2014) and *P. falciparum* antigen 332 (Glenister et al., 2009) have been shown to be essential for efficient delivery of PfEMP1 to the RBC surface.

REX1 is a peripheral membrane protein that is exported to the RBC cytoplasm in the very early ring stage of infection (~2 h p.i.) (McMillan et al., 2013), where it associates with a population of already formed Maurer's clefts (Gruring et al., 2012). This 712 amino acid protein possesses a recessed hydrophobic signal sequence (residues 37 – 58), a predicted coiled-coil region (residues 181 – 361), a highly charged repetitive sequence region (residues 362-579) and a C-terminal region (residues 580-712) (Figure 3.2). It has no predicted Plasmodium Export Element (PEXEL) and is thus considered to be a PEXEL-Negative Exported Protein (PNEP) (Gruring et al., 2012, Spielmann and Gilberger, 2010).

Previously we have shown that attachment of REX1 to the Maurer's clefts is mediated by a sequence within the predicted coiled-coil domain (Dixon et al., 2008). Interestingly, targeted truncation of REX1 leads to an altered Maurer's cleft architecture and a significant decrease in PfEMP1 surface exposure (Dixon et al., 2011, Hanssen et al., 2008a). However, complete genetic disruption of REX1 was found to be associated with concomitant deletion of the sub-telomeric region of chromosome 2, with resultant loss of the genes for a number of exported proteins, including the knob-associated histidine-rich protein (KAHRP). KAHRP forms the main structural component of the knobs at the infected RBC surface in which PfEMP1 is concentrated (Horrocks et al., 2005) and

promotes PfEMP1 presentation (Crabb et al., 1997). This makes it difficult to distinguish the direct effect of REX1 on PfEMP1 trafficking from an indirect effect due to the loss of knobs and other deleted chromosome 2 genes.

In this work, we have used the inducible ribozyme system (Prommana et al., 2013) to genetically attenuate the expression of REX1 and show that Maurer's cleft architecture changes can be achieved, independent of loss of the *kahrp* locus. We have mapped the key domain within REX1 that controls cleft architecture and forward trafficking of PfEMP1. That is, we show that removal of the repeat sequence region (residues 362-579) results in the formation of giant stacked Maurer's clefts. This is associated with significant loss of PfEMP1 surface delivery and decreased adhesion of infected RBCs. Using sophisticated prediction methods, we gain some insights into the physical nature of REX1 and its role in Maurer's clefts sculpting.

3.2.1 Plasmid constructs and *P. falciparum* transfection

The genomic region of REX1 corresponding to amino acids 1-579 was PCR-amplified from 3D7 gDNA using the REX1⁵⁷⁹fw (**cctaggtgccaactcgaaacttctgc**) and REX1⁵⁷⁹rv (**atcgatatcttttcagcttgagtaag**) primers (*AvrII* and *Clal* in bold). The resultant PCR products were directionally cloned into pHH1-DEST to get pHH1-REX1¹⁻⁵⁷⁹. The gene sequence used to generate the REX³⁷¹⁻⁵⁷⁹ parasites was synthesized by GeneScript™. This sequence contained *BamHI* and *PstI* sites at the 5' and 3' ends of the gene allowing directional cloning into the pEntry-GFP gateway compatible vector (Invitrogen). The pEntry-REX³⁷¹⁻⁵⁷⁹-GFP vector was recombined with the Gateway compatible Destination vector, pHH1-DEST, to yield the final transfection plasmid pHH1-REX³⁷¹⁻⁵⁷⁹.

The riboswitch-inducible knockdown construct was made by PCR amplifying the 3' region of REX1 with the REX1-glmS-fw (**ggatcctgccaactcgaaacttctgc**) and REX1-glmS-rv (**ctgcagattaaatacagaactttctag**) primers (*BamHI* and *PstI* in bold). This PCR product was directionally cloned into the pGLMS-HA plasmid (Elsworth et al., 2014) to get the pGLMS-REX1-HA construct. Transfections were performed as previously described (Deitsch et al., 2001).

3.2.2 Fluorescence microscopy

Fluorescence microscopy was performed on either paraformaldehyde/ glutaraldehyde (4%/0.0065%) or acetone-fixed thin blood smears as previously described (Spielmann et al., 2006). The following primary antibodies were used: anti-REX1 (rabbit, 1:2000) (Hawthorne et al., 2004), anti-REX1_N-term (mouse, 1:1000) (Hanssen et al., 2008a), anti-GFP (monoclonal antibody, Roche, 1:500), anti-GFP (rabbit, 1:1000) (Humphries et al., 2005), anti-SBP1 (rabbit, 1:2000) (Cooke et al., 2006), anti-MAHRP2 (rabbit, 1:200) (Pachlatko et al., 2010), anti-PfEMP1 ATS (mAb 1B/98-6H1-1, 1:100) (Adisa et al., 2007), anti-KAHRP (mouse, 1:200) and anti-PfEMP3 (mouse, 1:200) (Waterkeyn et al., 2000). Nuclei were visualized by addition of DAPI (1 µg ml⁻¹).

Samples were viewed on a DeltaVision DV Elite Restorative Widefield Deconvolution Imaging System (GE Healthcare/Applied Precision) using a 100X objective (1.4NA). Samples were excited by 390, 475, 542 or 632 nm LEDs and imaged using band pass filters at 435, 523, 994 or 676 nm. Images are presented as projections of whole cell z-stacks (taken at intervals of 0.2 µm) unless otherwise stated.

Structured Illumination Microscopy (Schermelleh et al., 2008) was performed on a

DeltaVision OMX V4 Blaze (GE Healthcare/Applied Precision). Samples were excited using 488, 568 or 642 nm lasers and imaged using band pass filters at 528, 608 and 683 nm with a 60X objective (1.42 NA). Images were processed using the SoftWorx imaging software (Applied Precision) or ImageJ software (NIH).

3.2.3 Immunoblotting

Trophozoite stage parasites were enriched from culture by magnetic separation or Percoll purification as previously described (Dixon et al., 2011). Purified cells were lysed with 0.03% saponin and fractionated into supernatant and pellet fractions as previously described (Dixon et al., 2008). Protein samples were adjusted for equal loading, mixed with 6x SDS loading dye and separated on 4-12% Bis-Tris gels (Life Technologies). Gels were transferred to nitrocellulose membranes and blocked for 1 h in 3.5% skim milk in PBS. The following primary antibodies were used in these study: anti-REX1 (rabbit, 1:2000) (Hawthorne et al., 2004b), anti-REX1 (mouse, 1:1000) (Hanssen et al., 2008a), anti-GFP (mAb, Roche; 1:500), anti-GFP (rabbit, 1:1000) (Humphries et al., 2005) and anti-GAPDH (rabbit, 1:1000). Anti-mouse or anti-rabbit horseradish peroxidase-conjugated secondary antibodies (1:25000, Promega) were incubated with the membranes for 1 h at room temperature. All membranes were washed 3 times for 10 min with 0.1% Tween-20 in PBS, following antibody incubations. Washed membranes were incubated with Clarity ECL reagents (Bio-Rad) and visualized on a Las3000 Imager (Fujifilm).

3.2.4 CD36 binding assays and PfEMP1 variant up-selection

Up-selection of parasites on immobilized CD36 was employed prior to binding experiments to maximize surface expression of PfEMP1. Recombinant human CD36 (125 $\mu\text{g ml}^{-1}$ in PBS) was immobilized on plastic petri dishes (Spycher et al., 2008). Dishes were blocked with 1% BSA in PBS and washed with RPMI-HEPES. Infected RBCs (1% haematocrit, 3% parasitaemia) in RPMI-HEPES were added and incubated for 1 h at 37°C. Unbound cells were gently washed from the dish with RPMI-HEPES. Fresh culture media and RBCs were added to the dish and cultures were maintained as described above.

Binding assays under constant flow conditions were performed in culture chambers (iBIDI μ -Slide I) loaded with recombinant human CD36 (125 $\mu\text{g ml}^{-1}$ in PBS) and incubated overnight at 4°C. Prior to use the chambers were blocked in 1% BSA in PBS

for 1 h at 37°C. Binding assays were performed on trophozoites >24 h post-invasion, synchronized to a 6-8 h window. Parasites (1% haematocrit, 3% parasitaemia) were resuspended in bicarbonate-free RPMI-HEPES and flowed through the chambers at 0.1 Pa using a programmable Harvard Elite 11 Syringe Pump. All assays were performed at 37°C and were visualized on a DeltaVision DV Elite Restorative Widefield Deconvolution Imaging System (Applied Precision) using a 60X objective. Parasites were flowed through the chamber for 5 min, prior to washing chamber for 5 min in bicarbonate-free RPMI-HEPES under constant flow conditions. The number of bound cells per field was counted for 10 randomly chosen fields.

3.3 Results

3.3.1 Knockdown of REX1 expression is associated with Maurer's cleft reorganization without loss of KAHRP

Genes with important functions in the asexual blood stage are difficult to study using conventional gene disruption strategies due to the haploid nature of the *P. falciparum* genome. Recently, methods have been introduced to target genes by incorporating a glucosamine-6-phosphate-activated ribozyme (*glmS*) into their 3' untranslated region (Figure 3.1 Schematic representation of strategy used to generate transfected parasites) (Prommana et al., 2013). In the presence of the cofactor glucosamine-6-phosphate, the *glmS* ribozyme degrades the mRNA encoding the targeted gene thereby reducing its expression.

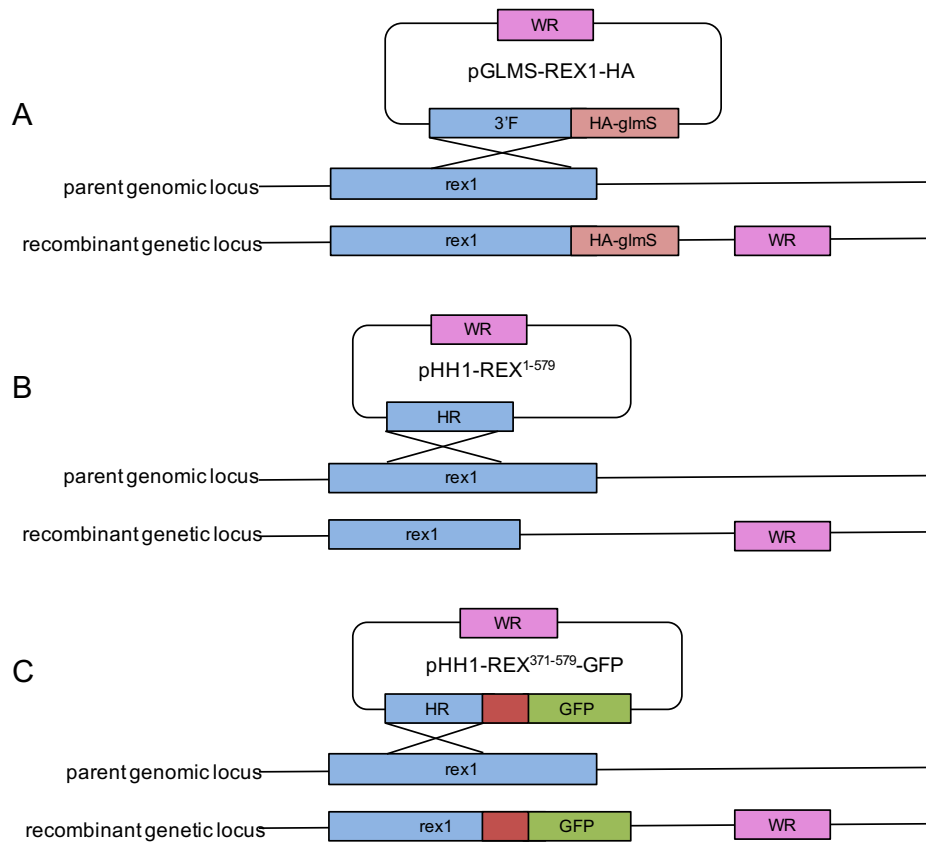


Figure 3.1 Schematic representation of strategy used to generate transfected parasites

- (A) REX1-HA-glmS, 3'F = 3' flank
- (B) REX1¹⁻⁵⁷⁹, HR = homologous region
- (C) REX1^(Δ371-579)- GFP

The glucosamine (GlcN)-inducible *gImS* ribozyme and a 3 x HA tag (Figure 3.2) were incorporated into the 3' untranslated region of the REX1 gene by homologous recombination. PCR and DNA sequencing confirmed correct integration of the *gImS* plasmid. Treatment of ring stage REX1-KD parasites with 2.5 mM GlcN (which is converted to glucosamine-6-phosphate) for 20 h, resulted in efficient (>90%) REX1 knockdown, as quantitated by loss of the HA-tagged REX1 (Figure 3.5A). By contrast, the level of a control protein, *PfGAPDH*, remained unchanged. This indicates that the decline in the REX1 level was not caused by defective or aborted development of parasites. Indeed, parasite growth was not affected by the significantly decreased expression of REX1; when monitored over a period of 48 h in the presence of 2.5 mM GlcN, no growth defect was observed in either 3D7 or REX1-KD parasites compared to untreated parasites. Parasitaemia levels were 106% of the controls, in both cases (Fig. Figure 3.3).

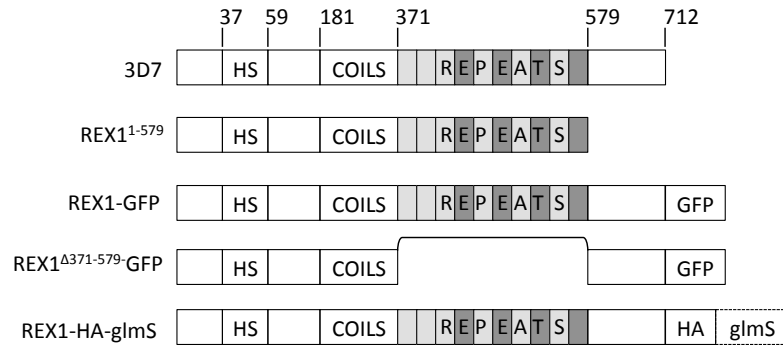


Figure 3.2 Schematics of REX1 and REX1 mutants

Full length 3D7 REX1 features a recessed hydrophobic signal sequence (HS), a predicted coiled-coil region and a repeat region. In REX1¹⁻⁵⁷⁹ transfectants the C-terminal region is deleted. REX1-GFP and REX1^(Δ371-579)-GFP transfectants express REX1 with a C-terminal GFP tag, with and without the repeat region. REX1_KD transfectants have a 3xHA tag and *glmS* sequence integration into the 3' untranslated region.

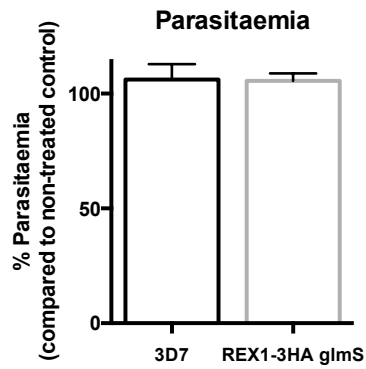


Figure 3.3 Analysis of the growth of 3D7 and REX1-KD parasites in the presence and absence of GlcN

Parasites were synchronized to a 2 h window and were treated, or not, with GlcN at 24 h post-invasion. 48 h later the infected RBCs were labelled with SYTO61 and parasitaemia levels were determined using flow cytometry. Results are presented as a percentage of untreated control + S.D.

Maurer's clefts can be observed by immunofluorescence microscopy following labelling with antibodies recognizing resident proteins such as MAHRP1 and SBP1 (Figure 3.4D; Figure 3.5B, D). In the absence of GlcN, we observed 16 ± 3 REX1-HA and SBP1-positive puncta in the REX1-KD parasites (Figure 3.5C), which is equivalent to the number found in wildtype 3D7 (see Figure 3.6C). These puncta correspond to individual Maurer's cleft cisternae that have a distributed organization within the RBC cytoplasm (Hanssen et al., 2008a).

Upon exposure to 2.5 mM GlcN, the REX1-KD parasites exhibited a decreased number (4 ± 1) of SBP1-positive puncta (Figure 3.5C; Figure 3.4D) indicating reorganization of Maurer's cleft architecture. Treatment of 3D7 parasites with 2.5 mM GlcN did not affect the number of Maurer's clefts puncta (data not shown). Deletion of the *rex1* gene has been reported to be associated with concomitant disruption of the chromosome 2 locus, which contains genes encoding KAHRP and other proteins such as *P. falciparum* Erythrocyte Membrane Proteins-3 (PfEMP3) (Dixon et al., 2011). Interestingly the GlcN-treated REX1-KD parasites retained expression of KAHRP (Figure 3.5D) and PfEMP3 (Figure 3.4C), indicating that Maurer's cleft restructuring can occur even in the presence of an intact chromosome 2 locus, and that reduction of REX1 levels does not affect the trafficking of these proteins to the RBC periphery.

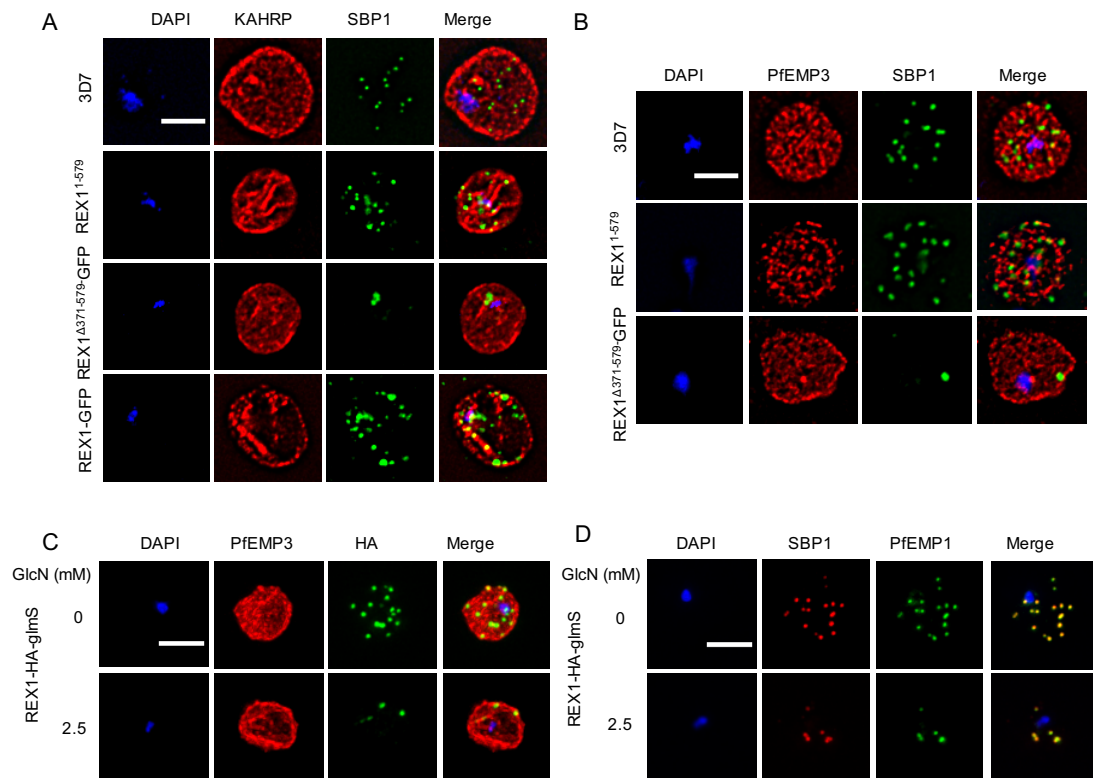


Figure 3.4 Immunofluorescence microscopy of KAHRP, PfEMP3 and PfEMP1.

(A, B) Acetone-fixed infected red blood cells probed with α KAHRP1, α SBP1 and α PfEMP3

(C, D) Paraformaldehyde-fixed infected red blood cells probed with α PfEMP3, α HA, α ATS or α SBP1.

Nuclei are stained with DAPI (blue). Scale bar = 3 μ m.

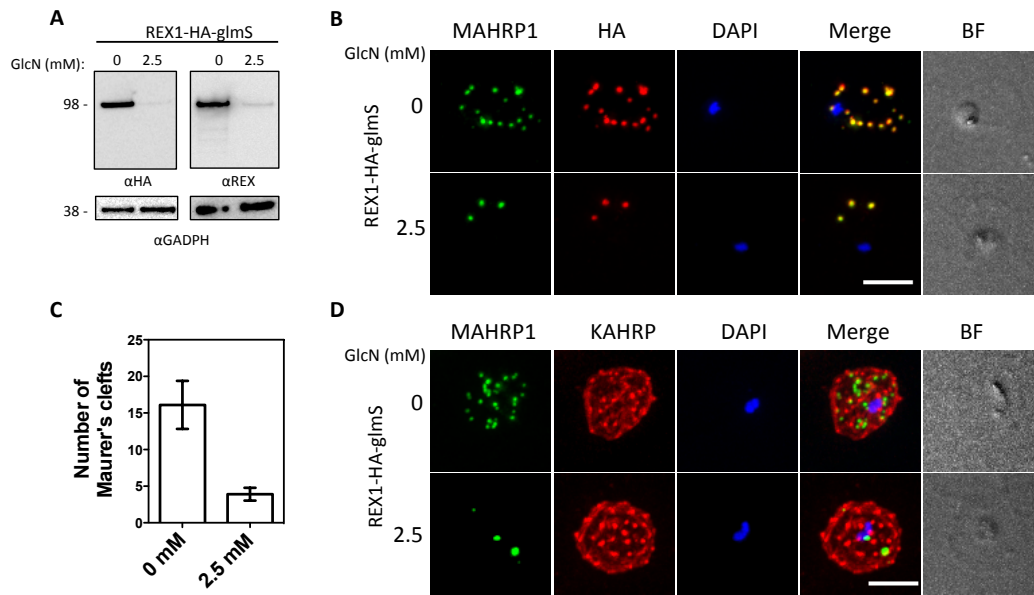


Figure 3.5 Inducible knockdown of REX1 using the glmS ribozyme system decreases the number of Maurer's cleft puncta

(A) Western blots confirming knockdown of expression of REX1 in REX1_KD transfectants probed with anti-HA and anti-REX1.

(B, D) Immunofluorescence microscopy of paraformaldehyde-fixed infected RBCs probed with Maurer's cleft marker anti-MAHRP1 (green) and anti-HA or anti-KAHRP (red). Nuclei are stained with DAPI (blue). Scale bar = 3 μ m.

(C) Quantitation of numbers of Maurer's clefts produced by REX1_KD transfectants in the presence and absence of 2.5 mM GlcN. The mean number of Maurer's clefts produced per singly nucleated infected RBC was determined by counting SBP1-labelled puncta in at least 10 cells. Error bars = S.D.

3.3.2 The repeat region of REX1 is involved in Maurer's cleft sculpting

In an effort to identify the region within REX1 that is responsible for maintaining normal Maurer's cleft architecture, we targeted the locus to modify the REX1 sequence. We found that removal of the C-terminal half of the REX1 protein, using an integration strategy (REX1¹⁻³⁶²) (see (Dixon et al., 2011); Figure 3.1 Schematic representation of strategy used to generate transfected parasites) is associated with a dramatic decrease in the number (3 ± 0.2) of SBP1-positive puncta (Figure 3.6A,C), similar to that observed with REX1 knock-down parasites. We next generated parasites in which REX1 is truncated at residue 579 (REX1¹⁻⁵⁷⁹; Figure 3.2) and used Western analysis to show that a protein of approximately 70 kDa was expressed (Figure 3.6B, left panel). These parasites exhibit 12 ± 3 SBP1-labelled puncta (Figure 3.6A, C), a Maurer's cleft profile that more closely resembles wildtype 3D7 ($p = 0.54$, unpaired t-test). This indicates that the region between amino acids 363 and 579 carries the major determinant that controls Maurer's cleft architecture.

To further investigate this we generated a REX1 construct in which the repeat sequence domain (371 – 579) was deleted (REX1^{Δ371-579}-GFP; Figure 3.2). For this transfectant, we used a GFP-tagged REX1 construct, to facilitate downstream characterization, and compared the mutants with transfectants expressing full-length REX1-GFP and with wild type 3D7. Western analysis confirms that full-length REX1-GFP migrates with an apparent molecular mass of 120 kDa as expected for the chimera, while the REX1^{Δ371-579}-GFP migrates with the expected molecular mass of 87 kDa (Figure 3.6B, right panel).

Immunofluorescence microscopy reveals that full-length REX1-GFP is correctly localized at the Maurer's clefts (Figure 3.6A) and that these transfectants exhibit an average number of puncta equivalent to that of the 3D7 parent (13 ± 2 ; $p = 0.59$, unpaired t-test; Figure 3.6C). By contrast, the REX1^{Δ371-579}-GFP parasites exhibited a striking Maurer's cleft phenotype, with only 2 ± 0.3 punctate structures observed in the infected RBC cytoplasm (Figure 3.6A, C). This is much less than in wildtype 3D7 and the REX1-GFP line (unpaired t-test, $p < 0.0001$) and even less than the number observed in the REX1 knockdown parasites. These structures were still labelled with SBP1, but appeared larger than the puncta in wildtype parasites.

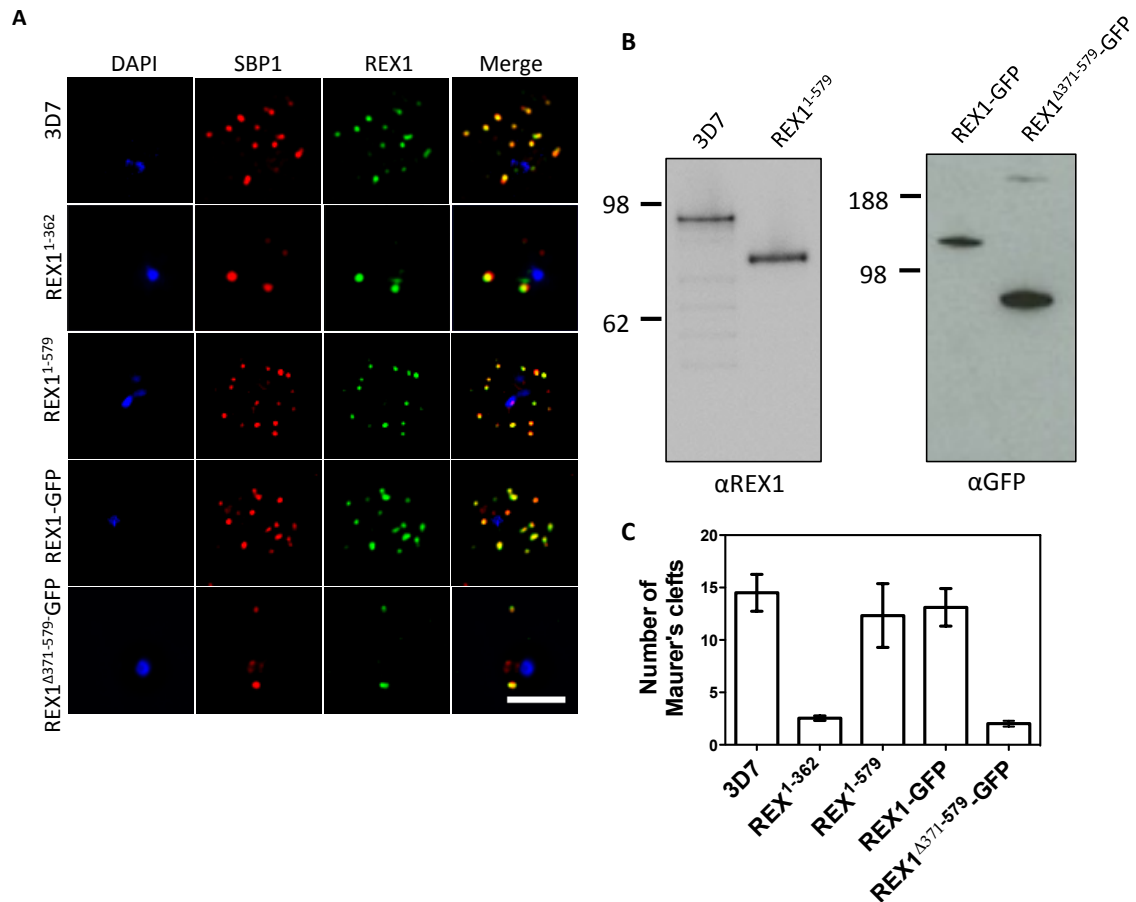


Figure 3.6 Deletion of the repeat region of REX1 decreases the number of Maurer's cleft puncta

(A) Immunofluorescence microscopy of acetone-fixed infected RBCs probed with anti-SBP1 (red) and anti-REX1 (green). Nuclei are stained with DAPI (blue). Scale bar = 3 μ m.

(B) Western blots confirming expression of REX1 in wildtype 3D7 and truncated REX1¹⁻⁵⁷⁹ (probed with anti-REX1), and REX1-GFP and REX1^(Δ 371-579)-GFP chimeras (probed with anti-GFP).

(C) Quantitation of numbers of Maurer's clefts produced by 3D7 and different REX1 transfectants in singly nucleated infected RBCs. Error bars = SD.

We performed immunofluorescence microscopy to determine if deletion of the REX1 repeat domain affected the expression or trafficking of other parasite proteins. An anti-KAHRP antiserum gave a roughly homogenous staining pattern at the periphery of RBCs infected with all parasite lines (Figure 3.4A). Similarly, a characteristic PfEMP3 profile at the RBC membrane was observed in all parasite lines (Figure 3.4B).

Maurer's cleft cisternae have a diameter that is close to the limit of resolution of conventional light microscopy. Therefore, it was not clear whether the decreased number of puncta in the REX1^{Δ371-579}-GFP line was due to a deficiency in generating Maurer's clefts or to the stacking of Maurer's cleft cisternae. We therefore examined these structures using 3D-Structured Illumination Microscopy (SIM), which provides an 8-fold increase in volume resolution (Hanssen et al., 2010, Schermelleh et al., 2008). Infected RBCs were permeabilized with the pore-forming toxin, Equinatoxin II (EqII) and labelled with an antibody recognizing GFP (Figure 3.7A). 3D-SIM reveals giant Maurer's clefts with an apparently convoluted surface. We also examined the relative organization of REX1^{Δ371-579}-GFP and SBP1 by dual labelled immunofluorescence after fixation and permeabilization (Figure 3.7B). A complementary organization of REX1^{Δ371-579}-GFP and SBP1 is evident, consistent with sub-compartmentalization of the Maurer's cleft lamella.

We co-labelled early stage REX1^{Δ371-579}-GFP parasites with the membrane probe, BODIPY-ceramide (Figure 3.7C) in an effort to determine the physical organization of the Maurer's clefts relative to the parasitophorous vacuole membrane (PVM) that surrounds the parasite. The lipid probe BODIPY-ceramide strongly labels membrane structures around the parasite, such as the PVM and the tubulovesicular network (Adisa et al., 2003). As observed in this doubly infected ring stage parasite, the REX1^{Δ371-579}-GFP appears to accumulate at discrete regions of the PVM. This accumulation is also seen in cells labelled with the PVM marker EXP2 (de Koning-Ward et al., 2009) (Figure 3.7D) and may represent either nascent Maurer's clefts budding from the PVM or a stack of Maurer's clefts that has become tethered to the PVM.

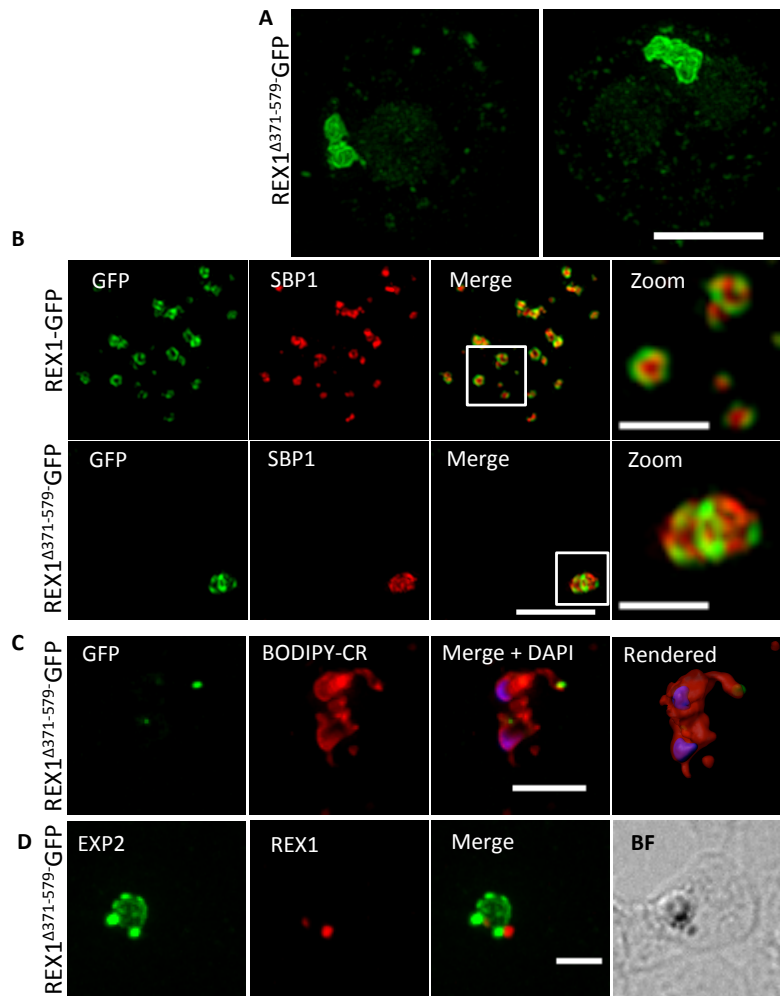


Figure 3.7 REX1^(Δ371-579)-GFP parasites exhibit giant Maurer's clefts

(A) REX1^(Δ371-579)-GFP-infected RBCs fixed with paraformaldehyde, permeabilized with EqII and labelled with anti-GFP.

(B) REX1-GFP and REX1^(Δ371-579)-GFP-infected RBCs were fixed with paraformaldehyde/ glutaraldehyde and probed with anti-GFP (green) and anti-SBP1 (red). Samples were examined using 3D-SIM.

(C) REX1^(Δ371-579)-GFP-infected RBCs were labelled with BODIPY-ceramide, fixed with paraformaldehyde/ glutaraldehyde, labelled with DAPI and imaged using widefield deconvolution microscopy. The right-hand panel shows rendering of the surface of the 3D structure using Imaris software.

(D) REX1^(Δ371-579)-GFP-infected RBCs were fixed with paraformaldehyde/ glutaraldehyde and probed with anti-EXP2 (green) and anti-REX1 (red). Samples were examined using deconvolution microscopy. Scale bars = 3 μm; zoom bar = 1 μm.

Transmission electron microscopy was performed to examine further the cleft phenotype in the REX1^{Δ371-579}-GFP parasites. The REX1-GFP parasites displayed an unstacked Maurer's cleft phenotype (Figure 3.8A, C) equivalent to that previously reported for the 3D7 strain (Hanssen et al., 2008a). Dramatically, the REX1^{Δ371-579}-GFP parasites showed very large stacks of Maurer's clefts (Figure 3.8B). For stacks cut in transverse section, it was possible to estimate the average number of layers in the stack as 6 ± 2 . The average distance between the lamellae was 20 ± 5 nm. The average thickness of the Maurer's cleft lamellae (lumen and both membranes) was 41 ± 8 and 38 ± 8 nm, respectively, for the REX1-GFP and REX1^{Δ371-579}-GFP lines. These data are consistent with the REX1^{Δ371-579}-GFP parasites producing a similar number of potential cisternae as REX1-GFP parasites but failing to separate them into individual structures.

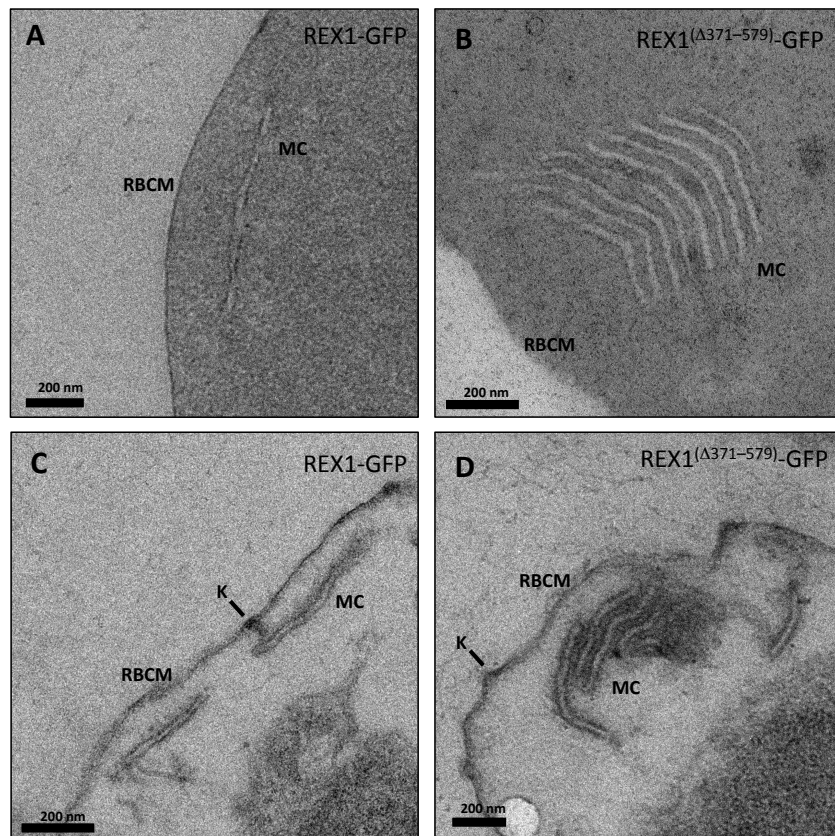


Figure 3.8 Transmission electron microscopy analysis of REX1-GFP and REX1(Δ 371–579)-GFP Maurer's clefts.

(A, B) TEM images of glutaraldehyde-fixed REX1-GFP and REX1(Δ 371–579)-GFP-infected RBCs (100 nm sections) revealing unstacked and highly stacked Maurer's clefts (MC) lamellae.

(C, D) TEM images of EqtII-permeabilized samples showing single Maurer's cleft lamellae and stacked lamellae (100 nm sections). Knobs (K) are indicated.

3.3.3 Tether-like structures accumulate on the stacked Maurer's clefts

In 3D7 parasites, Maurer's clefts are generated soon after invasion (Gruring et al., 2011, McMillan et al., 2013). During the first ~20 h of intraerythrocytic development, Maurer's clefts are often mobile within the RBC cytoplasm (McMillan et al., 2013). They then dock onto the RBC membrane in a process that involves tether-like structures as well as direct interactions with a remodeled RBC membrane skeleton (McMillan et al., 2013, Cyrklaff et al., 2011). To determine the organization of the tether-like structures in REX1^{Δ371-579}-GFP parasites, we made use of a previously described marker of the tethers, the membrane-associated histidine-rich protein-2 (MAHRP2) (Pachlatko et al., 2010). In REX1-GFP parasites, immunofluorescence reveals MAHRP2 labelling (Figure 3.10A) closely adjacent to the REX1-GFP labelled Maurer's clefts, as reported previously for wildtype 3D7 (McMillan et al., 2013). For the REX1^{Δ371-579}-GFP parasites, the MAHRP2 labelling partly overlaps with and partly sits outside the single puncta of GFP labelling. To examine this more closely we subjected these samples to 3D-SIM (Figure 3.10B). This indicates that MAHRP2 is present in small structures that decorate the Maurer's cleft stacks.

To obtain further insights into the Maurer's cleft architecture, REX1^{Δ371-579}-GFP transfectants were EqtII-permeabilized, then labeled with anti-GFP and protein A-gold. Sections (600 nm) were prepared for scanning transmission electron microscopy (STEM) tomography (Figure 3.10C). Rendering of the different features provides a 3D view of the stacked Maurer's cleft compartments (Figure 3.10D). Examination of the STEM tomogram indicated that the some of the Maurer's cleft layers are connected by a membrane continuum (Figure 3.10C, red), indicating a failure to separate the organelle into individual cisternae. It remains possible that the layered structure is more fully interconnected in regions that are out of the plane of the STEM tomogram. Protein A-gold-labeled anti-GFP is particularly concentrated on the edges of the REX1^{Δ371-579}-GFP Maurer's cleft cisternae, as previously reported for endogenous REX1 (Hanssen et al., 2008a). Several tubular tether structures with a diameter of ~25 nm are observed in the reconstructions (rendered in magenta).

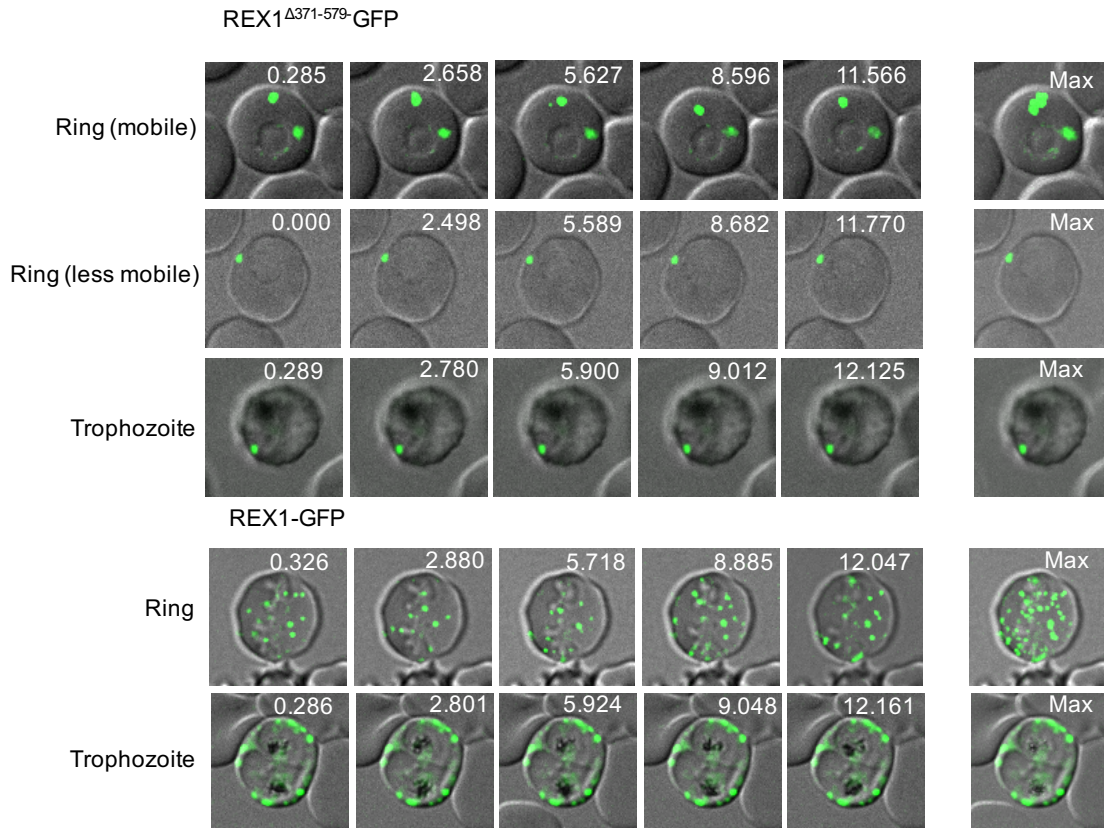


Figure 3.9 Live cell imaging of REX1-GFP and REX1^(Δ371-579)-GFP ring- and trophozoite- infected RBCs.

Top panel: A ring stage REX1^(Δ371-579)-GFP-infected RBC with mobile Maurer's clefts.

Second panel: A REX1^(Δ371-579)-GFP ring stage parasite with a Maurer's cleft with limited mobility.

Third panel: Immobilized Maurer's cleft from a REX1^(Δ371-579)-GFP trophozoite stage parasite.

Forth panel: Ring stage REX1-GFP parasites with mobile Maurer's clefts.

Fifth panel: Immobilized Maurer's clefts in a trophozoite stage REX1-GFP parasite.

Maximum projections of each of the series of five time points are presented on the far right. Times from beginning of acquisition are stamped on each image in seconds.

It is clear that some of the tether-like structures attached to the Maurer's clefts are not connected through to the RBC membrane; however, given the limited depth of the tomograms, it was difficult to ascertain whether any of the stacked cisternae is directly linked to the RBC membrane. To examine this further we undertook time-lapse imaging of live REX1-GFP and REX1^{Δ371-579}-GFP parasites. As previously reported (McMillan et al., 2013), the REX1-GFP labeled Maurer's clefts are highly mobile during the early to mid-ring stage of parasite development (Video S2; Figure 3.9). The majority of Maurer's clefts observed in REX1^{Δ371-579}-GFP ring stage-infected RBCs appear to have limited mobility, potentially due to linkage to the parasite surface or trapping in the limited physical space (Video S3; Figure 3.9). However, in some REX1^{Δ371-579}-GFP cells the Maurer's clefts are clearly mobile at the ring stage (Video S4; Figure 3.9). The Maurer's clefts of both REX1-GFP and REX1^{Δ371-579}-GFP immobilize at the trophozoite stage (Figure 3.9) consistent with docking onto the RBC membrane.

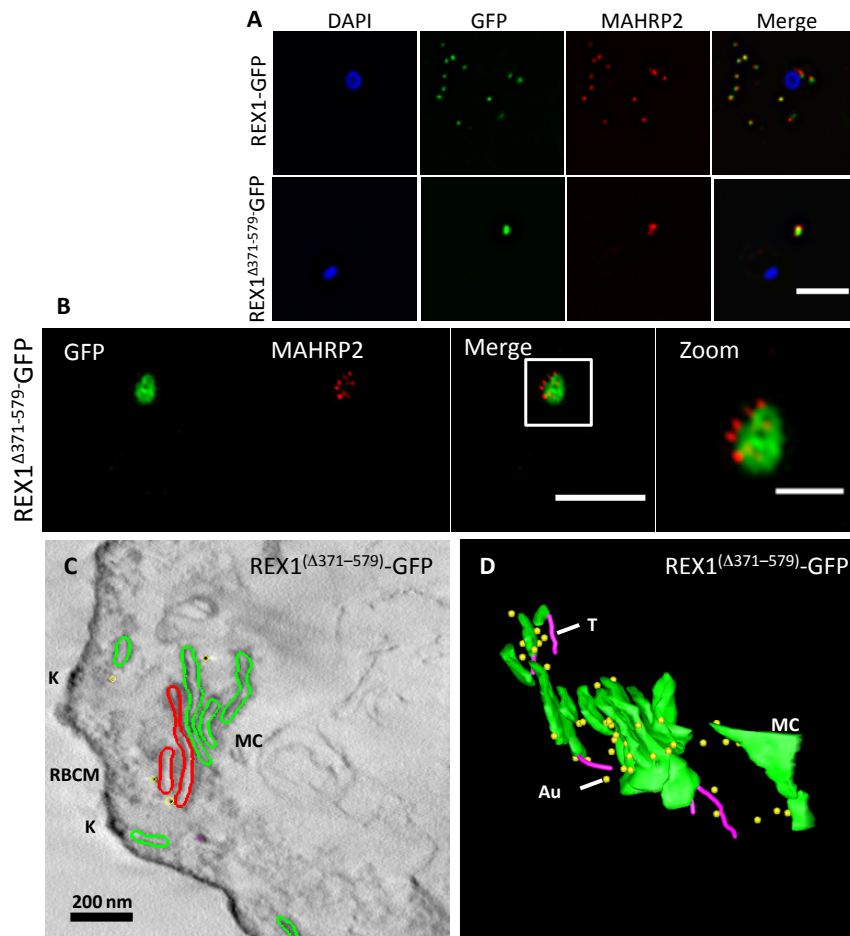


Figure 3.10 Analysis of the Maurer's clefts ultrastructure and distribution of tethers of REX1(Δ 371–579)-GFP parasites.

REX1-GFP and REX1(Δ 371–579)-GFP transfectants were fixed with paraformaldehyde/glutaraldehyde, permeabilized with Triton X-100, and probed with anti-GFP (green) and anti-MAHRP2 (red).

(A) Samples imaged using widefield deconvolution microscopy

(B) Samples imaged using 3D-SIM. Scale bars = 3 μ m; zoom bar = 1 μ m.

(C) STEM tomogram (600 nm section) of an EqII-permeabilized REX1(Δ 371–579)-GFP-infected RBC showing the stacked Maurer's clefts (MC) layers, and knobs (K) on the RBC membrane (RBCM). The lamella indicated in red share a membrane continuum.

(D) Rendered STEM tomogram of REX1(Δ 371–579)-GFP-infected RBC labelled with anti-GFP antibodies and protein A gold showing Maurer's clefts (MC, green), tethers (T, magenta) and gold particles (Au, yellow).

3.3.4 The repeat region of REX 1 is needed for efficient trafficking of PfEMP1 to the RBC surface

PfEMP1 trafficking requires export into the RBC cytoplasm and transport through the Maurer's cleft intermediate compartment, prior to insertion into the RBC membrane. We examined the organization of PfEMP1 in wildtype 3D7 and REX1 mutant parasites, using immunofluorescence microscopy on acetone-fixed cells. In agreement with previous studies (Blisnick et al., 2000, Wickham et al., 2001) we observed accumulation of PfEMP1 at the Maurer's clefts in the 3D7 wildtype parasites, as confirmed by co-labelling with the Maurer's cleft marker, SBP1 (Figure 3.11A). PfEMP1 is also delivered to the Maurer's clefts in the REX1¹⁻⁵⁷⁹, REX1-GFP and REX1^{Δ371-579}-GFP mutant parasite lines (Figure 3.11A) and in the REX-KD parasites (Figure 3.4D). Thus despite the aberrant morphology there is no obvious defect in trafficking of PfEMP1 from the parasite to the stacked Maurer's clefts.

Only a subpopulation of PfEMP1 is delivered to the infected RBC surface (Waterkeyn et al., 2000). This pool of PfEMP1 is oriented with its N-terminal domain exposed at the surface and is thus accessible to cleavage with trypsin (Kriek et al., 2003, Waterkeyn et al., 2000, Gardner et al., 1996). By contrast, intracellular pools of PfEMP1 are protected from protease cleavage. We undertook an analysis of the trypsin accessibility of PfEMP1 in RBCs infected with the different parasite lines. Intact magnet-purified mature stage-infected RBCs were subjected to treatment with PBS (P) or trypsin (T). The Triton-insoluble, SDS-soluble material (representing surface-exposed PfEMP1) was collected and subjected to SDS-PAGE and probed with an antibody recognizing the acidic terminal segment (ATS) domain of PfEMP1. Full length PfEMP1 from 3D7 parasites migrates with an apparent molecular mass of ~270 kDa (Figure 3.11B, D, F; red arrows). A cross-reaction of the PfEMP1 antibody with RBC spectrin (at ~250 kDa) is observed in variable intensity in the different samples (Figure 3.11B, D, F; yellow arrows). Cleavage products of ~75 kDa were observed in the trypsin-treated 3D7, REX1-GFP and REX1-KD (no GlcN) samples (green arrowheads). A similar cleavage product was observed in the REX1¹⁻⁵⁷⁹ sample as well as an additional product ~60 kDa, likely representing another PfEMP1 variant (Figure 3.11B). By contrast, the ~75 kDa cleavage products were not detected in the REX1^{Δ371-579}-GFP parasites (Figure 3.11D) and was reduced in the REX1-KD parasites treated with 2.5 mM GlcN (Figure 3.11F). This suggests a significant reduction of surface-exposed PfEMP1 in these parasites. By contrast, we observed no

obvious difference between the level of full-length Triton X-100-insoluble PfEMP1 in the GlcN-treated and control samples (three experiments). To control for the possibility of cell lysis during trypsin treatment, we used SBP1 as a control. There is no evidence for the SBP1 cleavage product that would be expected if the RBC membrane was breached during the trypsin treatment protocol (Figure 3.12).

To assess the functional consequences of the decreased surface-exposed PfEMP1, parasite-infected RBCs were panned on immobilized CD36, to enrich the population for CD36-binding variants of PfEMP1, and then examined for their ability to adhere to immobilized CD36 under flow at a pressure of 0.1 Pa (Figure 3.11C, E, G). Because binding levels differ depending on factors such as CD36 batch, it is important to compare matched pairs of samples strictly in parallel. The 3D7 parasites showed no significant difference in binding compared to REX1¹⁻⁵⁷⁹ ($p = 0.68$, unpaired t-test). The REX1 ^{Δ 371-579}-GFP mutants bound significantly less efficiently to CD36 (37% decrease; $p < 0.001$) than REX1-GFP. Similarly, addition of 2.5 mM GlcN to the REX1-KD parasites significantly decreased the binding to CD36 (35% decrease; $p < 0.001$). This confirms that loss of PfEMP1 surface exposure leads to a significant reduction in adhesion to endothelial ligands. To control for the possibility that treating with GlcN may affect parasite viability, we also measured the CD36 binding of GlcN-treated and untreated 3D7 parent parasites and found no difference (Figure 3.13; $p = 0.125$, unpaired t-test).

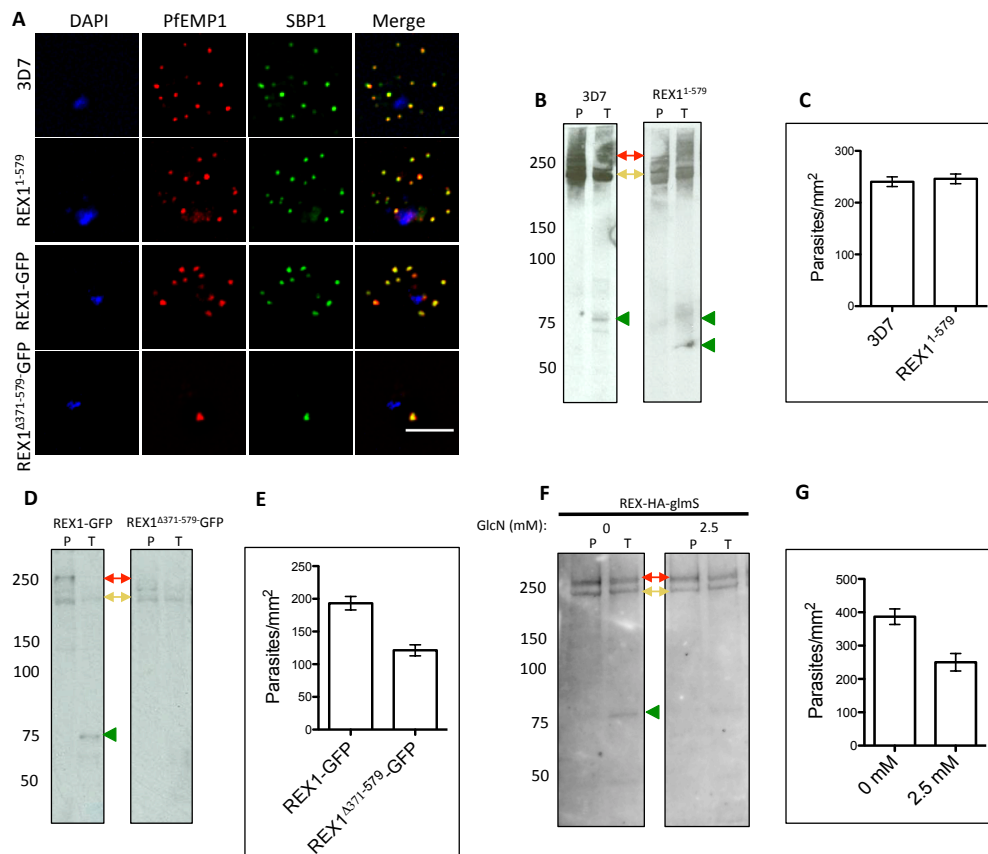


Figure 3.11 PfEMP1 surface-exposure and cytoadherence of REX1 transfectants

(A) Immunofluorescence microscopy of acetone-fixed RBCs infected with 3D7 and REX1 transfectants. Maurer's clefts were identified by immunolabeling with anti-SBP1 (green). Anti-PfEMP1 antibodies (red) revealed colocalization of the virulence protein with Maurer's clefts. The nuclei are stained with DAPI (blue). Scale bar = 3 μ m.

(B, D, F) Trypsin digestion of surface-exposed PfEMP1 in RBC infected with wildtype and REX1¹⁻⁵⁷⁹ transfectants in REX1-GFP and REX1^(Δ 371-579)-GFP transfectants (D) and in REX1-HA-GlmS parasites without or with treatment with 2.5 mM GlcN. Full-length PfEMP1 (~270 kDa, red arrows) and a cross-reactive spectrin band (~240 kDa, yellow arrows) are indicated. Trypsin cleavage products (75 kDa) are indicated with green arrowheads. The data are representative of three separate experiments.

(C, E, G) Adherence of trophozoite-stage infected RBCs to recombinant CD36 under flow conditions (0.1 Pa) \pm S.E.M. measured in 10 different areas in each of three separate experiments. REX1^(Δ 371-579)-GFP binding was significantly lower than REX1-GFP ($p < 0.0001$, unpaired t-test).

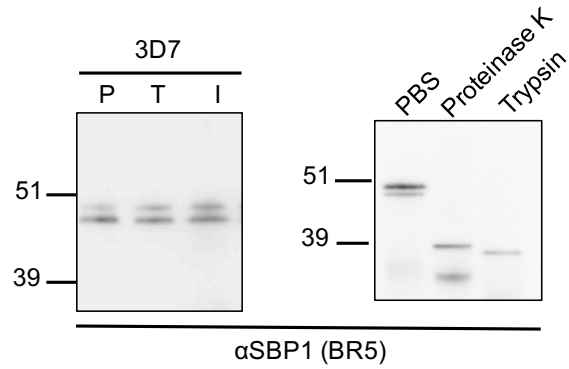


Figure 3.12 Control to monitor integrity of infected RBCs during trypsin digestion.

Left panel: 3D7 parasites were treated with PBS (P), PBS and trypsin (T) or PBS, trypsin and soybean trypsin inhibitor (I). The reaction was stopped with soybean trypsin inhibitor and the cells were permeabilized with EqtII to release hemoglobin. The samples were subjected to SDS-PAGE and Western blotting.

Right panel: 3D7 parasites were permeabilized with EqtII and treated with either PBS, proteinase K or trypsin. Proteins were precipitated with trichloroacetic acid and subjected to SDS-PAGE and Western blotting. The membranes were probed with an antibody recognizing the N-terminal fragment (BR5) of SBP1.

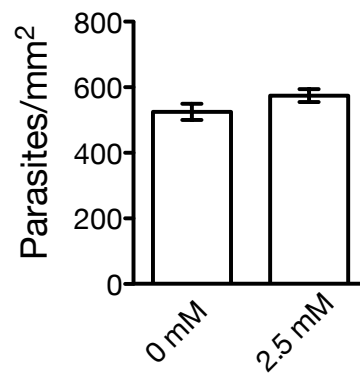


Figure 3.13 Binding of 3D7 parent parasites to CD36 under flow conditions.

Control (0 mM) or GlcN-treated (2.5 mM) infected RBCs (3% parasitaemia, 1% haematocrit) were flowed at 0.1 Pa over recombinant CD36. The number of bound infected RBCs was counted. $P = 0.125$, unpaired t-test. Error bars represent the S.E.M. of data collected in 3 separate experiments (10 fields each experiment).

3.4 Discussion

The virulence of *P. falciparum* is due, in part, to its ability to present PfEMP1 at the RBC surface, which enables sequestration of infected RBCs within the microvasculature of the host. Differences in the severity of malaria-induced pathologies are thought to arise from the expression of different PfEMP1 variants that bind to different endothelial cell receptors or to the same receptor with different affinities. However, differences in the efficiency of trafficking or presentation of PfEMP1 may also contribute to the adhesion phenotype. For example, alterations in Maurer's cleft architecture may directly or indirectly affect the efficiency of PfEMP1 trafficking to the RBC membrane.

Previous efforts to ablate the *rex1* gene resulted in concomitant loss of a subtelomeric region of chromosome 2, encoding KAHRP and other proteins. Because of the inefficiency of conventional knockout strategies in *P. falciparum*, several months of continuous culturing may be required to retrieve a knockout clone. If a genetic manipulation confers even a small growth disadvantage additional genetic changes may occur that relieve this disadvantage. For example, the loss of the sub-telomeric region of chromosome 2, which encodes several exported proteins that are not needed for survival in culture, is a frequent event during long-term culture.

In this work, we took advantage of a recently developed system for conditional knockdown of *P. falciparum* genes. We achieved >90% knockdown of REX1 upon addition of GlcN to REX1-KD parasites. This was not associated with a measureable growth defect over the period examined (48 h) but a disadvantage may manifest over a longer period, or upon complete deletion of REX1. Maurer's cleft reorganization was observed in these REX1-depleted parasites, confirming its important role in maintaining normal organization. No loss of the chromosome 2 proteins, KAHRP and PfEMP3, was observed indicating that it is possible to lose REX1 and maintain the expression of these other exported proteins. Nonetheless, REX1-KD mutants showed defective PfEMP1 surface presentation and defective binding under flow. This confirms that REX1 plays a role in PfEMP1 trafficking that is independent of effects on other exported protein. The level of this defect (~35% lower binding) was less than that reported for complete *rex1* deletion (Dixon et al., 2011). This likely indicates that the loss of knobs also contributes to the loss of adhesion in this REX1-deleted line, but may also reflect the fact that a small amount of REX1 is still expressed in the REX1 knockdown. Contrary to previous reports (Knuepfer et al., 2005, Wickham et al., 2001), we did not observe KAHRP or PfEMP3

colocating with Maurer's clefts proteins. This may be due to stage differences or to the fact that these previous studies used truncated constructs of KAHRP and PfEMP3 which may have affected protein localization.

We were interested to further dissect the region of REX1 that is responsible for Maurer's cleft sculpting and effective PfEMP1 trafficking. We showed that deletion of 341 amino acids from the C-terminus causes the formation of Maurer's cleft with an average of 3 stacked cisternae, and is associated with less efficient PfEMP1 trafficking, consistent with previous work (Dixon et al., 2011). By contrast deletion of the C-terminal 133 amino acids had no significant effect on Maurer's cleft stacking or PfEMP1 trafficking, indicating that the repeat region (371-579 amino acids) contains important functional motifs.

To further investigate the role of this region we generated transfectants in which the repeat sequence domain was deleted. These parasites exhibited a phenotype that is even more severe than the REX1¹⁻³⁶² transfectants. The Maurer's clefts became highly stacked with an average of six layers per stack. Lateral interactions between the cisternal layers membrane were evident, as well as a membrane continuum between some of the layers. Interestingly in early stage parasites the giant Maurer's clefts were attached to the PVM, which is consistent with the suggestion that Maurer's cleft lamellae are formed from a single focus. The appearance and dimensions of the individual cisternae were similar to that in wildtype parasites, and Maurer's cleft markers such as SBP1 were still trafficked to the stacked clefts and located in distinct sub-compartments, as for wildtype 3D7 (McMillan et al., 2013). The clefts were decorated with multiple 25-nm tether-like structures, indicating that this association still occurs; and they still docked onto the RBC membrane in the mature stage of development. The data suggest that the clefts are formed in a similar manner to wildtype Maurer's clefts, but fail to separate into individual cisternae.

It is evident that the repeat region plays an important role (either direct or indirect) in Maurer's cleft sculpting. An important caveat is that it is possible that deletion of the REX1 repeats alters the 3D structure of the REX1 protein in a way that is deleterious to its function.

The REX1^{Δ371-579} mutants exhibited an intact chromosome 2 locus, a normal distribution of KAHRP and PfEMP3, and normal knob morphology. This suggests that REX1 plays

no role in the trafficking of these proteins. Similarly, PfEMP1 appeared to be delivered efficiently to the Maurer's clefts indicating that REX1 is not involved in this transport step. By contrast, the REX1^{Δ371-579} mutants (like the GlcN-treated REX1-KD parasites) showed defective PfEMP1 surface presentation and defective binding under flow. It is possible that the repeat domain directly participates in PfEMP1 trafficking, for example by promoting the budding of PfEMP1-containing vesicles from the Maurer's clefts. Alternatively, deleting the repeat region of REX1 may exert an effect by altering the conformation of the protein. Another possibility is that the stacking of the Maurer's clefts may compromise lateral associations of individual Maurer's cleft cisternae with the RBC membrane that are needed for budding of vesicles or packaging of cargo.

Interestingly an analysis of the REX1 sequences available in PlasmoDB indicates that the repeat region is polymorphic (in sequence and length) in different *P. falciparum* strains. These differences in repeats do not seem to result in the dramatic change in Maurer's clefts morphology that are observed when this region is deleted. Nonetheless, it is possible that repeat region polymorphisms will affect the efficiency of PfEMP1 trafficking, which could in turn contribute to different levels of cytoadhesion, and thus virulence, of field strains. Further analysis of the role of REX1 in trafficking PfEMP1 may provide ways of interfering with its surface presentation. This could provide an important new strategy to combat this lethal human pathogen.

Chapter 4 : Enrichment and analysis of the Maurer's clefts

4.1 Introduction

Severe malaria caused by *P. falciparum* is in part due to the cytoadhesion of the infected red blood cells to ligands on the host vascular endothelium. The parasite protein PfEMP1 is the adhesin responsible for this process. In order for PfEMP1 to be presented on the red blood cell surface, it first must be exported to the red blood cell cytoplasm, transit through the Maurer's clefts and be trafficked from the clefts to the red blood cell surface. The Maurer's clefts are currently a "black box" in our understanding of the route of PfEMP1 trafficking. Only a handful of Maurer's clefts proteins have been characterised in-depth and the events surrounding the insertion of PfEMP1 to the clefts, and subsequent transport to the red blood cell membrane surface are poorly understood. Moreover, the composition of the Maurer's clefts changes throughout the parasite lifecycle as proteins are expressed and exported at distinct stages of asexual development (McMillan et al., 2013). In this study, we profile the protein content of the Maurer's clefts at the stage of the asexual parasite lifecycle where PfEMP1 trafficking is taking place.

A review describing Maurer's clefts as the 'enigma of *P. falciparum*' called for improved fractionation techniques in order to study these membranes (Mundwiler-Pachlatko and Beck, 2013). In the present study, we develop a new technique for enriching Maurer's clefts which combines cellular fractionation and co-precipitation. A similar approach has been used to enrich the apicoplast (Botte et al., 2013). The Maurer's clefts protein composition is analysed at 14-18 h post-invasion - a time point at which the clefts are mobile and are accumulating PfEMP1. A previous study has used mass spectrometry to analyse the protein composition of the Maurer's clefts (Vincensini et al., 2005). This study analysed deuterium-labelled trophozoite-infected red blood cell ghosts, as Maurer's clefts are found in the ghost fraction at this parasite stage. The resident Maurer's clefts protein SBP1 was used a positive control for the presence of Maurer's clefts in this fraction. From this work, two novel Maurer's clefts proteins, PfJ23 (PF3D7_1001900) and PfE60/PIESP2 (PF3D7_0501200) were identified that were confirmed by specific antibody or epitope-tagging (Vincensini et al., 2005, Mbengue et al., 2015). However, many other known Maurer's clefts proteins were not identified and the preparations included intracellular parasite and parasitophorous vacuole contaminants e.g. GAPDH (PF3D7_1462800) and serine repeat antigen 5 (PF3D7_0207600). Meanwhile, the use of

proteomic approaches to study exported *Plasmodium* proteins has become more common, with the ‘exportomes’ of both of *P. yoelii* and *P. berghei* recently being characterised (Siau et al., 2016, Pasini et al., 2013). The proteomic analysis of the Maurer’s clefts provides an important update to our understanding of these organelles.

We were interested in the proteins present in the Maurer’s clefts at the time when PfEMP1 trafficking is occurring. The timeframe of PfEMP1 appearing on the red blood cell surface ranges between 16 - 24 h post-invasion (Kriek et al., 2003, Leech et al., 1984, Gardner et al., 1996). One study, using flow cytometry, found that the majority of PfEMP1 appeared on the surface of infected red blood cells between 16-20 hours post-invasion, and plateaued at 24 h post-invasion (Kriek et al., 2003). In the present study, we captured the clefts at a stage where PfEMP1 is residing within the organelle and is beginning to be transported to the red blood cell surface.

We identify novel Maurer’s clefts proteins and generate epitope-tagged transfectant parasites. Analysis of these fluorescently tagged proteins leads to the identification of several novel Maurer’s clefts proteins. In a previous study, visualisation of Maurer’s clefts proteins by electron microscopy and super-resolution fluorescence microscopy revealed sub-compartmentalisation of proteins within the clefts. For example, REX1 is located around the edges of the clefts (McMillan et al., 2013), whereas SBP1 is more central (Hanssen et al., 2008b). In the present study, we examine the location of a number of novel and established Maurer’s clefts proteins using structured illumination microscopy (SIM).

It has been more than a decade since the original mass spectrometric analysis of Maurer’s clefts was published. In the years since, many more Maurer’s clefts proteins have been identified, nonetheless there remains a need for a defined protein profile of these organelles. In this study, we undertake a controlled and reproducible tandem mass spectrometric analysis of the Maurer’s clefts. Additionally, we identify a number of human proteins enriched at the Maurer’s clefts that have roles in membrane trafficking and lipid pathways. By providing new data on the spatial arrangement of proteins within the context of published protein knockout information, we provide an updated model for the structure and function of Maurer’s clefts.

4.2 Results

4.2.1 Validation of the method to enrich the Maurer's clefts

Red blood cells infected with wild type 3D7 and parasites expressing an episomally encoded REX1-GFP were synchronised to a 14 - 18 h post-invasion window. At this stage of the asexual cycle, Maurer's clefts are mobile and contain PfEMP1 (McMillan et al., 2013). Parasite-infected red blood cells were hypotonically lysed, extruded 10 times through a 27-gauge needle, made isotonic, pre-cleared, and then incubated with GFP-Trap® beads (Figure 4.1A; Section 2.5).

The GFP-Trap beads were washed and prepared for immunoblotting alongside fractions collected throughout the procedure from both REX1-GFP samples and a 3D7 control. Markers from different compartments within the infected red blood cell were used to assess the composition of each fraction (Figure 4.1B). The 'Total' fractions from both the 3D7 control and REX1-GFP samples contain host spectrin and parasite proteins GAPDH and EXP1. Although SBP1 is expected to be present in this fraction, it was not abundant enough for detection due to loading limits of this haemoglobin-containing fraction. The 'Input' fraction represents the supernatant after a low-speed centrifugation step that removes much of the red blood cell ghost material (as suggested by the decrease in spectrin signal in both 3D7 and REX1-GFP samples). After incubation with the GFP-Trap® beads, the 'Unbound' and 'Beads' fractions show the specific enrichment of SBP1 and REX1-GFP samples compared to markers from other compartments (Figure 4.1B). This is interpreted as Maurer's clefts membrane fragments that had bound specifically to the GFP-Trap® beads via REX1-GFP.

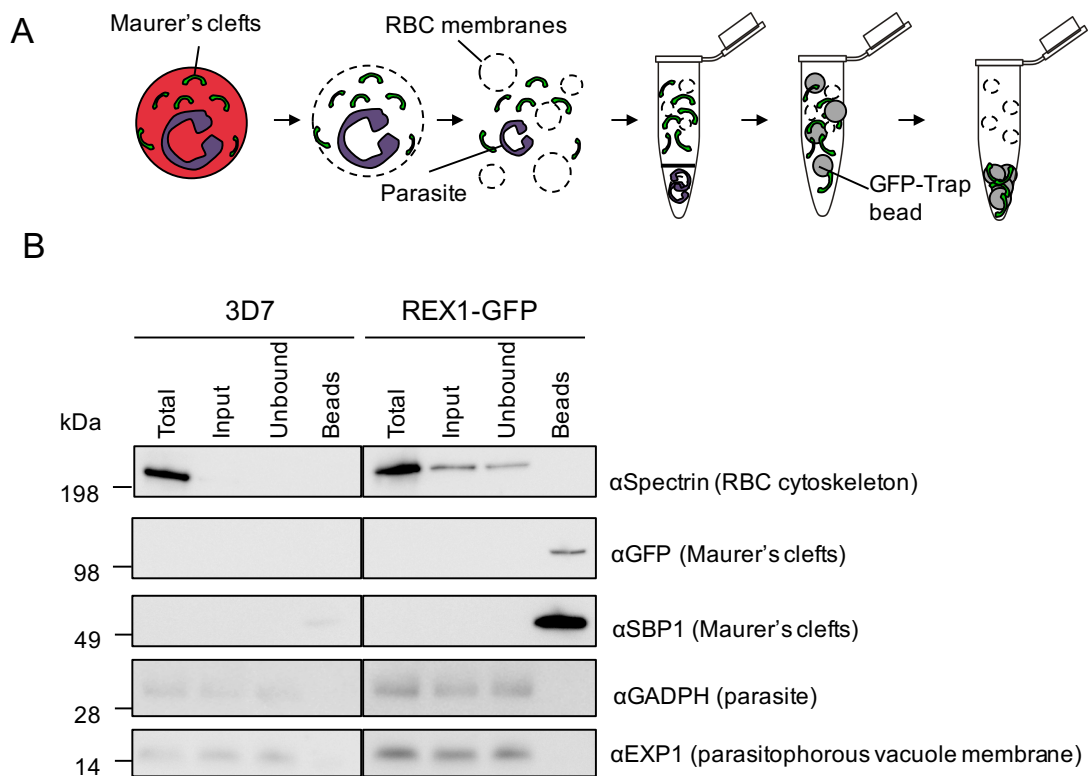


Figure 4.1 Enrichment and analysis of Maurer's clefts

(A) Schematic depicting the method used to enrich the Maurer's clefts from red blood cell infected with REX1-GFP transfectant parasites

(B) Western analysis of fractions from throughout the enrichment process. Total = infected red blood cell lysate, Input = fraction added to the GFP-Trap® beads, Unbound = supernatant after GFP-Trap® bead incubation, Beads = fraction eluted from GFP-Trap® beads. Molecular masses are shown in kDa

Having confirmed the enrichment of the Maurer's clefts relative to other cellular compartments, we next tested whether the integrity of the enriched Maurer's clefts membranes was maintained. This was assessed by proteinase K digestion followed by probing with an antibody to the luminal (amino terminal, BR5) segment of the integral membrane protein SBP1 (Blisnick et al., 2000). Protease digestion of SBP1 from permeabilised infected red blood cells results in a characteristic ~37 kDa fragment recognised by an α SBP1 antibody (Blisnick et al., 2000, McHugh et al., 2015). Bead fractions from 3D7 and REX1-GFP samples were treated with either PBS only, proteinase K only, or proteinase K and saponin (a compound that permeabilises the red blood cell, parasitophorous vacuole and Maurer's clefts membranes). Probing with α SBP1 showed that full-length SBP1 was present when the Maurer's clefts were enriched, but the cytoplasmic- and lumen-facing regions of SBP1 were degraded when treated with proteinase K (Figure 4.2B). This shows that the Maurer's clefts membrane integrity is disrupted during the enrichment process. Thus, a limitation of the enrichment protocol is that soluble proteins in the lumen of the Maurer's clefts may be lost.

Enriched Maurer's clefts bound to the GFP-Trap agarose beads® were analysed by fluorescence microscopy. Fluorescent puncta with a diameter $<1 \mu\text{m}$ were observed on the surface of the beads (Figure 4.2A). These REX1-GFP fluorescent puncta bear close resemblance with the size and appearance of fluorescently labelled Maurer's clefts, with some shaped like a characteristic 'horseshoe' (McMillan et al., 2013).

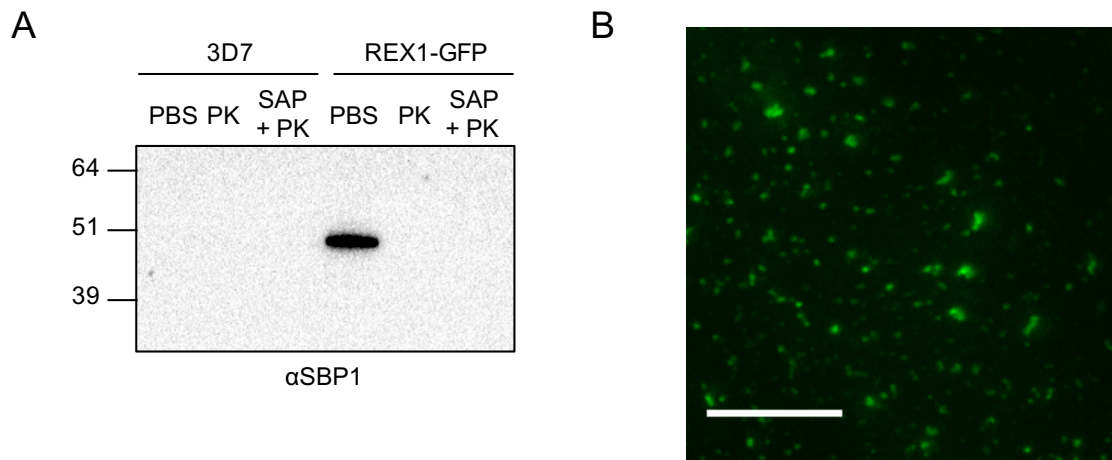


Figure 4.2 Analysis of the enriched Maurer's clefts fragments

(A) Protease accessibility analysis of the enriched Maurer's clefts. Washed beads were treated with either PBS only, PBS and proteinase K (1 mg/mL) or saponin (0.03% w/v) and proteinase K (1 mg/mL)

(B) Fluorescence microscopy of a 70 μm GFP-Trap agarose bead after incubation with REX1-GFP lysate. Scale bar = 10 μm

4.2.2 Mass spectrometric analysis of enriched Maurer's clefts

After validating the enrichment technique, the Maurer's clefts from REX1-GFP parasites and wild-type 3D7 controls were analysed by LC-MS/MS. Proteins were identified by searching the mass spectra using MASCOT (Matrix Science) against a database containing *P. falciparum* and *Homo sapiens* proteomes. Proteins were considered significant if at least 2 significant MS/MS spectra were detected in 2 separate experiments or were enriched 5 times in the REX1-GFP samples compared to 3D7 (Table 6). PfEMP1 variants detected are included in a separate table for readability (Table 7). A large number of the proteins known to be present at the Maurer's clefts at 14-18 h post-invasion were identified. A notable exception is REX2, which was identified in both replicates (4 and 5 significant MS/MS spectra respectively) but was excluded due to the presence of MS/MS spectra corresponding to REX2 in the 3D7 control. Eight of the proteins identified had no previously published localisation. Of these, two are homologues of known Maurer's clefts proteins: GEXP10 (orthologue of GEXP07) and PF3D7_1002000 (paralogue of PfJ23 and PTP5). A further three unlocalised proteins were identified: PF3D7_0501000, PF3D7_1353100 and STARP. Although there is no published location for PTP6, knockout of this protein arrests PfEMP1 transport at the Maurer's clefts, suggesting a possible function at the clefts for this protein (Maier et al., 2008). The remaining two unlocalised proteins, PF3D7_0301700 and PF3D7_0811600 are largely uncharacterised, except for one study that found that PF3D7_0811600 co-immunoprecipitated with PHIST protein PFE1605w (PF3D7_0532400) (Oberli et al., 2016). One likely parasite contaminant of unknown location met the criteria for inclusion in Table 6, a putative calyculin binding protein (PF3D7_1238100).

Table 6 Mass spectrometry analysis of enriched Maurer's clefts

PlasmoDB ID	Protein name	Number of significant ms/ms spectra			
		Expt. 1		Expt. 2	
		MCs	3D7	MCs	3D7
PF3D7_0935900	ring-exported protein 1 (REX1)	58	0	71	0
PF3D7_0830500	sporozoite and liver stage tryptophan-rich protein	32	0	46	0
PF3D7_0113900	Plasmodium exported protein (hyp8, GEXP10)	10	0	8	0
PF3D7_0811600	conserved Plasmodium protein (PF08_0091)	9	0	12	0
PF3D7_0702500	Plasmodium exported protein (PF07_0008)	9	0	18	0
PF3D7_1302000	EMP1-trafficking protein (PTP6)	8	0	10	0
PF3D7_1353100	Plasmodium exported protein (PF13_0275)	8	0	9	0
PF3D7_0702300	sporozoite threonine and asparagine-rich protein (STARP)	8	0	10	0
PF3D7_0601900	conserved Plasmodium protein (PFE0090w)	6	0	5	0
PF3D7_1002100	EMP1-trafficking protein (PTP5)	6	0	16	0
PF3D7_1001900	Plasmodium exported protein (hyp16, PfJ23)	6	0	8	0
PF3D7_0702400	small exported membrane protein 1 (SEMP1)	6	0	7	0
PF3D7_0202200	EMP1-trafficking protein (PTP1)	5	0	10	0
PF3D7_1002000	Plasmodium exported protein (hyp2)	5	0	8	0
PF3D7_1301700	Plasmodium exported protein (hyp8, GEXP07)	5	0	6	0
PF3D7_1238100	calcyclin binding protein, putative	4	0	3	0
PF3D7_1353200	membrane associated histidine-rich protein (MAHRP2)	4	0	3	0
PF3D7_0301700	Plasmodium exported protein (PFC0085c)	2	0	4	0
PF3D7_0501000	Plasmodium exported protein (PFE0050W)	2	0	4	0
PF3D7_1148900	Plasmodium exported protein (PF11_0505)	2	0	4	0
PF3D7_0501300	skeleton-binding protein 1 (SBP1)	2	0	4	0

Maurer's clefts proteins that are expressed in the trophozoite stage such as PIESP2 and trophozoite exported proteins 1 (TEX1) were either not detected or did not meet the threshold for inclusion. Multiple proteins from the PfEMP1 family were detected (Table 7). Export of PfEMP1 to the Maurer's clefts occurs by 16 h post-invasion or earlier, whilst clefts are still mobile (McMillan et al., 2013). This is consistent with our identification of PfEMP1 at the clefts. Whether transport of PfEMP1 to the red blood cell membrane takes place from mobile or arrested Maurer's clefts is still unclear. Of the proteins detected in the enriched Maurer's clefts, 10 are known or putative PNEPs (not including PfEMP1 variants), whilst 11 are PEXEL proteins. Any published protein localisation or knockout data is presented in Table 8.

Table 7 PfEMP1 variants detected in enriched Maurer's clefts

PlasmoDB ID	Protein name	Number of significant ms/ms spectra			
		Expt. 1		Expt. 2	
		MCs	3D7	MCs	3D7
PF3D7_0600200	erythrocyte membrane protein 1, PfEMP1 (VAR)	11	0	21	0
PF3D7_1300300	erythrocyte membrane protein 1, PfEMP1 (VAR)	9	0	30	0
PF3D7_1150400	erythrocyte membrane protein 1, PfEMP1 (VAR)	8	0	23	0
PF3D7_0632500	erythrocyte membrane protein 1, PfEMP1 (VAR)	4	0	21	0
PF3D7_0400400	erythrocyte membrane protein 1, PfEMP1 (VAR)	4	0	5	0
PF3D7_0800300	erythrocyte membrane protein 1, PfEMP1 (VAR)	4	0	6	0
PF3D7_1200400	erythrocyte membrane protein 1, PfEMP1 (VAR)	4	0	8	0
PF3D7_0800200	erythrocyte membrane protein 1, PfEMP1 (VAR)	4	0	11	0
PF3D7_0712300	erythrocyte membrane protein 1, PfEMP1 (VAR)	4	0	16	0
PF3D7_0833500	erythrocyte membrane protein 1, PfEMP1 (VAR)	4	0	6	0
PF3D7_0712900	erythrocyte membrane protein 1, PfEMP1 (VAR)	4	0	5	0
PF3D7_1100100	erythrocyte membrane protein 1, PfEMP1 (VAR)	4	0	8	0
PF3D7_0712400	erythrocyte membrane protein 1, PfEMP1 (VAR)	4	0	5	0
PF3D7_0425800	erythrocyte membrane protein 1, PfEMP1 (VAR)	3	0	9	0
PF3D7_0700100	erythrocyte membrane protein 1, PfEMP1 (VAR)	3	0	4	0
PF3D7_1219300	erythrocyte membrane protein 1, PfEMP1 (VAR)	3	0	3	0
PF3D7_1373500	erythrocyte membrane protein 1, PfEMP1 (VAR)	3	0	5	0
PF3D7_0300100	erythrocyte membrane protein 1, PfEMP1 (VAR)	3	0	6	0
PF3D7_0600400	erythrocyte membrane protein 1, PfEMP1 (VAR)	3	0	9	0
PF3D7_0533100	erythrocyte membrane protein 1 truncated, pseudogene (VAR1CSA)	2	0	2	0
PF3D7_1240300	erythrocyte membrane protein 1, PfEMP1 (VAR)	2	0	4	0
PF3D7_0400100	erythrocyte membrane protein 1, PfEMP1 (VAR)	2	0	5	0
PF3D7_1240600	erythrocyte membrane protein 1, PfEMP1 (VAR)	2	0	6	0
PF3D7_0712000	erythrocyte membrane protein 1, PfEMP1 (VAR)	2	0	7	0
PF3D7_0900100	erythrocyte membrane protein 1, PfEMP1 (VAR)	2	0	4	0
PF3D7_0712800	erythrocyte membrane protein 1, PfEMP1 (VAR)	2	0	4	0
PF3D7_0632800	erythrocyte membrane protein 1, PfEMP1 (VAR)	2	0	5	0
PF3D7_0711700	erythrocyte membrane protein 1, PfEMP1 (VAR)	2	0	3	0
PF3D7_0420900	erythrocyte membrane protein 1, PfEMP1 (VAR)	2	0	8	0
PF3D7_0412400	erythrocyte membrane protein 1, PfEMP1 (VAR)	2	0	5	0
PF3D7_0426000	erythrocyte membrane protein 1, PfEMP1 (VAR)	2	0	4	0
PF3D7_0100300	erythrocyte membrane protein 1, PfEMP1 (VAR)	2	0	7	0
PF3D7_0833300	erythrocyte membrane protein 1 (PfEMP1), exon 2, pseudogene	2	0	4	0

Table 8 Overview of proteins identified in the enriched Maurer's cleft

PlasmoDB ID	Protein name	Type	Location - red blood cell stage			Knockout		
			Compartment	Reference	Method	Disrupted	Reference	Phenotype
PF3D7_0935900	ring-exported protein 1 (REX1)	PNEP	MC	Hawthorne et al., 2004, Hanssen et al., 2008	SA*, GFP	Yes	Dixon et al., 2011	PfEMP1 stuck at clefts, stacked Maurer's clefts
PF3D7_0830500	sporozoite and liver stage tryptophan-rich protein	PNEP	MC and parasite	Heiber et al., 2013	GFP	No	-	-
PF3D7_0702500	Plasmodium exported protein (PF07_0008)	PNEP	MC and RBC cytoplasm	Heiber et al., 2013	GFP	No	-	-
PF3D7_1302000	EMP1-trafficking protein (PTP6)	PEXEL	Unknown	-	-	Yes	Maier et al., 2007	PfEMP1 stuck at clefts
PF3D7_1002100	EMP1-trafficking protein (PTP5)	PEXEL	MC	Batinovic et al., 2017	GFP	Yes	Maier et al., 2008	PfEMP1 stuck at clefts
PF3D7_0702300	sporozoite threonine and asparagine-rich protein (STARP)	PEXEL	Unknown	-	-	No	-	-
PF3D7_0811600	conserved Plasmodium protein (PF08_0091)	Unknown	Unknown	-	-	No	-	-
PF3D7_1001900	Plasmodium exported protein (hyp16, PfJ23)	PEXEL	MC	Vincensini et al., 2005	SA	No (refractory)	Maier et al., 2008	-
PF3D7_1353100	Plasmodium exported protein (PF13_0275)	PEXEL	Unknown	-	-	Yes	Maier et al., 2008	No effect
PF3D7_0202200	EMP1-trafficking protein (PTP1)	PEXEL	MC	Rug et al., 2014	SA, GFP, HA	Yes	Maier et al., 2008, Rug et al., 2014	PfEMP1 not exported, vesiculated Maurer's clefts
PF3D7_0601900	conserved Plasmodium protein (PFE0090w)	PNEP	MC	Heiber et al., 2013	GFP	No	-	-
PF3D7_0501300	skeleton-binding protein 1 (SBP1)	PNEP	MC	Blisnick et al. 2000	SA	Yes	Cooke et al., 2006, Maier et al., 2007	PfEMP1 stuck at clefts, PfEMP1 not exported
PF3D7_1002000	Plasmodium exported protein (hyp2, PF10_0024)	PEXEL	Unknown	-	-	Yes	Maier et al., 2008	No effect
PF3D7_0702400	small exported membrane protein 1 (SEMP1)	PNEP	MC and RBC cytoplasm	Heiber et al., 2013, Dietz et al., 2014	SA, GFP, HA	Yes	Dietz et al., 2014	No effect
PF3D7_1370300	membrane associated histidine-rich protein (MAHRP1)	PNEP	MC	Spycher et al., 2003, Spycher et al., 2006	SA, GFP	Yes	Spycher et al., 2008	PfEMP1 not exported
PF3D7_1301700	Plasmodium exported protein (hyp8, GEXP07)	PEXEL	MC	Sleebbs et al., 2014	GFP, HA	No (refractory)	Maier et al., 2008	-
PF3D7_0113900	Plasmodium exported protein (hyp8, GEXP10)	PEXEL	Unknown	-	-	No (refractory)	Maier et al., 2009	-
PF3D7_0301700	Plasmodium exported protein (PFC0085c)	PEXEL	Unknown	-	-	No	-	-
PF3D7_0501000	Plasmodium exported protein (PFE0050W)	PEXEL	Unknown	-	-	Yes	Maier et al., 2008	No effect
PF3D7_1353200	membrane associated histidine-rich protein (MAHRP2)	PNEP	Tethers	Pachlatko et al., 2010	SA, GFP	No (refractory)	Pachlatko et al., 2010	-
PF3D7_1148900	Plasmodium exported protein (PF11_0505)	PNEP	MC and parasite	Heiber et al., 2013	GFP	No	-	-
var gene family	P. falciparum erythrocyte membrane protein 1 (PfEMP1)	PNEP	MC and RBC surface	Kriek et al., 2003	SA	No	-	-
PF3D7_1238100	calcyclin binding protein, putative	N/A	Unknown	-	-	-	-	-

4.2.3 The Maurer's clefts are enriched in human proteins involved in membrane trafficking and lipid biogenesis

In addition to the *P. falciparum* proteins enriched at the Maurer's clefts, a number of human proteins were identified (Table 9). Proteins included in Table 9 were enriched in the Maurer's clefts sample at least 5 times compared to a 3D7 control. A number of these proteins have reported roles in membrane binding, membrane trafficking and lipid biogenesis. Two annexins - A4 and A11 - were identified. Annexins are characterised by Ca^{2+} -dependent binding to membranes and the presence of a 70 residue "annexin repeat" (Gerke and Moss, 2002). The *Plasmodium*-infected red blood cell has elevated levels of Ca^{2+} compared to uninfected red blood cells, and the $[\text{Ca}^{2+}]$ is higher in the cytosol of infected red blood cells than within the parasite (Kramer and Ginsburg, 1991). The top protein in Table 9, annexin A4, is involved in Ca^{2+} -dependent membrane vesicle aggregation and may play a role in the formation lipid rafts (Gerke et al., 2005). It is interesting to consider the possibility that annexin A4 plays a role in the formation of cholesterol rich domains at the Maurer's clefts as it has been suggested that such regions are an important requirement for PfEMP1 trafficking from the Maurer's clefts to the red blood cell surface (Frankland et al., 2006). Annexin A11 is a midbody protein and is required for cytokinesis, where it may regulate the incorporation of new membrane need for cytokinetic abscission (Gerke et al., 2005, Tomas et al., 2004). Another calcium-dependent membrane-binding protein, copine 3, was also enriched at the Maurer's clefts. Many of the enriched proteins are involved in endosomal/multivesicular body formation and trafficking. These include protein VAC14 homolog, which is involved in regulation of PI(3,5)P₂ levels, which in turn control membrane trafficking in the endosomal system (Sbrissa et al., 2007, Dong et al., 2010). Similarly, syntaxin 7 is present in late endosomes and is needed for fusion with lysosomes (Mullock et al., 2000). Both tumor susceptibility gene 101 protein (TSG101) and vacuolar protein sorting-associated protein 28 homolog (VPS28) are components of the ESCRT-I complex which regulates vesicular trafficking and exosome biogenesis (Baietti et al., 2012). This set of human proteins involved in membrane trafficking raises the tantalising possibility that remnants from the host cell's trafficking system are co-opted for use by the parasite. Investigating the localisation of these proteins in *P. falciparum*-infected red blood cells will help to ascertain these possible host-parasite interactions.

Table 9 *Homo sapiens* proteins enriched in the Maurer's clefts

Accession	Protein name	Number of significant ms/ms spectra			
		Expt. 1		Expt. 2	
		MCs	3D7	MCs	3D7
sp P09525 ANXA4_HUMAN	Annexin A4	18	0	26	1
sp P50995 ANX11_HUMAN	Annexin A11	15	0	18	0
sp O75131 CPNE3_HUMAN	Copine-3	9	0	11	0
sp Q15173 2A5B_HUMAN	Serine/threonine-protein phosphatase 2A 56 kDa regulatory subunit beta isoform	9	0	10	0
sp Q08AM6 VAC14_HUMAN	Protein VAC14 homolog	7	0	12	0
sp P53396 ACLY_HUMAN	ATP-citrate synthase	6	0	12	1
sp Q96FJ2 DYL2_HUMAN	Dynein light chain 2, cytoplasmic	3	0	3	0
sp B2RUZ4 SMIM1_HUMAN	Small integral membrane protein 1	2	0	2	0
sp O15400 STX7_HUMAN	Syntaxin-7	2	0	3	0
sp Q99816 TS101_HUMAN	Tumor susceptibility gene 101 protein	2	0	6	0
sp Q9UK41 VPS28_HUMAN	Vacuolar protein sorting-associated protein 28 homolog	2	0	4	0

4.2.4 Annexin A4 and protein VAC14 homolog partially co-localise with REX1 at the Maurer's clefts

We used immunofluorescence assays to investigate the location of two of the human proteins identified in Table 9 - annexin A4 (ANXA4) and protein VAC14 homolog (VAC14). In red blood cells infected with wildtype 3D7 parasites, ANXA4 partly co-localised with REX1 at the Maurer's clefts (Figure 4.3A). The parasitophorous vacuole (or possibly the parasite) is also labelled with ANXA4. Uninfected red blood cells showed a punctate distribution of ANXA4 throughout the cell. Likewise, VAC14 partly co-localised with REX1 at the Maurer's clefts in infected red blood cells, and showed a punctate distribution in uninfected cells (Figure 4.3B). The parasite nucleus was strongly labelled by the VAC14 antibody which could represent cross-reaction with a *P. falciparum* protein.

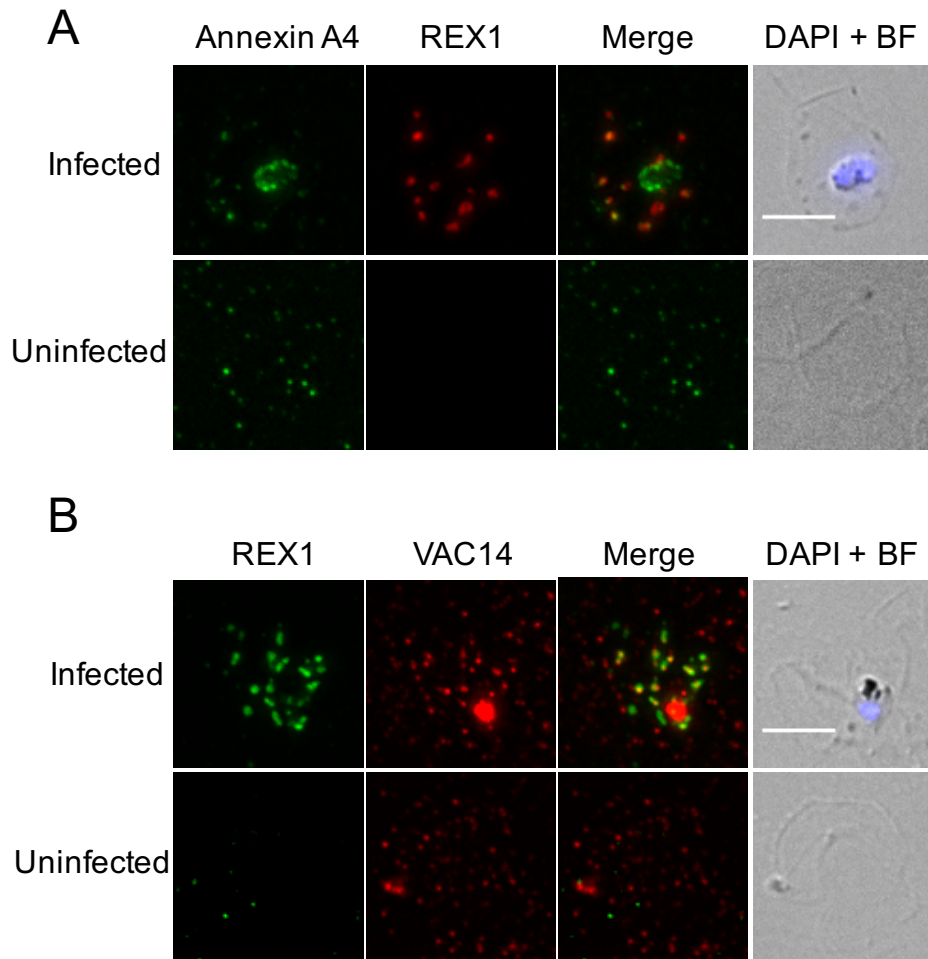


Figure 4.3 Annexin A4 and protein VAC14 homolog co-locate with REX1

Infected (wildtype 3D7) and uninfected red blood cells were fixed in an ice-cold solution of acetone and methanol (9:1) for 5 min. Alexa Fluor® 488- and Alexa Fluor® 568-conjugated secondary antibodies were used. DAPI was used to stain the nucleus. Scale bars = 5 μ m.

(A) Samples were probed with a mouse polyclonal α Annexin A4 and rabbit α REX1

(B) Samples were probed with mouse α REX1 and rabbit polyclonal α Protein VAC14 homolog

4.2.5 Epitope-tagging of established and putative Maurer's clefts proteins

Having identified a number of putative and established Maurer's clefts proteins by mass spectrometry, 8 were selected for GFP-tagging. Four proteins with unpublished localisation (GEXP10, PF13_0275, PTP5 and PTP6) and four known Maurer's clefts proteins (MAHRP1, REX2, GEXP07 and Pf11_0505) were targeted. Proteins were C-terminally GFP-tagged and expressed as episomes under the CRT promoter using the pGLUX vector (Boddey et al., 2009). The tagged proteins were a mixture of PEXEL and PNEPs and were of varied length with some containing features such as transmembrane domains (Figure 4.4A). Expression of the chimeric proteins was verified by Western blot of saponin-lysed parasite extracts (green arrowheads, Figure 4.4B). Parasites expressing MAHRP1-GFP showed a band close to the predicted molecular mass 56.0 kDa (Figure 4.4). The MAHRP1-GFP lane also has a band at approximately double the size ~97 kDa which possibly represents a dimeric form of the tagged protein, a possible artefact of overexpression. The proteins GEXP07-GFP and GEXP10-GFP show bands of the expected size after processing of the PEXEL motif (49.5 and 49.0 kDa respectively). The PNEPs REX1-GFP (expected mass 110.0 kDa), REX2-GFP (expected mass 37.8 kDa) and Pf11_0505-GFP (expected mass 37.3 kDa) all migrated close to their predicted molecular masses. The PEXEL proteins PTP5-GFP, PTP6-GFP and Pf13_0275-GFP also migrated close to their predicted molecular weights after PEXEL cleavage (90.1, 52.6 and 50.0 kDa respectively). Interestingly, PTP5-GFP shows a degradation pattern reminiscent of that observed for REX1 (Hawthorne et al., 2004a). All the GFP-tagged samples show a band (or bands) below the 28 kDa marker that probably represent degraded GFP (Figure 4.4).

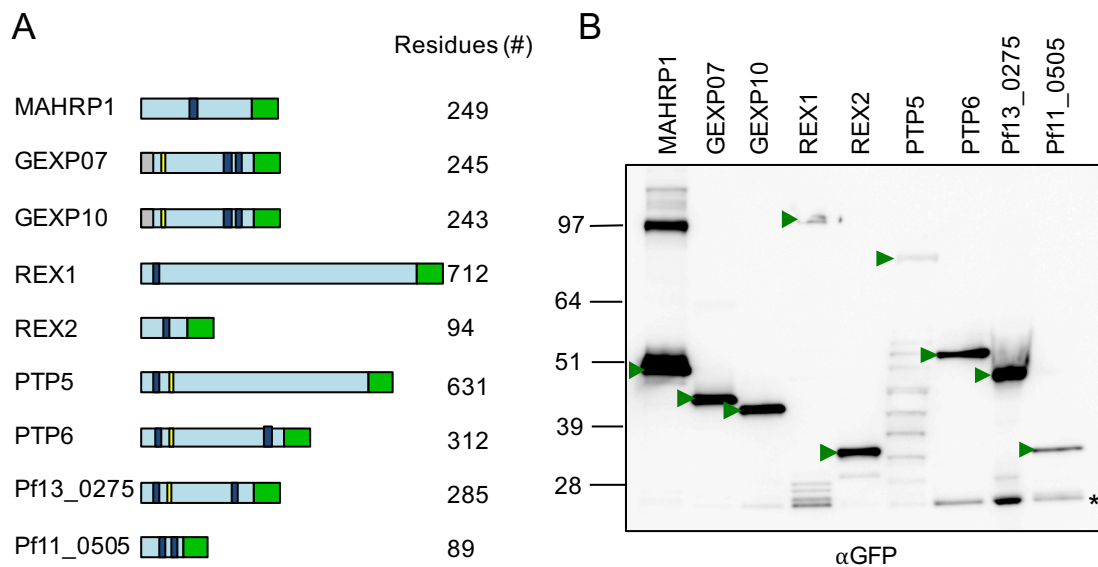


Figure 4.4 Schema and validation of exported proteins that were GFP-tagged

(A) Schematic representations of full-length GFP-tagged proteins with the residue length of the untagged protein. Grey = predicted signal peptide, dark blue = predicted transmembrane domain, yellow = PEXEL motif, green = GFP tag

(B) Western analysis of saponin lysates from transfectant parasites, probed with α GFP. Green arrowheads indicate bands that represent the full-length GFP-tagged chimeras. Molecular mass standard is in kDa. Asterisk (*) represents degraded GFP.

Having confirmed correct expression of the GFP chimaeric proteins, we next examined the localisation of the proteins by live-cell microscopy. Infected red blood cells were observed at the early trophozoite stage after the onset of immobilisation of the Maurer's clefts to facilitate image capture. All transfectants showed a punctate fluorescence pattern in the red blood cell cytoplasm (Figure 4.5). One protein, Pf11_0505-GFP, also showed significant fluorescence within the parasite or parasitophorous vacuole (Figure 4.5), which is consistent with a previous Pf11_0505-GFP transfectant (Heiber et al., 2013). The fluorescence pattern exhibited by the GFP-transfectants is typical of Maurer's clefts puncta. However, to confirm the Maurer's clefts localisation of the proteins, immunofluorescence microscopy was performed.

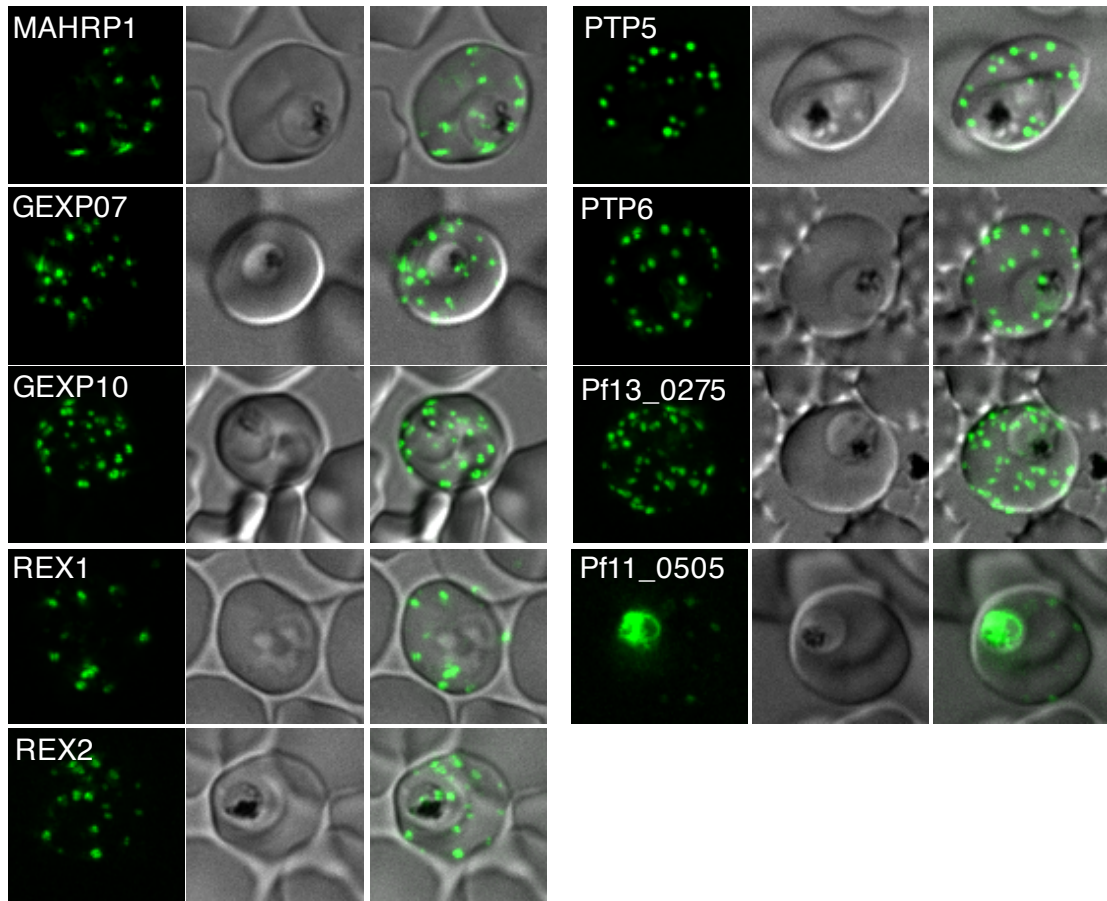


Figure 4.5 Live-cell fluorescence microscopy of GFP-tagged transfectant parasites

Infected red blood cells were suspended in RPMI and imaged on sealed glass coverslips at 37°C. The parasites are imaged at the early trophozoite stage after Maurer's clefts immobilisation. Dispersed puncta are present in all the transfectant-infected red blood cells. Significant fluorescence within the parasite is observed in the Pf11_0505-GFP sample.

Immunofluorescence assays were performed to confirm the location of the exported GFP-tagged proteins. The fixed cells were labelled with α GFP and α REX1. All the GFP-tagged proteins co-located with the Maurer's clefts marker REX1 (Figure 4.6). This confirms that GEXP10, PTP5, PTP6 and Pf13_0275 are located at the Maurer's clefts, and further validates the Maurer's clefts enrichment described above as a useful tool to identify novel Maurer's clefts proteins.

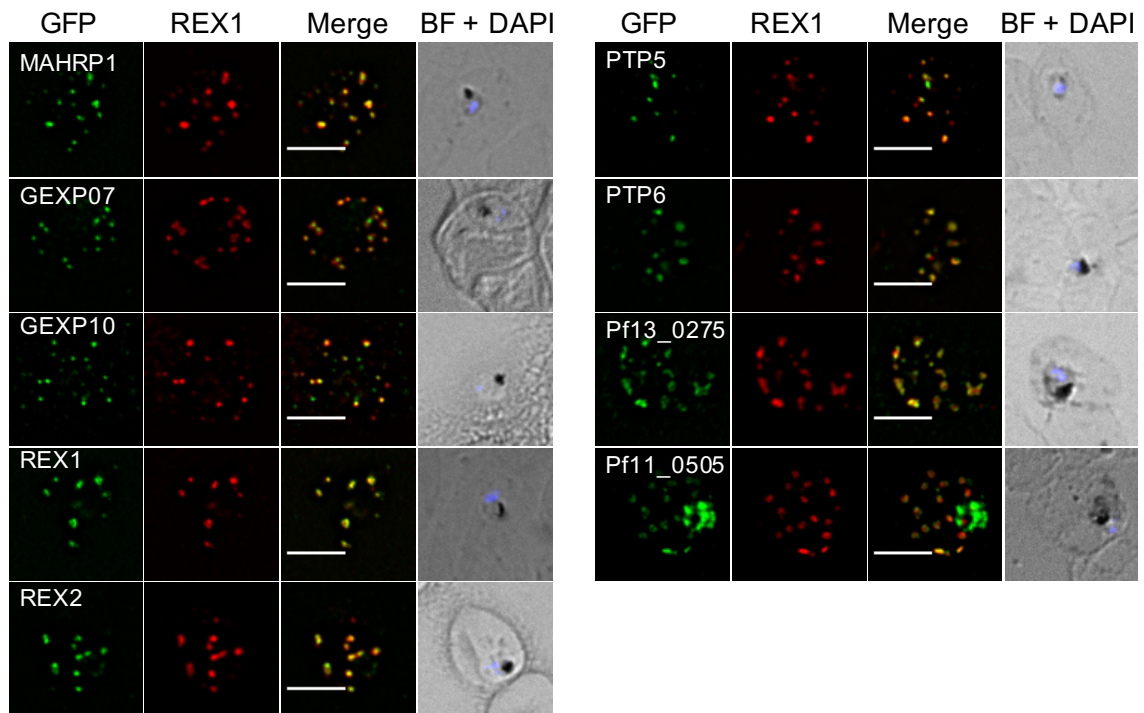


Figure 4.6 Immunofluorescence analysis of transfectant parasites

Infected red blood cells were fixed in ice-cold acetone and methanol (9:1) and labelled with α GFP (1:300) and α REX1 (1:1000), followed by Alexa Fluor® 488 and Alexa Fluor® 568 and nuclear stain DAPI. The Maurer's clefts are discrete REX1-labelled puncta. BF = bright field. Scale bars = 5 μ m.

4.2.6 Super-resolution analysis of protein localisation within the Maurer's clefts

Maurer's clefts are sub-compartmentalised, with some proteins localising quite distinctly to the centre, edges or tethers of the clefts (McMillan et al., 2013, Hanssen et al., 2008a). Yet other proteins such as PfEMP1 seem to have a broader distribution throughout the organelle (McMillan et al., 2013). The localisation of REX1 and MAHRP1 within the subdomains of the Maurer's clefts has been well described. The distribution of REX1 was quantitated by analysis of immuno-gold labelled electron micrographs, and is largely located on the Maurer's clefts edges and to a lesser extent on the tethers (Hanssen et al., 2008a). Similarly, previous 3D-SIM analysis has shown that REX1 localises to the Maurer's clefts periphery, forming a ring around a centralised MAHRP1-containing region.(McMillan et al., 2013). To expand our understanding of this spatial segregation, we mapped the locations of each of the GFP-tagged proteins within the Maurer's clefts. The orthologues GEXP07-GFP and GEXP10-GFP were labelled with Maurer's clefts markers and observed using 3D-SIM. One study showed by immuno-electron microscopy that a GEXP07-HA construct was trafficked to the Maurer's clefts (Sleebs et al., 2014). The immuno-labelling in these electron micrographs was concentrated around the centre of the Maurer's clefts, although no quantitation was performed (Sleebs et al., 2014). When co-labelled with α REX1, GEXP07-GFP appears to be in discrete puncta surrounded by the more dispersed REX1 fluorescence signal (Figure 4.7A, top panel). The GEXP07-GFP and MAHRP1 signals show co-localisation in what is presumably the central area of the Maurer's clefts' lamellae (Figure 4.7A, bottom panel). Similarly, GEXP10-GFP is located in the centre of the clefts, ringed by REX1 and partially co-localising with MAHRP1 (Figure 4.7B, top and bottom panels). The relative positions of PfEMP1 (probed with α ATS, which labels the cytoplasmic face of the protein) and GEXP10-GFP were also investigated. Although there was a degree of co-localisation, the distribution of PfEMP1 was more varied than that of GEXP10-GFP (Figure 4.7B, middle panel).

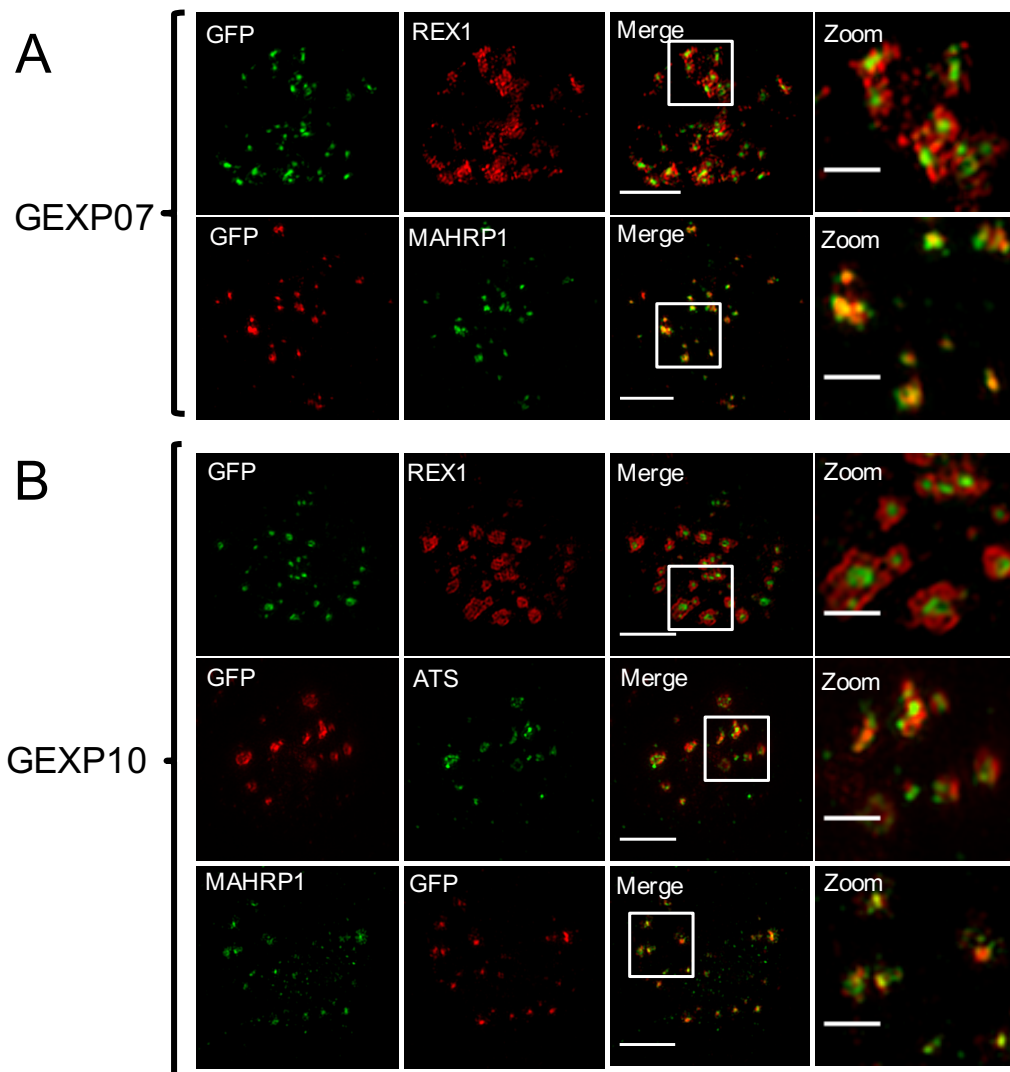


Figure 4.7 3D-SIM analysis GEXP07-GFP- and GEXP10-GFP-infected red blood cells.

Infected cells were acetone/methanol (9:1) fixed and Alexa Fluor 488 and Alexa Fluor 568 secondary antibodies were used.

(A) GEXP07-GFP-infected red blood cells probed with α GFP and either α REX1 or α MAHRP1.

(B) GEXP10-GFP-infected red blood cells probed with α GFP and either α REX1, α ATS or α MAHRP1. Images are average projections and have been adjusted for brightness and contrast. Merge scale bars = 3 μ m, zoom scale bars = 1 μ m.

Transfectants expressing two of the newly identified Maurer's clefts proteins, PTP5-GFP and PTP6-GFP were examined by 3D-SIM. In Figure 4.8A (top panel), PTP6-GFP appears to form a ring of fluorescence around REX1. Co-staining with α ATS show PfEMP1 is arranged in rings that are partially enclosed by PTP6-GFP (Figure 4.8A, bottom panel). The localisation of PTP5-GFP partly overlaps with REX1 (Figure 4.8B). Both PTP5-GFP and PTP6-GFP exhibit a ring-shaped pattern and it is likely that these proteins are on the outer edges of the Maurer's clefts. The circular (or occasionally "horse-shoe") distribution of PTP5-GFP around the clefts edges can be appreciated in Figure 4.8C.

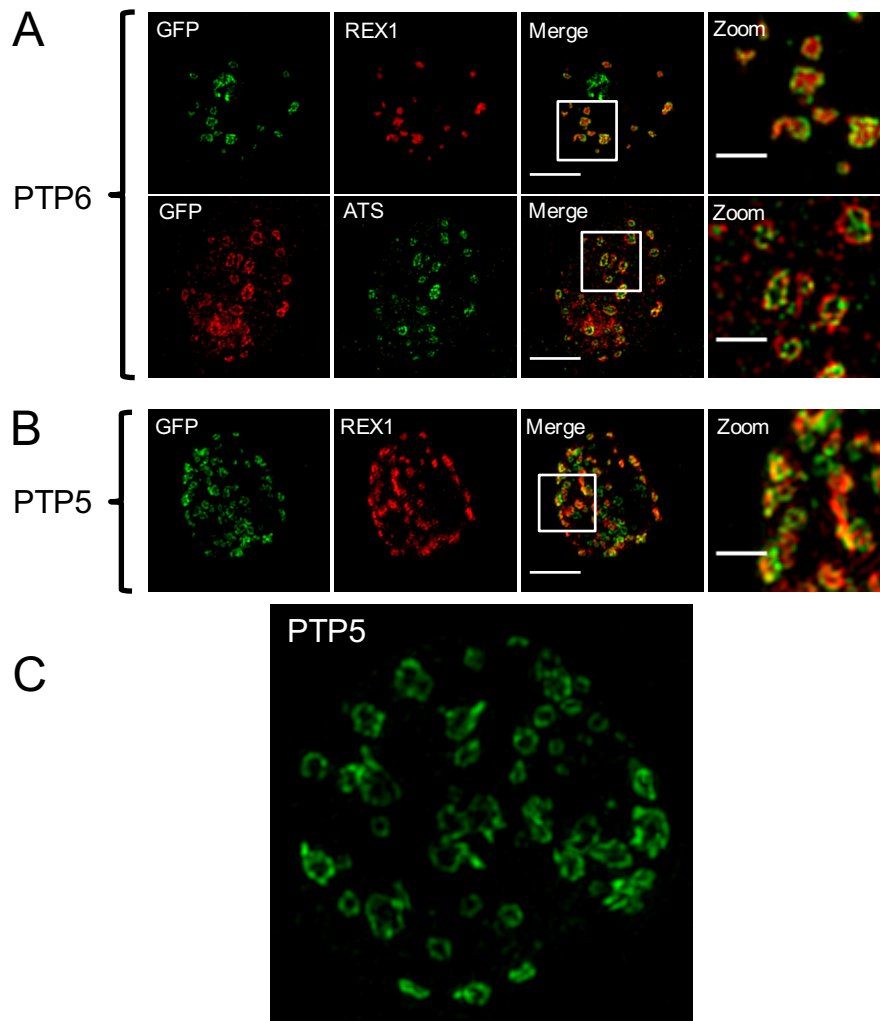


Figure 4.8 3D-SIM analysis of PTP5-GFP- and PTP6-GFP-infected red blood cells.

Samples were fixed in ice-cold acetone/methanol (9:1) before immuno-labelling. Alexa Fluor 488 and Alexa Fluor 568 secondary antibodies were used. Images shown are maximum projections

(A) PTP6-GFP-expressing parasitised red blood cells were labelled with α GFP, α REX1 and α ATS

(B and C) PTP5-GFP parasites were labelled with α GFP and α REX1 antibodies. Merge scale bars = 3 μ m, zoom scale bars = 1 μ m

As previously shown, REX1-GFP showed some co-localisation with PfEMP1 in the Maurer's clefts (Figure 4.9A) (McMillan et al., 2013). The PNEP REX2 has been extensively studied as a model protein for analyses of protein export motifs (Spielmann et al., 2006, Haase et al., 2009, Gruring et al., 2012). The function of REX2 is still unknown. As shown in Figure 4.9B (top panel), REX2-GFP is interspersed with REX1 around the edges of the Maurer's clefts. This protein shows limited overlap with PfEMP1 (Figure 4.9B, bottom panel). Lastly, we looked at the localisation of Pf13_0275-GFP. The distribution of Pf13_0275-GFP is ring-shaped around the edges of the clefts, punctuated in some regions with REX1 (Figure 4.9C). This survey of the sub-compartmentalisation of the Maurer's clefts provides information on the relative positions of proteins with the clefts, including the four novel Maurer's clefts proteins GEXP10, PTP5, PTP6 and Pf13_0275.

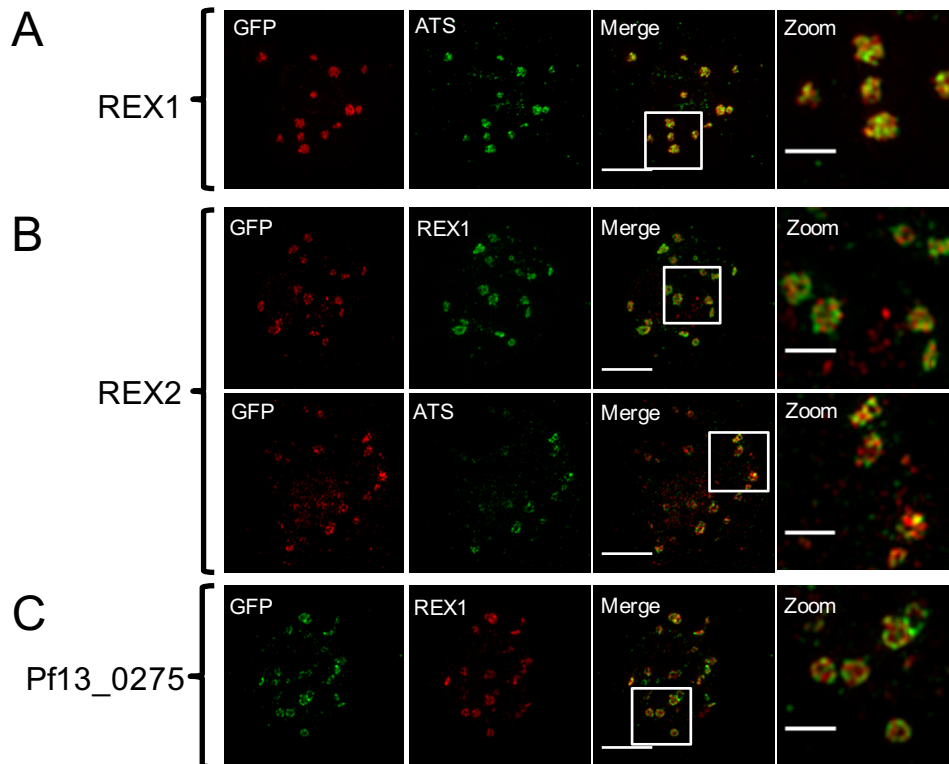


Figure 4.9 3D-SIM analysis of REX1-GFP, REX2-GFP and Pf13_0275-GFP localisation

Samples were fixed in ice-cold acetone/methanol (9:1) before immuno-labelling. Alexa Fluor 488 and Alexa Fluor 568 secondary antibodies were used. Images shown are maximum projections.

(A) REX1-GFP-infected red blood cells labelled with α GFP and α ATS.

(B) REX2-GFP-expressing parasites labelled with α GFP and α REX1 or α ATS.

(C) Pf13_0275-GFP-infected red blood cells labelled with α GFP and α REX1. Merge

scale bars = 3 μ m, zoom scale bars = 1 μ m.

4.3 Discussion

The Maurer's clefts are crucial for PfEMP1 trafficking to the red blood cell membrane. Characterising the properties of the Maurer's clefts as a discrete organelle has been difficult due to their close association with the red blood cell membrane during the trophozoite stage (Vincensini et al., 2005). The enrichment process developed here (Section 4.2.1) exploits the mobility of ring-stage Maurer's clefts, and provides a protein profile at a stage when PfEMP1 is transiting through the Maurer's clefts *en route* to the red blood cell membrane. In the past, identifying Maurer's clefts proteins has been made difficult by the presence of parasite and host contaminants in the Maurer's clefts preparations, and issues with antibody cross-reactivity with unidentified proteins (Adisa et al., 2001, Albano et al., 1999, Wickert et al., 2003a, Hayashi et al., 2001, Vincensini et al., 2005). The present study uses hypotonic lysis of high parasitaemia (but unpurified) ring-stage infected red blood cells, resulting in less contamination from irrelevant parasite proteins than methods using detergent solubilisation. The coupling of the purification with epitope-tagging and co-localisation studies has led to the localisation of GEXP10, PTP5, PTP6 and Pf13_0275 - four novel Maurer's clefts proteins. Additionally, a further five putative Maurer's clefts proteins were identified: Pf08_0091, Pf10_0024, STARP, PfE0050w and PfC0085c. These candidates should be investigated by epitope-tagging before they are considered *bona fide* Maurer's clefts proteins.

We were able to identify the majority of known ring-stage expressed Maurer's clefts proteins. However, there are some notable exceptions. One group is the FIKK kinase family members (FIKK4.1, FIKK9.3, FIKK9.6 and FIKK12) that have been reported (as data not shown) to localise to Maurer's clefts during the ring-stage (Nunes et al., 2007). These proteins may transiently interact with the Maurer's clefts, and may not be abundant enough to be identified using this method. A limitation of the current method for analysis of the Maurer's clefts protein profile is that the hypotonic lysis may result in the loss of some protein species. Although no proteins have yet been shown to be soluble within the lumen of the Maurer's clefts, if there are such proteins they would be lost due to the loss of Maurer's clefts membrane integrity.

A number of proteins are expressed and trafficked to the Maurer's clefts from ~24 h post-invasion (i.e. after Maurer's cleft docking) and as such were not identified in the present

analysis. Such proteins include PTP2, PfVAP, TEX1, MSPR6 (which associates with “cloudy” structures adjacent to the Maurer’s clefts membrane), PFL0065w (PF3D7_1201300), PFL2515c (PF3D7_1252300), PIESP2, PfCRMP1-2, PfEPF1, 3 and 4, and Pf332 (Nilsson et al., 2012, Heiber et al., 2013, Nacer et al., 2015, Kulangara et al., 2012, Thompson et al., 2007, Mbengue et al., 2013). Similarly, we did not detect proteins from the variant surface antigen families STEVOR, RIFIN or PfMC-2TM. A detailed analysis of the small variant surface antigens reported that these proteins localise primarily to the red blood cell membrane which may explain their absence from our preparation (Bachmann et al., 2015). Analysis of immobilised Maurer’s clefts may shed light on later processes occurring at these organelles.

The role (if any) of vesicle-mediated transport to or from the Maurer’s clefts remains the great mystery of *P. falciparum* protein trafficking, as the parasite does not export classical trafficking machinery. Despite being devoid of obvious membrane trafficking machinery, mature red blood cells evidently do contain proteins as remnants of systems such as endosomes/lysosomes (**Table 9**). We have identified a number of human proteins that are enriched at the Maurer’s clefts that may play a role in membrane trafficking at these organelles. Proteins such as VPS28, TSG101, syntaxin, and VAC14 are involved in the budding and fusion of membranes in the mammalian endocytic pathway. We confirm by immunofluorescence that both ANXA4 and VAC14 are recruited to the Maurer’s clefts in *P. falciparum*-infected red blood cells. Thus far, no *Plasmodium* Maurer’s clefts proteins show similarity to any known membrane trafficking proteins, making it a possibility that *P. falciparum* scavenges host proteins for building the exomembrane system. The use of host membrane trafficking systems by other pathogens has been described. For example, proteomic analysis of another intracellular parasite, *Chlamydia trachomatis*, provided evidence that this bacterium hijacks the host retrograde trafficking pathway (Aeberhard et al., 2015). Moreover, RNA viruses are known to co-opt host endocytic pathways (including proteins such as the ESCRT complex) for effective replication (Illynska et al., 2013, Barajas et al., 2014, Kovalev et al., 2016). In this context, the observation that the spiral scaffolding underpinning knobs closely resembles ESCRT-III-induced vesicle budding is especially interesting (Watermeyer et al., 2016). Enrichment and mass spectrometric studies of knobs could shed light on the possibility of human endocytic protein involvement in their formation. Instances of host protein hijacking by *P. falciparum* have been reported. These include the mining of host actin

from the red blood cell cytoskeleton to link to the Maurer's clefts, and the potential use of the human TRiC complex as a chaperone for exported *Plasmodium* proteins (Cyrklaff et al., 2011, Kilian et al., 2013, Rug et al., 2014, Dearnley et al., 2016, Batinovic et al., 2017).

Recently, a proteomics approach was used to study the *P. yoelii* 'remodellome' through subcellular fractionation and LC-MS/MS analysis, followed by validation by GFP-tagging (Siau et al., 2016). Structures that remodel the *P. falciparum*-infected red blood cell, such as knobs, EDVs and J-dots could potentially be investigated using methodology similar to our approach to profiling the Maurer's clefts proteins.

Sub-localisation within the Maurer's clefts has been described in the literature for a handful of proteins, and has been investigated by immuno-electron microscopy or super-resolution fluorescence microscopy. The proteins MAHRP1 and GEXP07 have been localised to the centre of the clefts (McMillan et al., 2013, Sleebs et al., 2014) and we show that the novel Maurer's clefts protein GEXP10 co-localises with MAHRP1. So far, three proteins (MAHRP1, SBP1 and PTP1) are known to be required for PfEMP1 to reach the Maurer's clefts (Spycher et al., 2008, Maier et al., 2007, Rug et al., 2014). The current understanding of protein export in *P. falciparum* is that proteins (including Maurer's clefts proteins and PfEMP1 itself) are translocated via PTEX to the red blood cell cytoplasm and may travel to the Maurer's clefts as chaperoned complexes (Gruring et al., 2012, Beck et al., 2014, Elsworth et al., 2014, Batinovic et al., 2017). It is possible that the centrally located Maurer's clefts proteins play roles in PfEMP1 stabilisation and insertion into the Maurer's cleft membrane. The lack of observable exported PfEMP1 in MAHRP1, SBP1 and PTP1 knockout parasites could be due to loss of this function.

Previous reports show that REX1, PTP1, and MAHRP2 are located on the edges of the clefts (Hanssen et al., 2008a, Rug et al., 2014, Pachlatko et al., 2010). In the present study, we show that PTP5, PTP6, Pf13_0275 and REX2 also localise primarily to the Maurer's clefts edges. Three of these Maurer's clefts edge proteins (REX1, PTP5 and PTP6) are thought to be involved in the transport PfEMP1 from the Maurer's clefts to red blood cell surface i.e. in their absence PfEMP1 is trafficked to the Maurer's clefts, but is not efficiently trafficked from there to the red blood cell membrane. Super-resolution microscopy showed that REX1 co-located with PfEMP1 and others have demonstrated a

direct interaction between these two proteins (Batinovic et al., 2017). It is possible that PfEMP1 is initially captured by the proteins in the centre of the Maurer's clefts, and is then transferred to proteins located at the periphery before being transported to the red blood cell membrane.

Chapter 5 : Investigation of protein interaction networks at the Maurer's clefts

5.1 Introduction

The many proteins exported by *P. falciparum* are thought to have diverse functions in enabling parasite survival and virulence. Recent studies have identified complexes of secreted proteins in the parasitophorous vacuole that play roles in facilitating export of parasite virulence determinants (Batinovic et al., 2017). However, little is currently known about how exported proteins interact in the red blood cell cytoplasm and at the Maurer's clefts in order to drive host cell remodelling.

Exported proteins may form interactions with other parasite proteins, or with host proteins. For example, the virulence protein PfEMP1 binds to the knob-forming protein KAHRP via electrostatic interactions, which in turn interacts with the cytoskeletal proteins spectrin, actin and band 4.1 (Voigt et al., 2000, Oh et al., 2000, Ganguly et al., 2015). These interactions underpin the mechanism of adhesion of infected red blood cells to blood vessel walls and also contribute to the host cell's increased rigidity (Rug et al., 2006, Ganguly et al., 2015, Watermeyer et al., 2016, Dearnley et al., 2016).

While knockout phenotype analysis and sub-localisation data is available for many individual Maurer's clefts proteins, protein-protein interactions at the Maurer's clefts have been less well studied. In the present study, we have shown that some Maurer's clefts proteins segregate within the organelle (Section 4.2.6). Proteins such as GEXP07, GEXP10 and MAHRP1 are located in the central region of the cleft compartment, whilst REX1, PTP5, PTP6 and others are located at the cleft periphery. The virulence protein PfEMP1 appears to be distributed throughout both the central and peripheral parts of the Maurer's clefts. Extensive knockout studies of exported proteins in *P. falciparum* point to important or essential functions of many of these Maurer's clefts proteins (Table 8) (Maier et al., 2008). With this information in hand, we wanted to analyse protein-protein interactions to contextualise the spatial organisation and function of different proteins. We used the parasite lines generated in Section 4.2.5 to investigate interactions between Maurer's clefts proteins. Eight epitope-tagged proteins were analysed by co-precipitation and tandem mass spectrometry across two biological replicates in order to identify protein-protein interactions. We found that spatial segregation of proteins within the

clefts correlates with their protein interactions as determined by mass spectrometry. Furthermore, we characterised a conditional knockdown of the Maurer's clefts protein GEXP07. Despite co-localising with, and co-precipitating with PfEMP1, knockdown of GEXP07 does not seem to affect PfEMP1 trafficking to the red blood cell surface.

5.2 Results

5.2.1 A network of protein-protein interactions in the centre of the Maurer's clefts

Immunofluorescence microscopy of transfectants expressing the chimaeras GEXP07-GFP and GEXP10-GFP and dual labelled with antibodies recognising endogenous MAHRP1 revealed that all three proteins are located in the central part of the Maurer's clefts, where GEXP10 also partially co-locates with PfEMP1 (Section 4.2.6). We went on to investigate protein-protein interactions using co-immunoprecipitation. Parasites expressing GEXP07-GFP, GEXP10-GFP and MAHRP1-GFP were harvested at the trophozoite stage, solubilised in Triton X-100 (1% v/v) and prepared for immunoprecipitation using GFP-Trap (for the complete method, see Section 2.6.5). Co-immunoprecipitated proteins were eluted from the GFP-Trap beads and analysed by Western blot. All three proteins were successfully immunoprecipitated (Figure 5.1A, green arrowheads). Endogenous MAHRP1 was strongly co-immunoprecipitated with GEXP07-GFP and more weakly precipitated with GEXP10-GFP (Figure 5.1B, blue arrowheads). The MAHRP1-GFP construct also appears to co-immunoprecipitate with endogenous MAHRP1 (open arrow), although it is also possible that this band represents a degradation product of MAHRP1-GFP (Figure 5.1B).

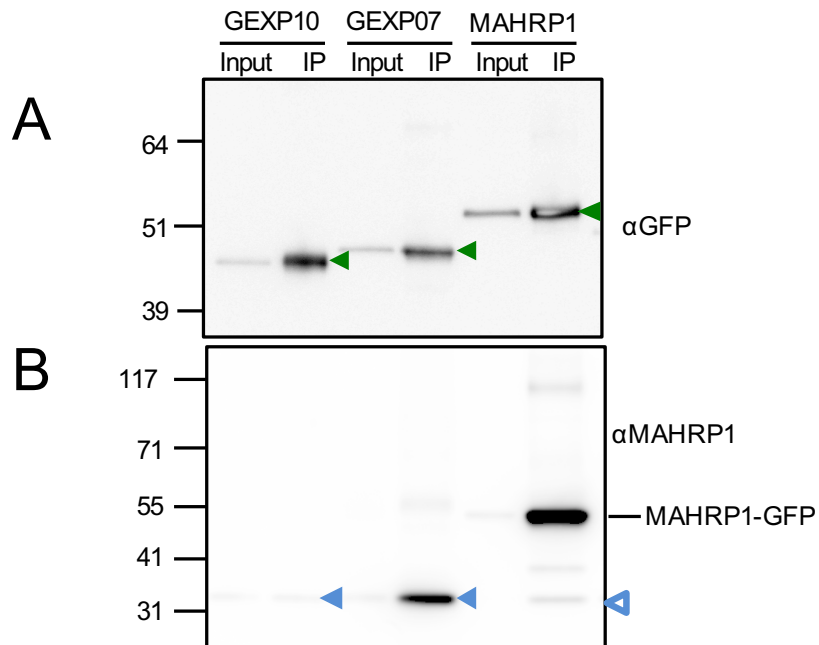


Figure 5.1 Immunoprecipitation analysis of GEXP10-GFP, GEXP07-GFP and MAHRP1-GFP.

- (A) Membrane was probed with α GFP (1:1000). Green arrowheads indicate the immunoprecipitated GFP-tagged protein.
- (B) Membrane was probed with α MAHRP1 (1:1000). Blue arrowheads indicate the co-immunoprecipitated MAHRP1 protein.

Signal was detected by the addition of HRP-conjugated secondary antibodies and chemiluminescent reactions. Input represents the pre-cleared Triton X-100-soluble material. Loading of 'Input' fractions was 4% of the total sample compared to 100% of the IP sample. Markers indicate molecular mass in kDa.

After Western blot confirmation, the immunoprecipitated proteins were subjected to LC-MS/MS. Two biological replicates were performed and the eluates from the transfectants were compared to mock precipitated samples of wild-type 3D7 run in parallel. Protein hits were considered significant if they were identified in both experiments and were at least 5 times enriched compared to the control, and had at least two significant MS/MS spectra in each replicate. Mass spectrometry analysis of the MAHRP1-GFP IP sample identified 4 exported interacting proteins: GEXP10, GEXP07, PIESP2 and the PEXEL-containing protein PF3D7_0501000 (Table 10). A previous study showed that PF3D7_0501000 and PIESP2 can be knocked out and that PfEMP1 trafficking and cytoadherence is unaffected in their absence (Maier et al., 2008). Although not detected in both replicates in the present study, PfEMP1 has been shown by Western blot to co-precipitate with MAHRP1-GFP (Batinovic et al., 2017). Two abundant cytoplasmic proteins, 60S ribosomal protein (PF3D7_1424100) and 14-3-3 protein (PF3D7_0818200) were also detected, probably due to non-specific binding.

Similarly to MAHRP1-GFP, GEXP07-GFP co-immunoprecipitated GEXP10, MAHRP1 and PF3D7_0501000 (Table 11). Two PTEX components (HSP101 and PTEX150) were also identified, possibly as a result of a portion of the overexpressed GEXP07-GFP construct accumulating in the parasitophorous vacuole where it is presumably exported by the PTEX. Interestingly, PfEMP1 also co-precipitated with GEXP07-GFP. Proteins co-precipitating with GEXP10-GFP (Table 12) were identical to the exported proteins co-precipitating with MAHRP1-GFP, as depicted in Figure 5.2A. Taken together, this suggests close association between GEXP07, MAHRP1, GEXP10 and PF3D7_0501000, and possibly PIESP2 and PfEMP1 (Figure 5.2B). The solubilisation process used in this immunoprecipitation study and the abundance of host proteins in samples lead to the identification of some human proteins by mass spectrometry. Human proteins that were significantly enriched from all samples analysed by LC-MS/MS are presented in Tables S1-S8.

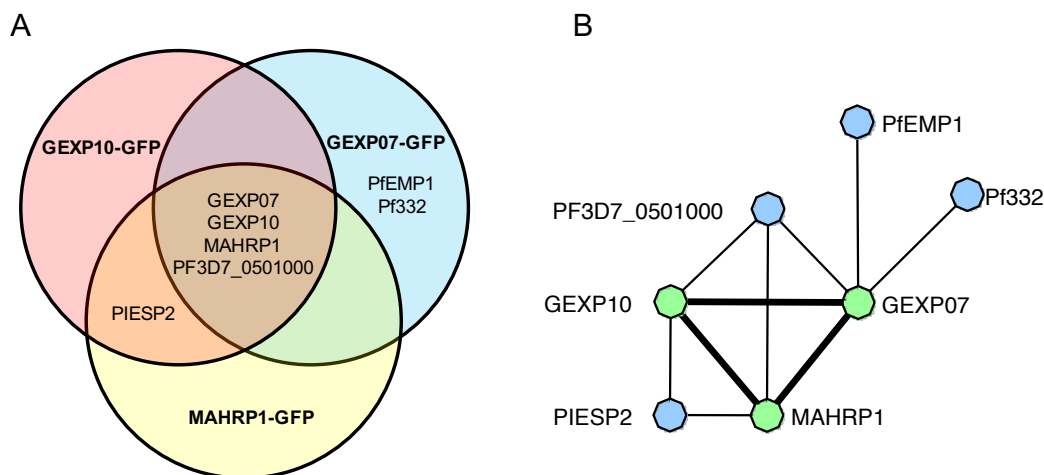


Figure 5.2 Diagrams of exported protein interactions identified by immunoprecipitation of MAHRP1-GFP, GEXP07-GFP and GEXP10-GFP.

(A) Venn diagram of exported proteins co-immunoprecipitating with each GFP-tagged protein.

(B) Network of co-precipitating exported proteins from MAHRP1-GFP, GEXP07-GFP and GEXP1-GFP tandem mass spectrometry experiments. Green nodes = GFP-tagged proteins, blue nodes = exported, thin edge = co-precipitated protein, thick edge = proteins co-precipitated each other. Network image was built using NAViGaTOR 2.3.

Table 10 Mass spectrometry analysis of MAHRP1-GFP co-precipitated proteins

PlasmoDB ID	Protein name	Number of significant ms/ms spectra			
		Experiment 1		Experiment 2	
		MAHRP1	3D7	MAHRP1	3D7
PF3D7_1370300	membrane associated histidine-rich protein (MAHRP1)	8	0	11	0
PF3D7_0818200	14-3-3 protein (14-3-3I)	8	1	8	1
PF3D7_1301700	Plasmodium exported protein (hyp8), (GEXP07)	8	0	9	0
PF3D7_0501200	parasite-infected erythrocyte surface protein (PIESP2)	4	0	10	0
PF3D7_0501000	Plasmodium exported protein	2	0	4	0
PF3D7_0113900	Plasmodium exported protein (hyp8), (GEXP10)	2	0	6	0
PF3D7_1424100	60S ribosomal protein L5, putative	2	0	5	0

Table 11 Mass spectrometry analysis of GEXP07-GFP co-precipitated proteins

PlasmoDB ID	Protein name	Number of significant ms/ms spectra			
		Experiment 1		Experiment 2	
		GEXP07	3D7	GEXP07	3D7
PF3D7_1301700	Plasmodium exported protein (hyp8), (GEXP07)	20	0	10	0
PF3D7_0706000	importin-7, putative	18	0	10	0
PF3D7_1116800	heat shock protein 101 (HSP101)	15	0	2	0
PF3D7_1436300	translocon component PTEX150 (PTEX150)	12	0	4	0
PF3D7_0113900	Plasmodium exported protein (hyp8), (GEXP10)	7	0	4	0
PF3D7_1370300	membrane associated histidine-rich protein (MAHRP1)	6	0	5	0
PF3D7_0501000	Plasmodium exported protein	4	0	4	0
PF3D7_1149000	antigen 332, DBL-like protein (Pf332)	6	0	3	0
PF3D7_0524000	karyopherin beta (KASbeta)	3	0	3	0
PF3D7_1240900	erythrocyte membrane protein 1, PfEMP1 (VAR)	7	0	3	0
PF3D7_1002900	conserved Plasmodium protein	2	0	2	0
PF3D7_1346100	protein transport protein SEC61 subunit alpha (SEC61)	2	0	4	0
PF3D7_1456800	V-type H(+)-translocating pyrophosphatase, putative (VP1)	2	0	2	0

Table 12 Mass spectrometry analysis of GEXP10-GFP co-precipitated proteins

PlasmoDB ID	Protein name	Number of significant ms/ms spectra			
		Experiment 1		Experiment 2	
		GEXP10	3D7	GEXP10	3D7
PF3D7_0113900	Plasmodium exported protein (hyp8), (GEXP10)	21	0	17	0
PF3D7_1301700	Plasmodium exported protein (hyp8), (GEXP07)	8	0	5	0
PF3D7_0501200	parasite-infected erythrocyte surface protein (PIESP2)	10	0	3	0
PF3D7_0501000	Plasmodium exported protein,	3	0	2	0
PF3D7_1370300	membrane associated histidine-rich protein (MAHRP1)	4	0	3	0

5.2.2 Generation of an inducible knockdown transfectant parasite line

In order to further investigate the role of GEXP07 in PfEMP1 trafficking, conditional knockdown parasites were generated (plasmids were a gift of Dr Paul Gilson, Burnet Institute). The GEXP07 protein comprises 245 residues, and has a canonical signal sequence, a PEXEL motif and two predicted transmembrane domains (Figure 5.3A). The GEXP07 gene was tagged by homologous recombination at the 3' end with a HA epitope and a glmS ribozyme/riboswitch sequence which allows conditional degradation of the GEXP07 mRNA (Prommana et al., 2013, McHugh et al., 2015).

Localisation of the GEXP07-HA-glmS construct to the Maurer's clefts was confirmed by colocalisation with the Maurer's clefts marker SBP1 (Figure 5.3B). Knockdown of the protein was achieved by the addition of increasing concentrations of glucosamine (0, 2.5, 5 and 10 mM) to trophozoite stage parasite culture. Parasites were harvested 48 h after the addition of glucosamine, followed by immunoblotting of the saponin-lysed infected red blood cells. Knockdown of the GEXP07-HA-glmS protein was observed. At the highest concentration of glucosamine (10 mM) the decrease was estimated to be ~90% when compared to GAPDH, a parasite housekeeping protein (Figure 5.3C).

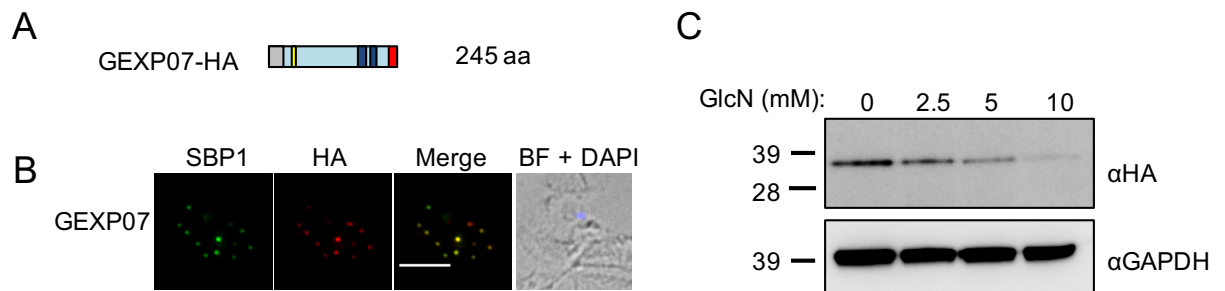


Figure 5.3 Characterisation of a GEXP07-HA-glmS conditional knockdown parasite line

- (A) Schematic representation of GEXP07-HA-glmS protein. Grey = predicted signal sequence, yellow = PEXEL, dark blue = predicted transmembrane domains, red = HA tag.
- (B) Immunofluorescence microscopy confirming expression of the HA-tagged GEXP07 co-localising with Maurer's clefts marker SBP1. Infected red blood cells were fixed in acetone and methanol (9:1). DAPI was used to stain the nucleus. Scale bar = 5 μ m.
- (C) Knockdown of GEXP07-HA-glmS with increasing concentrations of glucosamine (GlcN). Membranes were probed with α HA (1:1000) or α GAPDH (1:1000), then developed by the addition of HRP-conjugated secondary antibodies and chemiluminescent detection. Molecular masses are in kDa.

5.2.3 Partial knockdown of GEXP07 does not affect other exported proteins

The present study and a previous study (Sleebbs et al., 2014) localised GEXP07 to the Maurer's clefts. Considering the demonstrated interaction between GEXP07 and PfEMP1 (as well as other exported proteins, such as MAHRP1 which has been shown to play an important role in PfEMP1 export), we hypothesised that knockdown of GEXP07 may have an effect on transfer of PfEMP1 or other exported proteins to the Maurer's clefts. The GEXP07-HA-glmS-infected red blood cells were treated with either 0 mM or 10 mM glucosamine from ~24 h post-invasion for 48 h before acetone/methanol fixation and preparation for immunofluorescence assays. As higher concentrations of glucosamine may have an effect on parasite growth (Prommana et al., 2013) a 3D7 control was also included. The resident Maurer's clefts protein REX1 showed no difference in distribution at concentrations of 10 mM glucosamine in either 3D7- or GEXP07-HA-glmS-infected red blood cells, nor was there any change in numbers of Maurer's clefts based on the number of REX1-labelled fluorescent puncta (Figure 5.4). As expected, there was no labelling of the Maurer's clefts with α HA in 3D7 samples. Untreated GEXP07-HA-glmS samples showed HA-labelling at the Maurer's clefts as anticipated (Figure 5.4). Weaker HA-labelling was also detected in the 10 mM-treated GEXP07-HA-glmS sample indicating that knockdown of GEXP07-HA-glmS is incomplete. This is consistent with the ~10% GEXP07-HA detected by Western blotting (Figure 5.3C).

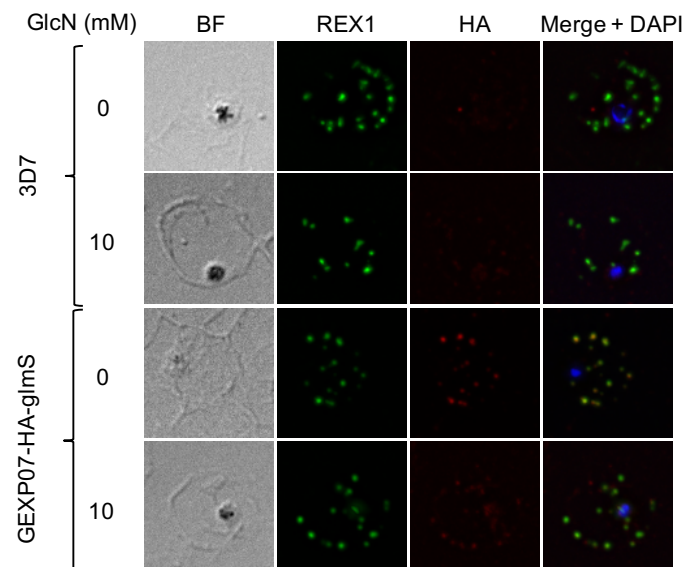


Figure 5.4 Immunofluorescence analysis of glucosamine-treated 3D7 and GEXP07-HA-glmS parasites

Wild-type 3D7- and GEXP07-HA-glmS-infected red blood cells were treated with either 0 mM or 10 mM glucosamine for 48 h, then fixed in acetone and methanol (9:1). Samples were probed with α REX1 (1:1000) and α HA (1:300), AlexaFluor® secondary antibodies and were co-labelled with the nuclear stain DAPI.

We next assessed the localisation of PfEMP1 (probing with α ATS) and the Maurer's clefts marker SBP1. Co-precipitation studies identified PfEMP1 as a possible interacting partner of GEXP07 (Table 11), so we hypothesised that knockdown of GEXP07 might affect PfEMP1 localisation at the Maurer's clefts. Trophozoite stage parasites were treated with either 0 or 10 mM glucosamine for 48 h. Both the 3D7 and GEXP07-HA-glmS samples showed PfEMP1 co-locating with SBP1 at the Maurer's clefts (Figure 5.5A), indicating that knockdown (albeit incomplete) does not affect PfEMP1 transport to the Maurer's clefts. Immunofluorescence analysis of KAHRP, a protein component of knobs, showed that the localisation of this protein at the red blood cell periphery showed no obvious perturbation associated with knockdown of GEXP07-HA-glmS parasites (Figure 5.5B).

Some Maurer's clefts proteins such as REX1, PTP5 and PTP6 are involved in the transport of PfEMP1 from the Maurer's clefts to the red blood cell surface (Dixon et al., 2011, Maier et al., 2008). To investigate the possibility that GEXP07 plays a role in this process, we analysed the binding of infected red blood cells to the human endothelial ligand CD36. Binding to CD36 is mediated by surface-exposed PfEMP1 presented on knobs at the red blood cell membrane and as such can be used as an indirect measurement of PfEMP1 on the red blood cell surface. Wild-type 3D7 and GEXP07-HA-glmS parasites (8 h window) were treated with either 0 or 10 mM glucosamine at the late ring stage, and were harvested for analysis 48 h later in the following asexual cycle. The infected red blood cells were flowed through a chamber coated with CD36 and the number of bound cells counted. As previously reported, there was no significant difference in mean between wild-type 3D7 glucosamine treated and untreated samples (Figure 5.5C; $p = 0.15$, unpaired t-test) (Batinovic et al., 2017). Likewise, there was no significant difference between the GEXP07-HA-glmS treated and untreated samples (Figure 5.5C; $p = 0.11$, unpaired t-test). This could suggest that GEXP07 does not have a role in PfEMP1 trafficking. Alternatively, it is possible that the decreased level of GEXP07 is still sufficient to enable its normal function.

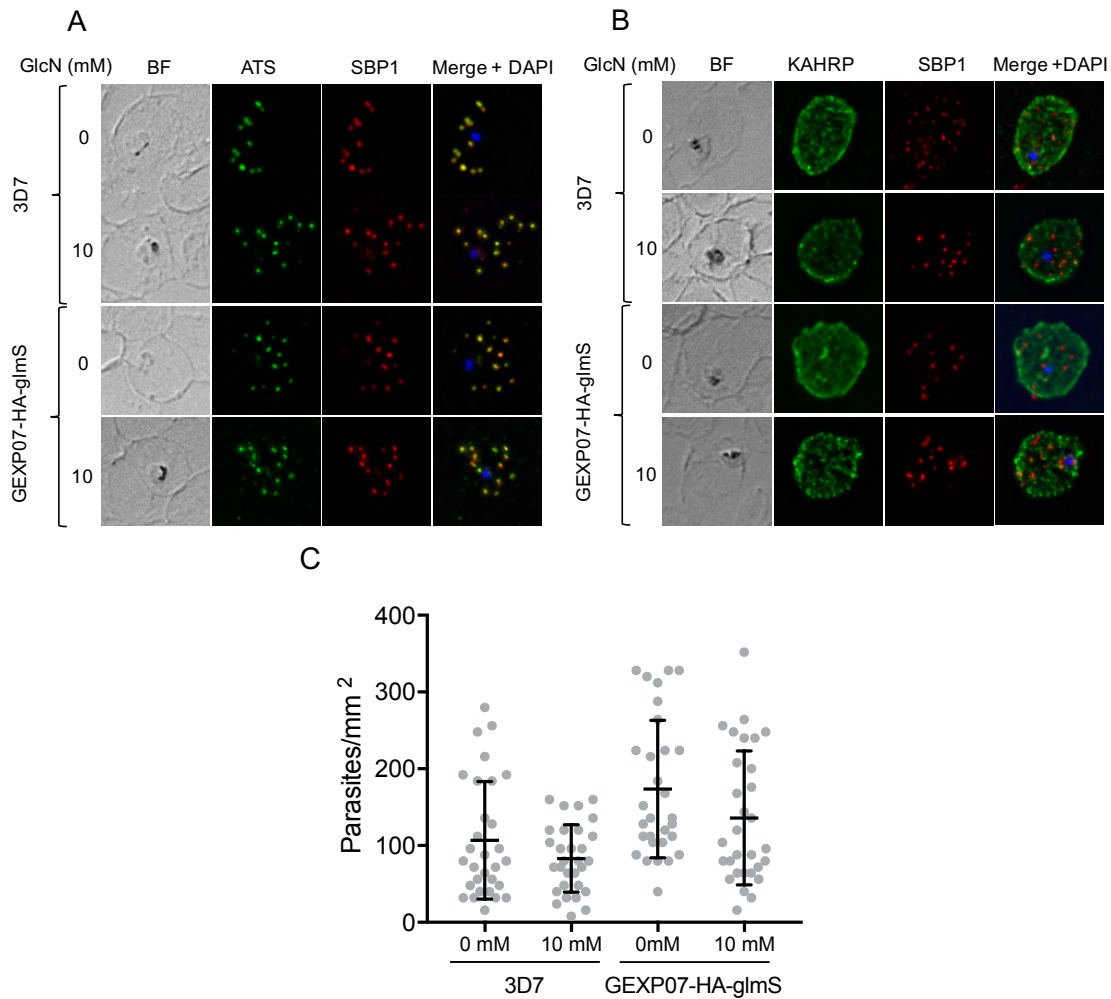


Figure 5.5 Analysis of the effect of GEXP07 knockdown on exported proteins

For immunofluorescence, infected red blood cells (wildtype 3D7 or GEXP07-HA-glmS) were treated with either 0 mM or 10 mM glucosamine for 48 h before fixation in acetone and methanol (9:1). AlexaFluor® secondary antibodies were used and DAPI (blue) was added to visualise nuclear material.

- (A) Samples were probed with α ATS (green; 1:100) and α SBP1 (red; 1:300)
- (B) Samples were probed with α KAHRP (green; 1:300) and α SBP1 (red; 1:300)
- (C) Analysis of binding of infected red blood cells to CD36. The infected red blood cells were flowed through a chamber coated with recombinant human CD36 at 0.1 Pa, washed with RPMI and the number of bound cells were counted for 10 randomly selected, pre-programmed fields of view. Counts are plotted as dots representing the amount of bound infected red blood cells per mm² in a field of view. Counts are from 3 biological replicates (n = 3). Error bars represent the SEM and the longer horizontal bar is the mean.

5.2.4 Two Maurer's clefts edge proteins co-immunoprecipitate and share similarities

We investigated the co-precipitating proteins of both REX1-GFP and PTP5-GFP-expressing parasites using immunoblotting and tandem mass spectrometry. Using GFP-Trap®, REX1-GFP was successfully immunoprecipitated (Figure 5.6A, green arrowhead). In Figure 5.6A, a ladder of ~5 smaller bands is evident as well as the full-length REX1-GFP band (as well as a band representing free GFP at ~28 kDa). This degradation of the N-terminal region of REX1 may reflect processing of putative PEST sequences within the protein (Hawthorne et al., 2004a). As expected, REX1-GFP co-precipitated with PfEMP1 (Figure 5.6B, blue arrowhead). The REX1-GFP immunoprecipitation fractions were analysed by tandem mass spectrometry in parallel with a wild-type 3D7 control. This analysis identified four variants of PfEMP1 that co-precipitated with REX1-GFP, strongly supporting an interaction between REX1 and PfEMP1 (Table 13). Despite its involvement in a complex interacting with PfEMP1 (Figure 5.2B) (Batinovic et al., 2017), the Maurer's clefts protein MAHRP1 did not co-precipitate with REX1 (Figure 5.6). One possible explanation for this is that PfEMP1 may be transferred to the edge of the Maurer's clefts (away from MAHRP1 and GEXP07) and interact with REX1 before transit to the red blood cell membrane. Interestingly, REX1-GFP co-precipitated with the tether protein MAHRP2 (Table 13).

Both REX1 and MAHRP2 have been observed by immunoelectron microscopy associated with tethers - tubular structures that protrude from the edge of Maurer's clefts and occasionally link them to the red blood cell membrane or parasitophorous vacuole membrane (Hanssen et al., 2008a, Pachlatko et al., 2010). Like REX1, MAHRP2 has also been shown to co-precipitate with PfEMP1 (Batinovic et al., 2017). Attempts to genetically ablate MAHRP2 have thus far been unsuccessful, suggesting that this gene may be essential (Pachlatko et al., 2010).

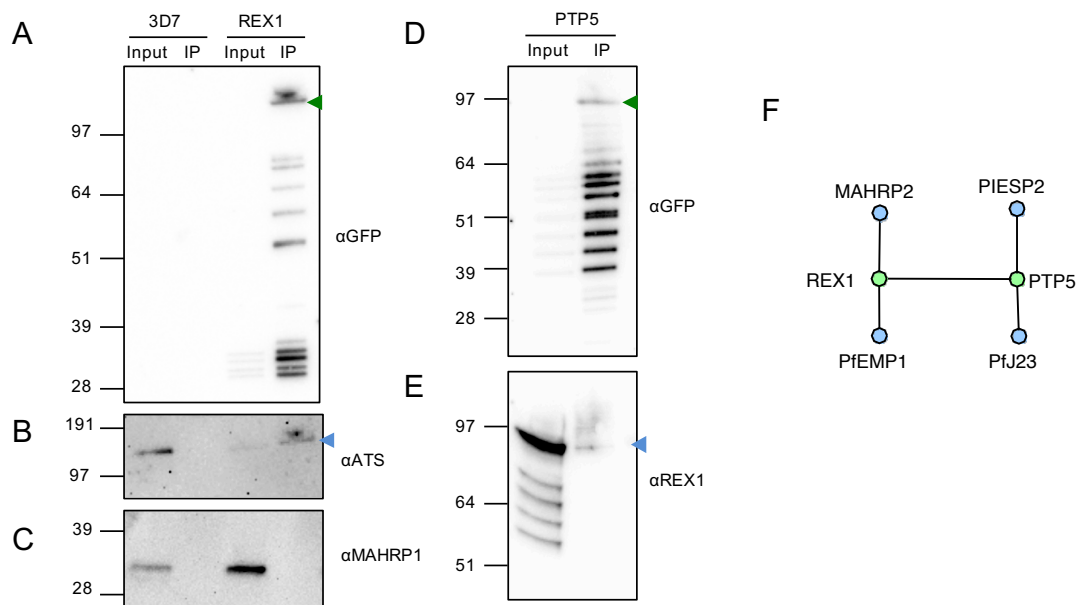


Figure 5.6 Immunoprecipitation of wild-type 3D7, REX1-GFP and PTP5-GFP parasite lines

Trophozoite-stage parasites were harvested and solubilised in 1% (v/v) Triton X-100 in PBS and subjected to immunoprecipitation using GFP-Trap. The bound material was eluted from the beads and either analysed by SDS-PAGE (4% input was loaded cf. IP) or mass spectrometry. Molecular masses are in kDa.

- (A) Wild-type 3D7 and REX1-GFP IPs probed with α GFP. Green arrowhead indicates full-length immunoprecipitated REX1-GFP
- (B) Wild-type 3D7 and REX1-GFP IPs probed with α ATS. Blue arrowhead indicates immunoprecipitated PfEMP1
- (C) Wild-type 3D7 and REX1-GFP IPs probed with α MAHRP1. MAHRP1 was not co-precipitated with REX1-GFP
- (D) PTP5-GFP IPs probed with α GFP. Green arrowhead indicates full-length immunoprecipitated PTP5-GFP
- (E) PTP5-GFP IPs probed with α REX1. Blue arrowhead indicates co-precipitated full-length REX1
- (F) Network of co-precipitating proteins from REX1-GFP and PTP5-GFP tandem mass spectrometry. Green nodes = GFP-tagged proteins, blue nodes = exported proteins, thin edge = co-precipitated protein. Network image was built using NAViGaTOR 2.3.

Full-length PTP5-GFP was co-precipitated from Triton X-100-soluble infected red blood cell material using GFP-Trap beads (Figure 5.6D, green arrowhead). A ladder pattern presumably representing N-terminally truncated PTP5-GFP was also which is reminiscent of the pattern observed in the REX1-GFP sample (Figure 5.6A). The sequence of PTP5 has 11 predicted PEST sites (EMBOSS epestfind; emboss.bioinformatics.nl/cgi-bin/emboss/epestfind). There are ~15 bands in the PTP5-GFP IP lane of Figure 5.6D, 3 of which are between 28-39 kDa and likely represent degraded GFP. It is possible that proteolytic cleavage of PTP5 and REX1 occurs at the putative PEST sequences. Whether this processing is important for protein function is unclear.

Tandem mass spectrometry analysis of proteins co-precipitating with PTP5-GFP identified REX1 as the protein with the highest number of significant MS/MS spectra (Table 14). Probing immunoblots with α REX1 showed that full-length REX1 was weakly co-immunoprecipitated with PTP5-GFP (Figure 5.6E). Another two Maurer's clefts proteins, PfJ23 (a paralogue of PTP5) and PIESP2, also co-precipitated with PTP5-GFP (Table 14). Both PfJ23 and PIESP2 (also referred to as PfE60) were identified in the original proteomic analysis of the Maurer's clefts (Vincensini et al., 2005). Knockout of PIESP2 in the CS2 parasite strain did not result in significantly decreased surface-exposed PfEMP1 after upselection on CSA (Maier et al., 2008). In the same study, PfJ23 was unable to be knocked out (Maier et al., 2008). The PfJ23 and PTP5 proteins have an additional paralogue, Pf10_0024, which was successfully disrupted and did not affect PfEMP1 surface exposure (Maier et al., 2008). Although not detected by mass spectrometry in the present study, previous immunoblotting work showed that PTP5-GFP co-precipitates with PfEMP1 (Batinovic et al., 2017). Both REX1 and PTP5 are required for efficient transfer of PfEMP1 from the Maurer's clefts to the red blood cell membrane, possibly with the involvement of two essential proteins (MAHRP2 and PfJ23) (Maier et al., 2008, Dixon et al., 2011, Pachlatko et al., 2010). A representation of the co-precipitating proteins (including non-exported proteins) of both REX1-GFP and PTP5-GFP is presented in Figure 5.6F.

Table 13 Mass spectrometry analysis of REX1-GFP co-precipitated proteins

PlasmoDB ID	Protein name	Number of significant ms/ms spectra			
		Experiment 1		Experiment 2	
		REX1	3D7	REX1	3D7
PF3D7_0935900	ring-exported protein 1 (REX1)	127	0	91	0
PF3D7_1318800	translocation protein SEC63 (SEC63)	47	0	31	0
PF3D7_0600200	erythrocyte membrane protein 1, PfEMP1 (VAR)	16	0	34	0
PF3D7_0632500	erythrocyte membrane protein 1, PfEMP1 (VAR)	6	0	18	0
PF3D7_0705500	inositol-phosphate phosphatase, putative	6	0	10	0
PF3D7_1412500	actin II (ACT2)	6	0	5	0
PF3D7_1100100	erythrocyte membrane protein 1, PfEMP1 (VAR)	3	0	2	0
PF3D7_0927100	conserved Plasmodium protein, unknown function	2	0	2	0
PF3D7_1200400	erythrocyte membrane protein 1, PfEMP1 (VAR)	2	0	2	0
PF3D7_1353200	membrane associated histidine-rich protein (MAHRP2)	2	0	3	0

Table 14 Mass spectrometry analysis of PTP5-GFP co-precipitated proteins

PlasmoDB ID	Protein name	Number of significant ms/ms spectra			
		Experiment 1		Experiment 2	
		PTP5	3D7	PTP5	3D7
PF3D7_1002100	EMP1-trafficking protein (PTP5)	27	2	53	0
PF3D7_0935900	ring-exported protein 1 (REX1)	14	0	10	0
PF3D7_1001900	Plasmodium exported protein (hyp16), (PfJ23)	9	0	10	0
PF3D7_0524000	karyopherin beta (KASbeta)	5	0	5	0
PF3D7_0721100	conserved Plasmodium protein, unknown function	5	0	4	0
PF3D7_0501200	parasite-infected erythrocyte surface protein (PIESP2)	2	0	3	0

5.2.5 Networks of exported protein interactions at the Maurer's clefts

Efforts were made to identify parasite proteins that co-precipitate four additional GFP-tagged Maurer's clefts proteins. One protein, Pf11_0505-GFP, was not efficiently co-precipitated by GFP-Trap and was not analysed further. Three proteins (REX2-GFP, PTP6-GFP and Pf13_0275-GFP) were successfully co-precipitated (Figure 5.7A, B; green arrowheads).

REX2-GFP co-precipitated with two components of the EPIC complex, PV1 and EXP3 (Table 17). Co-precipitation studies with epitope-tagged PV1 identified REX2 as an interacting protein, suggesting that REX2 may associate with the EPIC complex prior to export through the PTEX (Batinovic et al., 2017). We did not identify any Maurer's clefts proteins interacting with REX2 - this may be due to inefficient export of the REX2-GFP construct from the parasitophorous vacuole. Only one exported protein, MAHRP2, was identified in mass spectrometric analysis of Pf13_0275-GFP co-precipitating proteins (Table 16). These genes encoding these proteins are adjacent. Immunofluorescence analysis showed PF13_0275 to be located near the edges of Maurer's clefts, whilst MAHRP2 is known to localise to tethers (Pachlatko et al., 2010). It is possible that PF13_0275-GFP functions in the link between the Maurer's clefts and the tethers.

PTP6-GFP was apparently not connected to the wider network of Maurer's clefts proteins (Figure 5.8A) but did co-precipitate with several other exported proteins: STARP, MESA, PF3D7_0702500 (a Maurer's clefts protein; previously PF07_0008), PF3D7_1002000 (previously PF10_0024) and PF3D7_031700 (previously PFC0085c) (Table 15) (Heiber et al., 2013). Except for MESA (which is associated with the red blood cell cytoskeleton), all of these proteins were identified in the Maurer's clefts protein analysis in Table 6 (Section 4.2.2) (Coppel et al., 1988). Previous work showed that a PTP6 knockout parasite line had disrupted transport of PfEMP1 to the red blood cell membrane, yet the majority of the PTP6-interacting proteins found here are relatively uncharacterised (Maier et al., 2008). Further investigation into the roles of these proteins may provide insight into how PTP6 influences PfEMP1 transport.

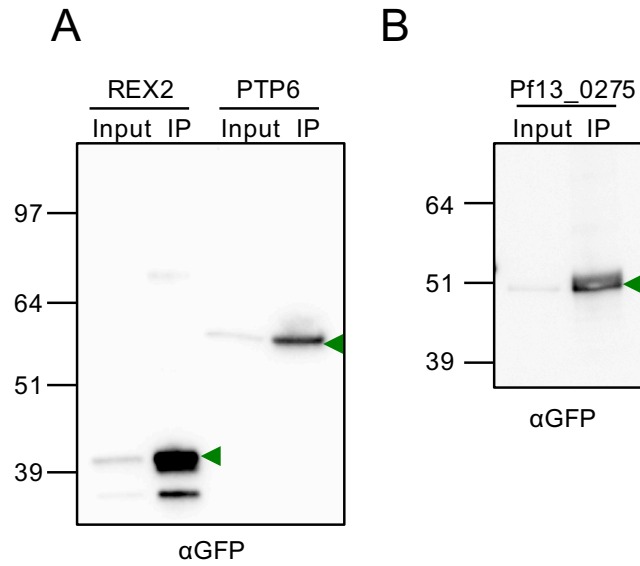


Figure 5.7 Immunoprecipitation with REX2-GFP, PTP6-GFP and Pf13_0275-GFP

Trophozoite-stage parasites were harvested and solubilised in 1% (v/v) Triton X-100 in PBS and subjected to co-immunoprecipitation by GFP-Trap. The bound material was eluted from the beads and either analysed by SDS-PAGE (4% input was loaded cf. IP) or tandem mass spectrometry. Molecular masses are in kDa.

(A) REX2-GFP and PTP6-GFP IPs probed with α GFP. Green arrowhead indicates the full-length GFP-tagged protein. Another band above the 64 kDa marker is likely to represent a dimerised form of the tagged protein.

(B) Pf13_0275-GFP IP probed with α GFP. Green arrowhead indicates the full-length GFP-tagged protein

Table 15 Mass spectrometry analysis of PTP6-GFP co-precipitated proteins

PlasmoDB ID	Protein name	Number of significant ms/ms spectra			
		Experiment 1		Experiment 2	
		PTP6	3D7	PTP6	3D7
PF3D7_1302000	EMP1-trafficking protein (PTP6)	22	0	26	0
PF3D7_0702500	Plasmodium exported protein, unknown function	12	0	4	0
PF3D7_0500800	mature parasite-infected erythrocyte surface antigen (MESA)	9	0	4	0
PF3D7_0301700	Plasmodium exported protein, unknown function	8	0	7	0
PF3D7_0702300	sporozoite threonine and asparagine-rich protein (STARP)	8	0	10	0
PF3D7_1002000	Plasmodium exported protein (hyp2), unknown function	7	0	13	0
PF3D7_0109900.1	unspecified product	2	0	2	0
PF3D7_1221900	conserved Plasmodium membrane protein, unknown function	2	0	2	0

Table 16 Mass spectrometry analysis of Pf13_0275-GFP co-precipitated proteins

PlasmoDB ID	Protein name	Number of significant ms/ms spectra			
		Experiment 1		Experiment 2	
		PF13_0275	3D7	PF13_0275	3D7
PF3D7_0524000	karyopherin beta (KASbeta)	42	0	29	0
PF3D7_1353100	Plasmodium exported protein (Pf13_0275)	26	0	21	0
PF3D7_0706000	importin-7, putative	23	0	7	0
PF3D7_1246200	actin I (ACT1)	23	4	3	0
PF3D7_0815200	importin beta, putative	9	0	3	0
PF3D7_0422400	40S ribosomal protein S19 (RPS19)	7	1	2	0
PF3D7_0628300	choline/ethanolaminephosphotransferase, putative (CEPT)	4	0	6	0
PF3D7_1038000.1	antigen UB05	3	0	2	0
PF3D7_1353200	membrane associated histidine-rich protein (MAHRP2)	3	0	3	0

Table 17 Mass spectrometry analysis of REX2-GFP co-precipitated proteins

PlasmoDB ID	Protein name	Number of significant ms/ms spectra			
		Experiment 1		Experiment 2	
		REX2	3D7	REX2	3D7
PF3D7_1129100	parasitophorous vacuolar protein 1 (PV1)	13	1	16	0
PF3D7_0936000	ring-exported protein 2 (REX2)	7	0	8	0
PF3D7_0524000	karyopherin beta (KASbeta)	4	0	16	0
PF3D7_1024800	exported protein 3 (EXP3)	4	0	15	0
PF3D7_1228600	merozoite surface protein 9 (MSP9)	4	0	2	0

5.2.6 Analysis of the Maurer's clefts protein interaction network

The exported proteins from the co-precipitation studies from 8 epitope-tagged proteins described here are summarised in an interaction network in Figure 5.8A. Within this network, there is a four-node true clique termed the 'inner clique' as the proteins localise to the central subcompartment of the Maurer's clefts (Figure 5.8B). This clique includes MAHRP1 (and is connected to PfEMP1 through GEXP07) and could represent a protein complex involved in transport and insertion of PfEMP1 into the Maurer's clefts (Spycher et al., 2008).

Mass spectrometry co-immunoprecipitation studies with two resident Maurer's clefts proteins (PTP1 and SEMP1) and the Maurer's clefts cargo protein PfEMP1 have been published (Rug et al., 2014, Dietz et al., 2014, Batinovic et al., 2017). A network summary of published Maurer's clefts protein mass spectrometry co-immunoprecipitation studies and data from the present study is presented in Figure 5.8C.

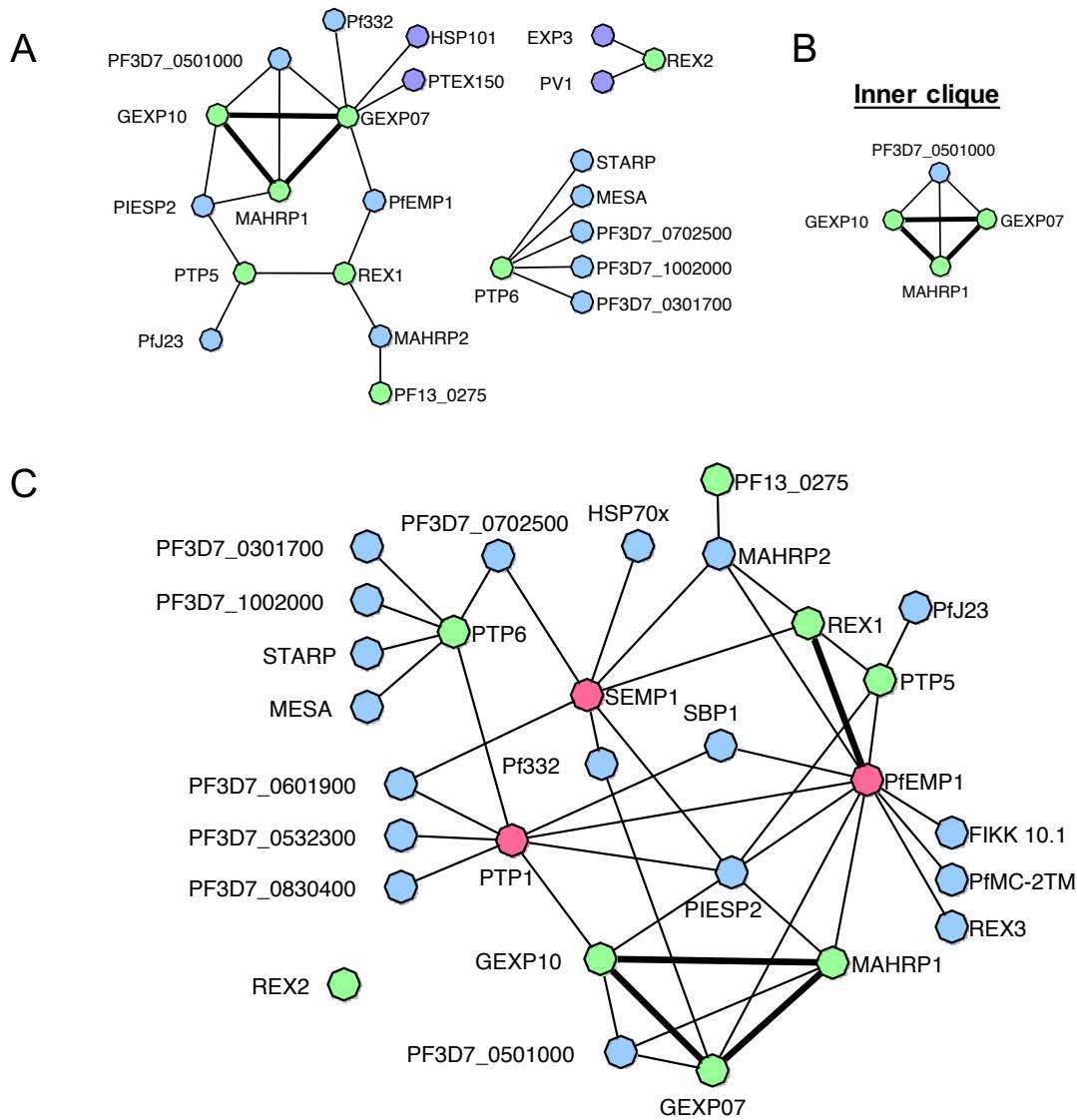


Figure 5.8 Network map and analysis of co-precipitating proteins

- (A) Network of exported and parasitophorous vacuole-located co-precipitating proteins from all GFP-tagged proteins analysed by GFP-Trap and tandem mass spectrometry. Green nodes = GFP-tagged proteins, blue nodes = exported proteins, purple nodes = parasitophorous vacuole proteins, thin edge = co-precipitated protein, thick edge = proteins co-precipitated each other. Network image was built using NAViGaTOR 2.3.
- (B) Clique identified within the network map that contains proteins that localise to the centre of the Maurer's clefts.
- (C) The interaction network map represents co-immunoprecipitated exported proteins from the present study and the literature, where SEMP1-HA, PTP1-HA and PfEMP1B-GFP were precipitated (Dietz et al., 2014, Rug et al., 2014,

Batinovic et al., 2017). Green nodes = GFP-tagged proteins from this study, pink nodes = epitope-tagged proteins from other studies, blue nodes = exported proteins (parasitophorous vacuole proteins not included). Thin edges = protein was co-immunoprecipitated, thick edges = proteins co-immunoprecipitated each other. Image was created using NAViGaTOR 2.3.

5.3 Discussion

In the present study, we describe the protein-protein interaction partners identified by co-precipitation and tandem mass spectrometry for 8 epitope-tagged Maurer's clefts proteins. We identify GEXP07 and GEXP10 as central components of the PfEMP1-interacting network at the Maurer's clefts. This is consistent with 3D-SIM studies showing that GEXP10, GEXP07 and MAHRP1 are located in the centre of the clefts. These proteins co-precipitate each other, and GEXP07 also co-precipitated with PfEMP1.

MAHRP1 was shown to be required for PfEMP1 localisation to the Maurer's clefts and red blood cell surface, whilst GEXP07 and GEXP10 have been thus far refractory to genetic deletion (Spycher et al., 2008, Maier et al., 2008, Sleebs et al., 2014). After export through PTEX, PfEMP1 is proposed to be transported in a soluble chaperoned state to mobile Maurer's clefts (Batinovic et al., 2017). Because GEXP07 co-precipitated with PfEMP1 and MAHRP1, we proposed that MAHRP1 and GEXP07 may function together for PfEMP1 to reach the Maurer's clefts. Using the glmS knockdown system, we were able to reduce expression of a GEXP07-HA construct. However, this knockdown of GEXP07 had no effect on PfEMP1 localisation at the Maurer's clefts, nor was there any apparent effect on parasite development, Maurer's clefts numbers, or MAHRP1 localisation. We also measured adherence of the knocked down infected red blood cells to CD36 under flow conditions as an indirect measure of virulence complex assembly and PfEMP1 surface exposure. There was no significant difference in binding upon knockdown of GEXP07. These results are surprising considering that GEXP07 (and GEXP10) have been reported to be refractory to genetic deletion, which suggests essentiality for parasite survival (Maier et al., 2008, Sleebs et al., 2014). We suggest that GEXP07 has no role in PfEMP1 trafficking. However, it remains possible that the level of GEXP07-HA expressed even after knockdown with 5 or 10 mM GlcN was sufficient for normal protein function.

Of interest, a recent study found that antibodies to GEXP10 (referred to as CBP1) and GEXP07 (CBP2) blocked adhesion of infected red blood cells to the chemokine, CX3CL1 (Hermann et al., 2016). This study also used antibodies to GEXP07 and GEXP10 to localise these proteins by immunofluorescence analysis. In contrast to our findings, they do not detect GEXP07 and GEXP10 in ring stage infected red blood cells and assert that

these proteins are located on the red blood cell surface in late trophozoites (Hermand et al., 2016). However, epitope-tagged GEXP07 parasites analysed by us and others (Sleebbs et al., 2014) find that GEXP07 is expressed in rings and is located at the Maurer's clefts. It remains possible that a small proportion of GEXP07 and GEXP10 is transported to the red blood cell surface, although further validation is needed. Two other proteins that co-precipitated with this clique, PIESP2 and PFE0050w, have previously been shown not to be required for efficient transport of PfEMP1 to the red blood cell surface (Maier et al., 2008)

We performed co-precipitation on REX1-GFP and PTP5-GFP-expressing parasites. The Maurer's clefts proteins REX1 and PTP5 have several similarities. They co-precipitate, and both are localised to the edges of the Maurer's clefts (Figure 4.8 and Figure 4.9). Knockout studies have shown that REX1 and PTP5 are required for efficient transport of PfEMP1 from the Maurer's clefts to the red blood cell membrane (Hanssen et al., 2008b, Dixon et al., 2011, McHugh et al., 2015, Maier et al., 2008). Knockout of REX1 and PTP5 does not affect PfEMP1 transfer to the Maurer's clefts, but instead affects the amount of surface-exposed PfEMP1 (Maier et al., 2008, Dixon et al., 2011). A previous study showed that a PfEMP1 mini protein co-precipitated with both REX1 and PTP5, and that PTP5-GFP co-precipitated with PfEMP1 (Batinovic et al., 2017). These proteins may therefore be involved in packaging or transporting PfEMP1 from the Maurer's clefts to the red blood cell membrane. These previous findings are consistent with our data showing that REX1-GFP co-precipitates with PfEMP1. Furthermore, a proximity ligation assay between α REX1 and α ATS showed that these two epitopes were within 40 nm (Batinovic et al., 2017), suggesting a direct interaction.

Immunoblot analysis of REX1-GFP and PTP5-GFP reveals a ladder pattern that is consistent with possible cleavage at putative PEST sequences within each protein. PEST sequences target proteins for proteolytic degradation via a pathway that can be conditional upon activation (e.g. by phosphorylation) (Rechsteiner and Rogers, 1996). The exact function of these PEST sequences is not clear. If PTP5 and REX1 are involved in vesicle budding from the Maurer's clefts as peripheral coat proteins, they may be degraded after vesicle uncoating and fusion at the red blood cell membrane. Another possibility is that degradation of PTP5 and REX1 is required for Maurer's clefts collapse before merozoite

egress. Two essential Maurer's clefts proteins - PfJ23 and MAHRP2 - are associated with PTP5 and REX1 respectively (Maier et al., 2008, Pachlatko et al., 2010). The essentiality of Maurer's clefts proteins in *in vitro* culture is puzzling, considering that the known new permeability pathway proteins (e.g. RhopH complex proteins) do not transit through these organelles.

Both REX1 (712 residues) and PTP5 (631 residues) have a hydrophobic stretch near the N-terminus that may function as a recessed signal sequence. Following the non-canonical signal sequence PTP5 has a PEXEL whereas REX1 does not. A significant portion of the REX1 and PTP5 polypeptide sequences are comprised of repeating sequences. The repeat region of REX1 has been extensively investigated and has been shown to be required for Maurer's clefts dispersion within the red blood cell cytoplasm and for efficient transport of PfEMP1 to the red blood cell membrane (Chapter 3) (McHugh et al., 2015). In REX1, the repeat region has an overall negative charge (pI = 4.92) and has two types of repeats: PQAEKDASKLTTTYDQTKEVK (pI = 6.62) and PQAEKDALAKTENQNGELL (pI = 4.41). The repeat region in PTP5 is positively charged (pI = 8.86) and consists of a repeating sequence of TSSKKAQEKSVEPTKKPSKYTMNLDSPLLKGSSGSE. The charged repeat regions within PTP5 and REX1 could represent points of electrostatic interactions between the two proteins.

The PTP6 protein is required for PfEMP1 transport from Maurer's clefts to the red blood cell membrane. Parasites (CS2 strain) lacking PTP6 do not adhere to CSA under flow conditions even though PfEMP1 is still transferred to the Maurer's clefts (Maier et al., 2008). We assessed the protein-protein interactions of PTP6-GFP by co-precipitation and identified a suite of proteins different to those interacting with the other tagged Maurer's clefts proteins under investigation. The PTP6-GFP-interacting proteins are relatively uncharacterised compared to other Maurer's clefts proteins, yet all (except MESA) were identified in the Maurer's clefts protein profile. Two PTP6-GFP co-precipitating proteins, STARP and PF3D7_0301700, have not been localised by microscopy nor genetically deleted. Characterisation of the PTP6-interacting cluster will assist in understanding how this protein influences PfEMP1 trafficking. Another study identified PTP6 as possible interacting partner of PTP1 in CS2 parasites (Rug et al., 2014). Although we identified PTP1 in tandem mass spectrometry analysis of Maurer's clefts proteins (Table 6), we did not identify PTP1 in co-precipitation analyses of PTP6-GFP nor with any other GFP-

tagged parasite line. We infer from the Maurer's clefts morphology that PTP1 is in fact expressed in these parasites (Figure 4.6). Differing sample preparation methods may account for the different Maurer's clefts protein interaction partners identified.

Protein-protein interaction data has been previously published for two Maurer's clefts proteins: PTP1 and SEMP1, and for PfEMP1 (Dietz et al., 2014, Rug et al., 2014, Batinovic et al., 2017). Indeed, a recent analysis of a PfEMP1-GFP mini-protein identified many exported proteins, including MAHRP1, PTP5, REX1, SBP1 and MAHRP2 (Batinovic et al., 2017). These studies involved pre-treatment of infected red blood cells with the amine-reactive chemical crosslinker DSP (dithiobis(succinimidyl propionate)) to stabilise interacting partners. We found that uncrosslinked REX1-GFP co-precipitated PfEMP1, but PTP5-GFP did not. Integrating the interaction data from the present study with data from (Batinovic et al., 2017), SEMP1 and PTP1 mass spectrometry co-precipitation studies reveals multiple cliques involving PfEMP1.

The PEXEL-containing protein, PTP1, was first identified as a mediator of PfEMP1 export in a large-scale exported protein knock-out study (Maier et al., 2008). It is a Maurer's clefts protein that is required for maintenance of the discoid structure of Maurer's clefts, as well as PfEMP1 trafficking from the parasitophorous vacuole. It may also function to link the Maurer's clefts to the cytoskeleton by aiding actin polymerisation (Maier et al., 2008, Rug et al., 2014). The published mass spectrometry analysis of PTP1-interacting proteins (one replicate) identified 6 PEXEL proteins (Rug et al., 2014). An additional 45 non-PEXEL proteins were also identified (including known Maurer's clefts proteins PFF0090w [PF3D7_0601900] and PF08_0004 [PF3D7_0830400]) (Rug et al., 2014). Some of the interactions between PTP1 and other proteins identified in the mass spectrometry analysis (SBP1, PfEMP1 and PIESP2) were confirmed by Western blotting (Rug et al., 2014). Additionally, 2D Blue Native PAGE provided evidence that PTP1 exists in a 420 kDa complex (Rug et al., 2014).

The small Maurer's clefts protein, SEMP1, was not identified as an interacting protein in the present study (possibly because of its size), but an epitope-tagged SEMP1 parasite line has been analysed by co-immunoprecipitation and mass spectrometry by others (Dietz et al., 2014). They found that SEMP1 co-immunoprecipitated with REX1, PF3D7_0702500, MAHRP2, PF3D7_0601900 and other exported proteins (Dietz et al.,

2014). The exact function of SEMP1 is still unclear, but it may bind to REX1 and MAHRP2 (a tether protein). Evaluating the existing spatial and interaction data of known Maurer's clefts proteins in the context of the network presented in this study is an important step to understanding Maurer's clefts function.

Chapter 6 : Summary and conclusion

6.1 New understanding of the function of ring-exported protein-1

Ring exported protein 1 is a 712 residue protein that is amongst the most well studied Maurer's clefts components. The REX1 gene was identified within a region of chromosome 9 associated with cytoadherence and was only the second Maurer's clefts protein described (Hawthorne et al., 2004a). Although it is a PEXEL-negative exported protein, the region of REX1 required for export has been identified as the 10 amino acids proximal to the hydrophobic stretch (Dixon et al., 2008). The downstream predicted coiled-coil region targets REX1 to the Maurer's clefts, where it is located primarily on the edges and tethers (Dixon et al., 2008, Hanssen et al., 2008a). Truncation of REX1 at residue 362 (just prior to the repeat region) results in stacking of the Maurer's clefts lamellae (Hanssen et al., 2008a). Residues 362-579 of REX1 comprise an acidic repeat region while residues 579-712 comprise a unique domain with no obvious motifs. The stacking of Maurer's clefts may be caused by failure of the lamellae to separate during genesis, or by aggregation whilst the Maurer's clefts are mobile in the red blood cell cytoplasm. We created two REX1 truncation parasite lines in order to determine which portion of the protein is required for separating Maurer's clefts lamellae. The parasite line lacking the C-terminal segment of the protein (termed REX1¹⁻⁵⁷⁹) showed no difference in Maurer's clefts morphology, exported protein localisation or virulence protein trafficking (McHugh et al., 2015). As such, the role of the C-terminal segment of REX1 is still unclear. In contrast, a parasite line expressing a truncated form of REX1 that lacked only the repeat region (REX1^{Δ371-579}-GFP) exhibited stacked Maurer's clefts (McHugh et al., 2015).

As well as being an important contributor to Maurer's clefts architecture, REX1 also plays a part in trafficking of the virulence protein PfEMP1. Genetic ablation of REX1 caused decreased adherence of infected red blood cells to CD36, and decreased trypsin-cleavable PfEMP1 on the red blood cell surface (Dixon et al., 2011). However, knockout of REX1 was consistently associated with truncation of chromosome 2 distal to the gene

encoding KAHRP. We created a REX1 inducible knockdown parasite line in order to study the function of REX1 in parasites that were expressing KAHRP. When REX1 was knocked down, the amount of surface exposed PfEMP1 decreased but was not completely ablated (McHugh et al., 2015). Similarly, REX1 knockdown parasites showed decreased binding to CD36 under flow conditions. The Maurer's clefts in REX1 knockdown parasites became stacked, as observed in the REX1^{Δ371-579}-GFP parasites. Knockout of some Maurer's clefts proteins such as SBP1, PTP1 and MAHRP1 completely ablates trafficking of PfEMP1 to the red blood cell surface (Maier et al., 2007, Spycher et al., 2008, Rug et al., 2014). Whilst knockdown of REX1 does not stop PfEMP1 trafficking to the red blood cell surface, it does decrease the trafficking efficiency reservoir (McHugh et al., 2015). This was interpreted as likely being due to the altered Maurer's clefts morphology being suboptimal for PfEMP1 transport. However, subsequent work (by others and in the present study) has demonstrated direct interactions between PfEMP1, REX1 and PTP5 (Batinovic et al., 2017). This suggests the alternative or additional possibility that disrupting REX1 decreases the efficiency of PfEMP1 transfer from the Maurer's clefts edges to the red blood cell membrane. Understanding this step in PfEMP1 trafficking is crucial for targeting the Maurer's clefts to impede the virulence of *P. falciparum*.

6.2 A more complete picture of Maurer's clefts

We have developed a method to enrich Maurer's clefts from *P. falciparum*-infected red blood cells. We have used tandem-mass spectrometry to profile the proteins of the Maurer's clefts at 14 - 18 h post-invasion. At this stage of the asexual lifecycle, PfEMP1 has arrived at the clefts and may be at the early stages of transferring to the red blood cell membrane (Kriek et al., 2003). We successfully identify all known ring-stage expressed Maurer's clefts proteins as well as a number of putative novel Maurer's clefts proteins. This list will provide a useful resource for others wishing to study Maurer's clefts. Interestingly, a number of human proteins involved in various aspects of membrane trafficking and lipid pathways were identified as enriched within the Maurer's clefts. This suggests a possible co-optation of host proteins for parasite virulence protein trafficking.

To validate the Maurer's clefts enrichment technique, a number of parasite lines were generated expressing epitope-tagged putative and established Maurer's clefts proteins.

This resulted in the localisation of four novel Maurer's clefts proteins: PTP6, GEXP10, Pf13_0275 and also PTP5 which we recently published (Batinovic et al., 2017). These new Maurer's clefts proteins, along with tagged established clefts proteins, were localised by super-resolution microscopy to sub-compartments within the Maurer's cleft organelle (Figure 6.1). We next looked at protein-protein interactions at the Maurer's clefts using co-precipitation/tandem mass spectrometry with eight epitope-tagged parasite lines. With this data, we map a Maurer's cleft interaction network that can be placed within the spatial context of the clefts. We identified two Maurer's clefts proteins, GEXP07 and REX1 that co-precipitated with PfEMP1. A conditional knockdown of GEXP07-HA showed that reduced levels of GEXP07 had no effect on PfEMP1 localisation or adherence of infected red blood cells to CD36 under flow conditions. GEXP07, GEXP10 and MAHRP1 localise and interact within the central compartment of the Maurer's clefts (Figure 6.1), where MAHRP1 is responsible for the transport of PfEMP1 to the Maurer's clefts (Spycher et al., 2008). We propose that a second interaction hub, including REX1 and PTP5 at the Maurer's clefts periphery, is involved in transport of PfEMP1 from the clefts to the red blood cell surface. The transport of PfEMP1 from the Maurer's clefts to the red blood cell surface has been suggested to be mediated by EDVs such as those observed to label with PTP2 (McMillan et al., 2013, Regev-Rudzki et al., 2013). Future work investigating this process will provide insights into trafficking of PfEMP1 - a key mediator of severe malaria.

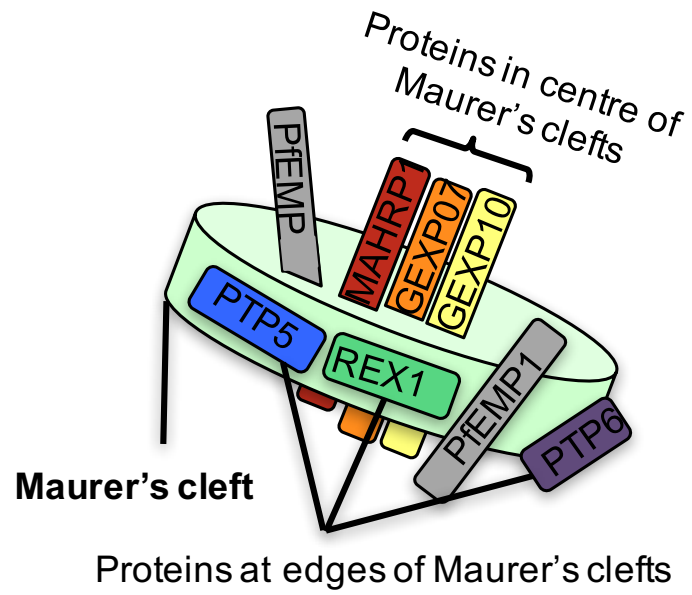


Figure 6.1 Schematic representing protein locations within the Maurer's clefts

6.3 Conclusions

The Maurer's clefts of *P. falciparum* have been studied for over 100 years, yet their function is still not fully understood. This study dissected the specific region of a Maurer's clefts protein, REX1, that is required for the dispersed clefts phenotype observed in wild-type parasite-infected red blood cells. The proteomic analysis of the Maurer's clefts defines the proteins at these organelles at the time of virulence protein trafficking. We show how proteins are spatially related within subcompartments of the Maurer's clefts and tie-in this information with protein-protein interaction data from co-immunoprecipitation and from the literature. This leads us to a model for PfEMP1 transport through the clefts where it is received at the clefts by a centrally located group of proteins and is shuttled to the clefts edges before transport to the red blood cell membrane. These insights further our understanding of how *P. falciparum* remodels the host red blood cell.

Supplementary

Table S1 Human proteins enriched in PTP5-GFP LC-MS/MS

Accession	Protein name	Number of significant ms/ms spectra			
		Experiment 1		Experiment 2	
		PTP5	3D7	PTP5	3D7
sp Q9BVA1 TBB2B_HUMAN	Tubulin beta-2B chain	6	0	2	0
sp Q5XKE5 K2C79_HUMAN	Keratin, type II cytoskeletal 79	3	0	2	0

Table S2 Human proteins enriched in PTP6-GFP LC-MS/MS

Accession	Protein name	Number of significant ms/ms spectra			
		Experiment 1		Experiment 2	
		PTP6	3D7	PTP6	3D7
sp P29144 TPP2_HUMAN	Tripeptidyl-peptidase 2	32	0	50	2
sp P69891 HBG1_HUMAN	Hemoglobin subunit gamma-1	3	0	2	0
sp O94919 ENDD1_HUMAN	Endonuclease domain-containing 1 protein	2	0	2	0
sp P17980 PRS6A_HUMAN	26S protease regulatory subunit 6A	2	0	7	1

Table S3 Human proteins enriched in REX1-GFP LC-MS/MS

Accession	Protein name	Number of significant ms/ms spectra			
		Experiment 1		Experiment 2	
		REX1	3D7	REX1	3D7
sp P68032 ACTC_HUMAN	Actin, alpha cardiac muscle 1	10	0	6	0
sp P04220 MUCB_HUMAN	Ig mu heavy chain disease protein	10	0	12	0
sp Q86X55 CARM1_HUMAN	Histone-arginine methyltransferase CARM1	4	0	3	0
sp Q9H0R4 HDHD2_HUMAN	Haloacid dehalogenase-like hydrolase domain-containing protein 2	3	0	2	0
sp Q6XQN6 PNCB_HUMAN	Nicotinate phosphoribosyltransferase	3	0	3	0
sp Q96M27 PRRC1_HUMAN	Protein PRRC1	2	0	9	0

Table S4 Human proteins enriched in REX2-GFP LC-MS/MS

Accession	Protein name	Number of significant ms/ms spectra			
		Experiment 1		Experiment 2	
		REX2	3D7	REX2	3D7
sp Q86VP6 CAND1_HUMAN	Cullin-associated NEDD8-dissociated protein 1	6	0	23	4
sp Q13200 PSMD2_HUMAN	26S proteasome non-ATPase regulatory subunit 2	4	0	11	2
sp P17858 PFKAL_HUMAN	ATP-dependent 6-phosphofructokinase, liver type	3	0	13	1
sp O43242 PSMD3_HUMAN	26S proteasome non-ATPase regulatory subunit 3	2	0	7	0
sp Q92526 TCPW_HUMAN	T-complex protein 1 subunit zeta-2	2	0	3	0
sp Q96P70 IPO9_HUMAN	Importin-9	2	0	9	0

Table S5 Human proteins enriched in MAHRP1-GFP LC-MS/MS

Accession	Protein name	Number of significant ms/ms spectra			
		Experiment 1		Experiment 2	
		MAHRP1	3D7	MAHRP1	3D7
sp P07203 GPX1_HUMAN	Glutathione peroxidase 1	6	1	3	0
sp P62979 RS27A_HUMAN	Ubiquitin-40S ribosomal protein S27a	5	0	3	0
sp Q00013 EM55_HUMAN	55 kDa erythrocyte membrane protein	5	0	4	0
sp P08779 K1C16_HUMAN	Keratin, type I cytoskeletal 16	3	0	3	0
sp P11171 41_HUMAN	Protein 4.1	3	0	12	0

Table S6 Human proteins enriched in GEXP07-GFP LC-MS/MS

Accession	Protein name	Number of significant ms/ms spectra			
		Experiment 1		Experiment 2	
		GEXP07	3D7	GEXP07	3D7
sp P08779 K1C16_HUMAN	Keratin, type I cytoskeletal 16	4	0	6	0

Table S7 Human proteins enriched in GEXP10-GFP LC-MS/MS

Accession	Protein name	Number of significant ms/ms spectra			
		Experiment 1		Experiment 2	
		GEXP10	3D7	GEXP10	3D7
sp P11171 41_HUMAN	Protein 4.1	11	0	8	0
sp Q7Z794 K2C1B_HUMAN	Keratin, type II cytoskeletal 1b	3	0	6	0
sp Q5XKE5 K2C79_HUMAN	Keratin, type II cytoskeletal 79	2	0	8	0

Table S8 Human proteins enriched in PF13_0275-GFP LC-MS/MS

Accession	Protein name	Number of significant ms/ms spectra			
		Experiment 1		Experiment 2	
		PF13_0275	3D7	PF13_0275	3D7
sp O95373 IPO7_HUMAN	Importin-7	44	0	47	0
sp Q86VP6 CAND1_HUMAN	Cullin-associated NEDD8-dissociated protein 1	41	0	58	0
sp O00410 IPO5_HUMAN	Importin-5	33	0	32	0
sp Q14974 IMB1_HUMAN	Importin subunit beta-1	27	0	27	0
sp Q93008 USP9X_HUMAN	Probable ubiquitin carboxyl-terminal hydrolase FAF-X	22	0	53	0
sp Q96P70 IPO9_HUMAN	Importin-9	22	0	18	0
sp Q9C0E2 XPO4_HUMAN	Exportin-4	15	0	19	0
sp O00507 USP9Y_HUMAN	Probable ubiquitin carboxyl-terminal hydrolase FAF-Y	12	0	18	0
sp P30153 2AAA_HUMAN	Serine/threonine-protein phosphatase 2A 65 kDa regulatory subunit A alpha isoform	9	0	14	0
sp Q9Y5L0 TNPO3_HUMAN	Transportin-3	9	0	9	0
sp O14980 XPO1_HUMAN	Exportin-1	7	0	12	0
sp Q5T4S7 UBR4_HUMAN	E3 ubiquitin-protein ligase UBR4	7	0	31	0
sp Q08AM6 VAC14_HUMAN	Protein VAC14 homolog	6	0	7	0
sp P27348 1433T_HUMAN	14-3-3 protein theta	3	0	5	0
sp P54920 SNAA_HUMAN	Alpha-soluble NSF attachment protein	3	0	17	0
sp Q14C86 GAPD1_HUMAN	GTPase-activating protein and VPS9 domain-containing protein 1	3	0	23	0
sp Q7Z3U7 MON2_HUMAN	Protein MON2 homolog	3	0	7	0
sp Q96IU4 ABHEB_HUMAN	Protein ABHD14B	3	0	3	0
sp Q9UIA9 XPO7_HUMAN	Exportin-7	3	0	11	0
sp Q9UPN7 PP6R1_HUMAN	Serine/threonine-protein phosphatase 6 regulatory subunit 1	3	0	5	0
sp O60518 RNBP6_HUMAN	Ran-binding protein 6	2	0	3	0
sp O75155 CAND2_HUMAN	Cullin-associated NEDD8-dissociated protein 2	2	0	4	0
sp O94919 ENDD1_HUMAN	Endonuclease domain-containing 1 protein	2	0	2	0
sp P62258 1433E_HUMAN	14-3-3 protein epsilon	2	0	10	0
sp Q92973 TNPO1_HUMAN	Transportin-1	2	0	9	0
sp Q96ER3 SAAL1_HUMAN	Protein SAAL1	2	0	3	0
sp Q9BSL1 UBAC1_HUMAN	Ubiquitin-associated domain-containing protein 1	2	0	8	0
sp Q9BYX7 ACTBM_HUMAN	Putative beta-actin-like protein 3	2	0	3	0
sp Q9NPQ8 RIC8A_HUMAN	Synembryn-A	2	0	6	0

References

- ADISA, A., ALBANO, F. R., REEDER, J., FOLEY, M. & TILLEY, L. 2001. Evidence for a role for a *Plasmodium falciparum* homologue of Sec31p in the export of proteins to the surface of malaria parasite-infected erythrocytes. *J Cell Sci*, 114, 3377-86.
- ADISA, A., FRANKLAND, S., RUG, M., JACKSON, K., MAIER, A. G., WALSH, P., LITHGOW, T., KLONIS, N., GILSON, P. R., COWMAN, A. F. & TILLEY, L. 2007. Re-assessing the locations of components of the classical vesicle-mediated trafficking machinery in transfected *Plasmodium falciparum*. *Int J Parasitol*, 37, 1127-41.
- ADISA, A., RUG, M., KLONIS, N., FOLEY, M., COWMAN, A. F. & TILLEY, L. 2003. The signal sequence of exported protein-1 directs the green fluorescent protein to the parasitophorous vacuole of transfected malaria parasites. *J Biol Chem*, 278, 6532-42.
- AEBERHARD, L., BANHART, S., FISCHER, M., JEHLICH, N., ROSE, L., KOCH, S., LAUE, M., RENARD, B. Y., SCHMIDT, F. & HEUER, D. 2015. The Proteome of the Isolated Chlamydia trachomatis Containing Vacuole Reveals a Complex Trafficking Platform Enriched for Retromer Components. *PLoS Pathog*, 11, e1004883.
- AIKAWA, M. 1988. Morphological changes in erythrocytes induced by malarial parasites. *Biol Cell*, 64, 173-81.
- AIKAWA, M., MILLER, L. H. & RABBEGE, J. 1975. Caveola--vesicle complexes in the plasmalemma of erythrocytes infected by *Plasmodium vivax* and *P. cynomolgi*. Unique structures related to Schuffner's dots. *Am J Pathol*, 79, 285-300.

- AIKAWA, M., UNI, Y., ANDRUTIS, A. T. & HOWARD, R. J. 1986. Membrane-associated electron-dense material of the asexual stages of *Plasmodium falciparum*: evidence for movement from the intracellular parasite to the erythrocyte membrane. *Am J Trop Med Hyg*, 35, 30-6.
- AKINYI, S., HANSEN, E., MEYER, E. V., JIANG, J., KORIR, C. C., SINGH, B., LAPP, S., BARNWELL, J. W., TILLEY, L. & GALINSKI, M. R. 2012. A 95 kDa protein of *Plasmodium vivax* and *P. cynomolgi* visualized by three-dimensional tomography in the caveola-vesicle complexes (Schuffner's dots) of infected erythrocytes is a member of the PHIST family. *Mol Microbiol*, 84, 816-31.
- ALBANO, F. R., BERMAN, A., LA GRECA, N., HIBBS, A. R., WICKHAM, M., FOLEY, M. & TILLEY, L. 1999. A homologue of Sar1p localises to a novel trafficking pathway in malaria-infected erythrocytes. *Eur J Cell Biol*, 78, 453-62.
- ARIEY, F., WITKOWSKI, B., AMARATUNGA, C., BEGHAIN, J., LANGLOIS, A. C., KHIM, N., KIM, S., DURU, V., BOUCHIER, C., MA, L., LIM, P., LEANG, R., DUONG, S., SRENG, S., SUON, S., CHUOR, C. M., BOUT, D. M., MENARD, S., ROGERS, W. O., GENTON, B., FANDEUR, T., MIOTTO, O., RINGWALD, P., LE BRAS, J., BERRY, A., BARALE, J. C., FAIRHURST, R. M., BENOIT-VICAL, F., MERCEREAU-PUIJALON, O. & MENARD, D. 2014. A molecular marker of artemisinin-resistant *Plasmodium falciparum* malaria. *Nature*, 505, 50-5.
- BACHMANN, A., SCHOLZ, J. A., JANSSEN, M., KLINKERT, M. Q., TANNICH, E., BRUCHHAUS, I. & PETTER, M. 2015. A comparative study of the localization and membrane topology of members of the RIFIN, STEVOR and PfMC-2TM protein families in *Plasmodium falciparum*-infected erythrocytes. *Malar J*, 14, 274.

- BAIETTI, M. F., ZHANG, Z., MORTIER, E., MELCHIOR, A., DEGEEST, G., GEERAERTS, A., IVARSSON, Y., DEPOORTERE, F., COOMANS, C., VERMEIREN, E., ZIMMERMANN, P. & DAVID, G. 2012. Syndecan-syntenin-ALIX regulates the biogenesis of exosomes. *Nat Cell Biol*, 14, 677-85.
- BARAJAS, D., XU, K., DE CASTRO MARTIN, I. F., SASVARI, Z., BRANDIZZI, F., RISCO, C. & NAGY, P. D. 2014. Co-opted oxysterol-binding ORP and VAP proteins channel sterols to RNA virus replication sites via membrane contact sites. *PLoS Pathog*, 10, e1004388.
- BARUCH, D. I., PASLOSKE, B. L., SINGH, H. B., BI, X., MA, X. C., FELDMAN, M., TARASCHI, T. F. & HOWARD, R. J. 1995. Cloning the *P. falciparum* gene encoding PfEMP1, a malarial variant antigen and adherence receptor on the surface of parasitized human erythrocytes. *Cell*, 82, 77-87.
- BATINOVIC, S., MCHUGH, E., CHISHOLM, S. A., MATTHEWS, K., LIU, B., DUMONT, L., CHARNAUD, S. C., SCHNEIDER, M. P., GILSON, P. R., DE KONING-WARD, T. F., DIXON, M. W. A. & TILLEY, L. 2017. An exported protein-interacting complex involved in the trafficking of virulence determinants in Plasmodium-infected erythrocytes. *Nat Commun*, 8, 16044.
- BECK, J. R., MURALIDHARAN, V., OKSMAN, A. & GOLDBERG, D. E. 2014. PTEX component HSP101 mediates export of diverse malaria effectors into host erythrocytes. *Nature*, 511, 592-5.
- BEESON, J. G. & BROWN, G. V. 2002. Pathogenesis of *Plasmodium falciparum* malaria: the roles of parasite adhesion and antigenic variation. *Cell Mol Life Sci*, 59, 258-71.
- BEESON, J. G., CHAN, J. A. & FOWKES, F. J. 2013. PfEMP1 as a target of human immunity and a vaccine candidate against malaria. *Expert Rev Vaccines*, 12, 105-8.

- BEESON, J. G., REEDER, J. C., ROGERSON, S. J. & BROWN, G. V. 2001. Parasite adhesion and immune evasion in placental malaria. *Trends Parasitol*, 17, 331-7.
- BHATTACHARJEE, S., STAHELIN, R. V., SPEICHER, K. D., SPEICHER, D. W. & HALDAR, K. 2012. Endoplasmic reticulum PI(3)P lipid binding targets malaria proteins to the host cell. *Cell*, 148, 201-12.
- BHATTACHARJEE, S., VAN OOIJ, C., BALU, B., ADAMS, J. H. & HALDAR, K. 2008. Maurer's clefts of *Plasmodium falciparum* are secretory organelles that concentrate virulence protein reporters for delivery to the host erythrocyte. *Blood*, 111, 2418-26.
- BLISNICK, T., MORALES BETOULLE, M. E., BARALE, J., UZUREAU, P., BERRY, L., DESROSES, S., FUJIOKA, H., MATTEI, D. & BRAUN BRETON, C. 2000. Pfsbp1, a Maurer's cleft *Plasmodium falciparum* protein, is associated with the erythrocyte skeleton. *Mol. Biochem. Parasitol.*, 111, 107-21.
- BODDEY, J. A., HODDER, A. N., GUNTHER, S., GILSON, P. R., PATSIOURAS, H., KAPP, E. A., PEARCE, J. A., DE KONING-WARD, T. F., SIMPSON, R. J., CRABB, B. S. & COWMAN, A. F. 2010. An aspartyl protease directs malaria effector proteins to the host cell. *Nature*, 463, 627-31.
- BODDEY, J. A., MORITZ, R. L., SIMPSON, R. J. & COWMAN, A. F. 2009. Role of the Plasmodium export element in trafficking parasite proteins to the infected erythrocyte. *Traffic*, 10, 285-99.
- BODDEY, J. A., O'NEILL, M. T., LOPATICKI, S., CARVALHO, T. G., HODDER, A. N., NEBL, T., WAWRA, S., VAN WEST, P., EBRAHIMZADEH, Z., RICHARD, D., FLEMMING, S., SPIELMANN, T., PRZYBORSKI, J., BABON, J. J. & COWMAN, A. F. 2016. Export of malaria proteins requires co-translational processing of the PEXEL motif independent of phosphatidylinositol-3-phosphate binding. *Nat Commun*, 7, 10470.

- BOTTE, C. Y., YAMARYO-BOTTE, Y., RUPASINGHE, T. W., MULLIN, K. A., MACRAE, J. I., SPURCK, T. P., KALANON, M., SHEARS, M. J., COPPEL, R. L., CRELLIN, P. K., MARECHAL, E., MCCONVILLE, M. J. & MCFADDEN, G. I. 2013. Atypical lipid composition in the purified relict plastid (apicoplast) of malaria parasites. *Proc Natl Acad Sci U S A*, 110, 7506-11.
- BULLEN, H. E., CHARNAUD, S. C., KALANON, M., RIGLAR, D. T., DEKIWADIA, C., KANGWANRANGSAN, N., TORII, M., TSUBOI, T., BAUM, J., RALPH, S. A., COWMAN, A. F., DE KONING-WARD, T. F., CRABB, B. S. & GILSON, P. R. 2012. Biosynthesis, localization, and macromolecular arrangement of the *Plasmodium falciparum* translocon of exported proteins (PTEX). *J Biol Chem*, 287, 7871-84.
- BURKHARD, P., STETEFELD, J. & STRELKOV, S. V. 2001. Coiled coils: a highly versatile protein folding motif. *Trends Cell Biol*, 11, 82-8.
- CHANG, H. H., FALICK, A. M., CARLTON, P. M., SEDAT, J. W., DERISI, J. L. & MARLETTA, M. A. 2008. N-terminal processing of proteins exported by malaria parasites. *Mol Biochem Parasitol*, 160, 107-15.
- COOKE, B. M., BUCKINGHAM, D. W., GLENISTER, F. K., FERNANDEZ, K. M., BANNISTER, L. H., MARTI, M., MOHANDAS, N. & COPPEL, R. L. 2006. A Maurer's cleft-associated protein is essential for expression of the major malaria virulence antigen on the surface of infected red blood cells. *J Cell Biol*, 172, 899-908.
- COPPEL, R. L., LUSTIGMAN, S., MURRAY, L. & ANDERS, R. F. 1988. MESA is a *Plasmodium falciparum* phosphoprotein associated with the erythrocyte membrane skeleton. *Mol Biochem Parasitol*, 31, 223-31.
- COUNIHAN, N. A., CHISHOLM, S. A., BULLEN, H. E., SRIVASTAVA, A., SANDERS, P. R., JONSDOTTIR, T. K., WEISS, G. E., GHOSH, S., CRABB,

- B. S., CREEK, D. J., GILSON, P. R. & DE KONING-WARD, T. F. 2017. *Plasmodium falciparum* parasites deploy RhopH2 into the host erythrocyte to obtain nutrients, grow and replicate. *Elife*, 6.
- CRABB, B. S., COOKE, B. M., REEDER, J. C., WALLER, R. F., CARUANA, S. R., DAVERN, K. M., WICKHAM, M. E., BROWN, G. V., COPPEL, R. L. & COWMAN, A. F. 1997. Targeted gene disruption shows that knobs enable malaria-infected red cells to cytoadhere under physiological shear stress. *Cell*, 89, 287-96.
- CSERTI, C. M. & DZIK, W. H. 2007. The ABO blood group system and *Plasmodium falciparum* malaria. *Blood*, 110, 2250-8.
- CYRKLAFF, M., SANCHEZ, C. P., KILIAN, N., BISSEYE, C., SIMPORE, J., FRISCHKNECHT, F. & LANZER, M. 2011. Hemoglobins S and C interfere with actin remodeling in *Plasmodium falciparum*-infected erythrocytes. *Science*, 334, 1283-6.
- DANIYAN, M. O., BOSHOFF, A., PRINSLOO, E., PESCE, E. R. & BLATCH, G. L. 2016. The Malarial Exported PFA0660w Is an Hsp40 Co-Chaperone of PfHsp70-x. *PLoS One*, 11, e0148517.
- DE KONING-WARD, T. F., DIXON, M. W., TILLEY, L. & GILSON, P. R. 2016. Plasmodium species: master renovators of their host cells. *Nat Rev Microbiol*, 14, 494-507.
- DE KONING-WARD, T. F., GILSON, P. R., BODDEY, J. A., RUG, M., SMITH, B. J., PAPENFUSS, A. T., SANDERS, P. R., LUNDIE, R. J., MAIER, A. G., COWMAN, A. F. & CRABB, B. S. 2009. A newly discovered protein export machine in malaria parasites. *Nature*, 459, 945-9.

- DE MORAES, L. V., TADOKORO, C. E., GOMEZ-CONDE, I., OLIVIERI, D. N. & PENHA-GONCALVES, C. 2013. Intravital placenta imaging reveals microcirculatory dynamics impact on sequestration and phagocytosis of Plasmodium-infected erythrocytes. *PLoS Pathog*, 9, e1003154.
- DE NIZ, M., ULLRICH, A. K., HEIBER, A., BLANCKE SOARES, A., PICK, C., LYCK, R., KELLER, D., KAISER, G., PRADO, M., FLEMMING, S., DEL PORTILLO, H., JANSE, C. J., HEUSSLER, V. & SPIELMANN, T. 2016. The machinery underlying malaria parasite virulence is conserved between rodent and human malaria parasites. *Nat Commun*, 7, 11659.
- DEARNLEY, M., CHU, T., ZHANG, Y., LOOKER, O., HUANG, C., KLONIS, N., YEOMAN, J., KENNY, S., ARORA, M., OSBORNE, J. M., CHANDRAMOHANADAS, R., ZHANG, S., DIXON, M. W. & TILLEY, L. 2016. Reversible host cell remodeling underpins deformability changes in malaria parasite sexual blood stages. *Proc Natl Acad Sci U S A*, 113, 4800-5.
- DEITSCH, K., DRISKILL, C. & WELLEMS, T. 2001. Transformation of malaria parasites by the spontaneous uptake and expression of DNA from human erythrocytes. *Nucleic Acids Res*, 29, 850-3.
- DIETZ, O., RUSCH, S., BRAND, F., MUNDWILER-PACHLATKO, E., GAIDA, A., VOSS, T. & BECK, H. P. 2014. Characterization of the Small Exported Plasmodium falciparum Membrane Protein SEMP1. *PLoS One*, 9, e103272.
- DIXON, M. W., HAWTHORNE, P. L., SPIELMANN, T., ANDERSON, K. L., TRENHOLME, K. R. & GARDINER, D. L. 2008a. Targeting of the ring exported protein 1 to the Maurer's clefts is mediated by a two-phase process. *Traffic*, 9, 1316-26.
- DIXON, M. W., KENNY, S., MCMILLAN, P. J., HANSEN, E., TRENHOLME, K. R., GARDINER, D. L. & TILLEY, L. 2011a. Genetic ablation of a Maurer's

cleft protein prevents assembly of the *Plasmodium falciparum* virulence complex. *Mol Microbiol*, 81, 982-93.

DONG, X. P., SHEN, D., WANG, X., DAWSON, T., LI, X., ZHANG, Q., CHENG, X., ZHANG, Y., WEISMAN, L. S., DELLING, M. & XU, H. 2010. PI(3,5)P(2) controls membrane trafficking by direct activation of mucolipin Ca(2+) release channels in the endolysosome. *Nat Commun*, 1, 38.

ELFORD, B. C., COWAN, G. M. & FERGUSON, D. J. 1995. Parasite-regulated membrane transport processes and metabolic control in malaria-infected erythrocytes. *Biochem J*, 308 (Pt 2), 361-74.

ELSWORTH, B., MATTHEWS, K., NIE, C. Q., KALANON, M., CHARNAUD, S. C., SANDERS, P. R., CHISHOLM, S. A., COUNIHAN, N. A., SHAW, P. J., PINO, P., CHAN, J. A., AZEVEDO, M. F., ROGERSON, S. J., BEESON, J. G., CRABB, B. S., GILSON, P. R. & DE KONING-WARD, T. F. 2014. PTEX is an essential nexus for protein export in malaria parasites. *Nature*, 511, 587-91.

FRANKLAND, S., ADISA, A., HORROCKS, P., TARASCHI, T. F., SCHNEIDER, T., ELLIOTT, S. R., ROGERSON, S. J., KNUEPFER, E., COWMAN, A. F., NEWBOLD, C. I. & TILLEY, L. 2006. Delivery of the malaria virulence protein PfEMP1 to the erythrocyte surface requires cholesterol-rich domains. *Eukaryot Cell*, 5, 849-60.

GANGULY, A. K., RANJAN, P., KUMAR, A. & BHAVESH, N. S. 2015. Dynamic association of PfEMP1 and KAHRP in knobs mediates cytoadherence during Plasmodium invasion. *Sci Rep*, 5, 8617.

GARDNER, J. P., PINCHES, R. A., ROBERTS, D. J. & NEWBOLD, C. I. 1996. Variant antigens and endothelial receptor adhesion in *Plasmodium falciparum*. *Proc Natl Acad Sci U S A*, 93, 3503-8.

- GEHDE, N., HINRICHS, C., MONTILLA, I., CHARPIAN, S., LINGELBACH, K. & PRZYBORSKI, J. M. 2009. Protein unfolding is an essential requirement for transport across the parasitophorous vacuolar membrane of *Plasmodium falciparum*. *Mol Microbiol*, 71, 613-28.
- GERKE, V., CREUTZ, C. E. & MOSS, S. E. 2005. Annexins: linking Ca²⁺ signalling to membrane dynamics. *Nat Rev Mol Cell Biol*, 6, 449-61.
- GERKE, V. & MOSS, S. E. 2002. Annexins: from structure to function. *Physiol Rev*, 82, 331-71.
- GLENISTER, F. K., COPPEL, R. L., COWMAN, A. F., MOHANDAS, N. & COOKE, B. M. 2002. Contribution of parasite proteins to altered mechanical properties of malaria-infected red blood cells. *Blood*, 99, 1060-3.
- GLENISTER, F. K., FERNANDEZ, K. M., KATS, L. M., HANSEN, E., MOHANDAS, N., COPPEL, R. L. & COOKE, B. M. 2009. Functional alteration of red blood cells by a megadalton protein of *Plasmodium falciparum*. *Blood*, 113, 919-28.
- GRURING, C., HEIBER, A., KRUSE, F., FLEMMING, S., FRANCI, G., COLOMBO, S. F., FASANA, E., SCHOELER, H., BORGESE, N., STUNNENBERG, H. G., PRZYBORSKI, J. M., GILBERGER, T. W. & SPIELMANN, T. 2012. Uncovering common principles in protein export of malaria parasites. *Cell Host Microbe*, 12, 717-29.
- GRURING, C., HEIBER, A., KRUSE, F., UNGEFEHR, J., GILBERGER, T. W. & SPIELMANN, T. 2011. Development and host cell modifications of *Plasmodium falciparum* blood stages in four dimensions. *Nat Commun*, 2, 165.

- HAASE, S., HANSEN, E., MATTHEWS, K., KALANON, M. & DE KONING-
WARD, T. F. 2013. The exported protein PbCP1 localises to cleft-like structures
in the rodent malaria parasite *Plasmodium berghei*. *PLoS One*, 8, e61482.
- HAASE, S., HERRMANN, S., GRURING, C., HEIBER, A., JANSEN, P. W.,
LANGER, C., TREECK, M., CABRERA, A., BRUNS, C., STRUCK, N. S.,
KONO, M., ENGELBERG, K., RUCH, U., STUNNENBERG, H. G.,
GILBERGER, T. W. & SPIELMANN, T. 2009. Sequence requirements for the
export of the *Plasmodium falciparum* Maurer's clefts protein REX2. *Mol
Microbiol*, 71, 1003-17.
- HANSEN, E., CARLTON, P., DEED, S., KLONIS, N., SEDAT, J., DERISI, J. &
TILLEY, L. 2010. Whole cell imaging reveals novel modular features of the
exomembrane system of the malaria parasite, *Plasmodium falciparum*. *Int J
Parasitol*, 40, 123-34.
- HANSEN, E., HAWTHORNE, P., DIXON, M. W., TRENHOLME, K. R.,
MCMILLAN, P. J., SPIELMANN, T., GARDINER, D. L. & TILLEY, L.
2008a. Targeted mutagenesis of the ring-exported protein-1 of *Plasmodium
falciparum* disrupts the architecture of Maurer's cleft organelles. *Mol Microbiol*,
69, 938-53.
- HANSEN, E., SOUGRAT, R., FRANKLAND, S., DEED, S., KLONIS, N.,
LIPPINCOTT-SCHWARTZ, J. & TILLEY, L. 2008b. Electron tomography of
the Maurer's cleft organelles of *Plasmodium falciparum*-infected erythrocytes
reveals novel structural features. *Mol Microbiol*, 67, 703-18.
- HARTL, F. U., BRACHER, A. & HAYER-HARTL, M. 2011. Molecular chaperones in
protein folding and proteostasis. *Nature*, 475, 324-32.
- HAWTHORNE, P. L., TRENHOLME, K. R., SKINNER-ADAMS, T. S.,
SPIELMANN, T., FISCHER, K., DIXON, M. W. A., ORTEGA, M. R.,
ANDERSON, K. L., KEMP, D. J. & GARDINER, D. L. 2004b. A novel

Plasmodium falciparum ring stage protein, REX, is located in Maurer's clefts. *Molecular and Biochemical Parasitology*, 136, 181-189.

HAYASHI, M., TANIGUCHI, S., ISHIZUKA, Y., KIM, H. S., WATAYA, Y., YAMAMOTO, A. & MORIYAMA, Y. 2001. A homologue of N-ethylmaleimide-sensitive factor in the malaria parasite *Plasmodium falciparum* is exported and localized in vesicular structures in the cytoplasm of infected erythrocytes in the brefeldin A-sensitive pathway. *J Biol Chem*, 276, 15249-55.

HEIBER, A., KRUSE, F., PICK, C., GRURING, C., FLEMMING, S., OBERLI, A., SCHOELER, H., RETZLAFF, S., MESEN-RAMIREZ, P., HISS, J. A., KADEKOPPALA, M., HECHT, L., HOLDER, A. A., GILBERGER, T. W. & SPIELMANN, T. 2013. Identification of new PNEPs indicates a substantial non-PEXEL exportome and underpins common features in *Plasmodium falciparum* protein export. *PLoS Pathog*, 9, e1003546.

HENRICH, P., KILIAN, N., LANZER, M. & CYRKLAFF, M. 2009. 3-D analysis of the *Plasmodium falciparum* Maurer's clefts using different electron tomographic approaches. *Biotechnol J*, 4, 888-94.

HERMAND, P., CICERON, L., PIONNEAU, C., VAQUERO, C., COMBADIÈRE, C. & DETERRE, P. 2016. *Plasmodium falciparum* proteins involved in cytoadherence of infected erythrocytes to chemokine CX3CL1. *Sci Rep*, 6, 33786.

HILLER, N. L., BHATTACHARJEE, S., VAN OOIJ, C., LIOLIOS, K., HARRISON, T., LOPEZ-ESTRANO, C. & HALDAR, K. 2004. A host-targeting signal in virulence proteins reveals a secretome in malarial infection. *Science*, 306, 1934-7.

HINTERBERG, K., SCHERF, A., GYSIN, J., TOYOSHIMA, T., AIKAWA, M., MAZIE, J. C., DA SILVA, L. P. & MATTEI, D. 1994. *Plasmodium falciparum*: the Pf332 antigen is secreted from the parasite by a brefeldin A-dependent

pathway and is translocated to the erythrocyte membrane via the Maurer's clefts. *Exp Parasitol*, 79, 279-91.

- HORROCKS, P., PINCHES, R. A., CHAKRAVORTY, S. J., PAPAKRIVOS, J., CHRISTODOULOU, Z., KYES, S. A., URBAN, B. C., FERGUSON, D. J. & NEWBOLD, C. I. 2005. PfEMP1 expression is reduced on the surface of knobless *Plasmodium falciparum* infected erythrocytes. *J Cell Sci*, 118, 2507-18.
- HTUT, Z. W. 2009. Artemisinin resistance in *Plasmodium falciparum* malaria. *N Engl J Med*, 361, 1807-8; author reply 1808.
- HUMPHRIES, A. D., STREIMANN, I. C., STOJANOVSKI, D., JOHNSTON, A. J., YANO, M., HOOGENRAAD, N. J. & RYAN, M. T. 2005. Dissection of the mitochondrial import and assembly pathway for human Tom40. *J Biol Chem*, 280, 11535-43.
- ILNYTSKA, O., SANTIANA, M., HSU, N. Y., DU, W. L., CHEN, Y. H., VIKTOROVA, E. G., BELOV, G., BRINKER, A., STORCH, J., MOORE, C., DIXON, J. L. & ALTAN-BONNET, N. 2013. Enteroviruses harness the cellular endocytic machinery to remodel the host cell cholesterol landscape for effective viral replication. *Cell Host Microbe*, 14, 281-93.
- INGMUNDSON, A., NAHAR, C., BRINKMANN, V., LEHMANN, M. J. & MATUSCHEWSKI, K. 2012. The exported *Plasmodium berghei* protein IBIS1 delineates membranous structures in infected red blood cells. *Mol Microbiol*, 83, 1229-43.
- IQBAL, J., SIDDIQUE, A., JAMEEL, M. & HIRA, P. R. 2004. Persistent histidine-rich protein 2, parasite lactate dehydrogenase, and panmalarial antigen reactivity after clearance of *Plasmodium falciparum* mono-infection. *J Clin Microbiol*, 42, 4237-41.

- KATS, L. M., FERNANDEZ, K. M., GLENISTER, F. K., HERRMANN, S., BUCKINGHAM, D. W., SIDDIQUI, G., SHARMA, L., BAMERT, R., LUCET, I., GUILLOTTE, M., MERCEREAU-PUIJALON, O. & COOKE, B. M. 2014. An exported kinase (FIKK4.2) that mediates virulence-associated changes in *Plasmodium falciparum*-infected red blood cells. *Int J Parasitol*, 44, 319-28.
- KILIAN, N., DITTMER, M., CYRKLAFF, M., OUERMI, D., BISSEYE, C., SIMPORE, J., FRISCHKNECHT, F., SANCHEZ, C. P. & LANZER, M. 2013. Haemoglobin S and C affect the motion of Maurer's clefts in *Plasmodium falciparum*-infected erythrocytes. *Cell Microbiol*, 15, 1111-26.
- KNUEPFER, E., RUG, M., KLONIS, N., TILLEY, L. & COWMAN, A. F. 2005. Trafficking determinants for PfEMP3 export and assembly under the *Plasmodium falciparum*-infected red blood cell membrane. *Mol Microbiol*, 58, 1039-53.
- KOVALEV, N., DE CASTRO MARTIN, I. F., POGANY, J., BARAJAS, D., PATHAK, K., RISCO, C. & NAGY, P. D. 2016. Role of Viral RNA and Co-opted Cellular ESCRT-I and ESCRT-III Factors in Formation of Tombusvirus Spherules Harboring the Tombusvirus Replicase. *J Virol*, 90, 3611-26.
- KRAMER, K. J., KAN, S. C. & SIDDIQUI, W. A. 1982. Concentration of *Plasmodium falciparum*-infected erythrocytes by density gradient centrifugation in Percoll. *J Parasitol*, 68, 336-7.
- KRAMER, R. & GINSBURG, H. 1991. Calcium transport and compartment analysis of free and exchangeable calcium in *Plasmodium falciparum*-infected red blood cells. *J Protozool*, 38, 594-601.
- KRIEK, N., TILLEY, L., HORROCKS, P., PINCHES, R., ELFORD, B. C., FERGUSON, D. J., LINGELBACH, K. & NEWBOLD, C. I. 2003. Characterization of the pathway for transport of the cytoadherence-mediating

protein, PfEMP1, to the host cell surface in malaria parasite-infected erythrocytes. *Mol Microbiol*, 50, 1215-27.

KULANGARA, C., LUEDIN, S., DIETZ, O., RUSCH, S., FRANK, G., MUELLER, D., MOSER, M., KAJAVA, A. V., CORRADIN, G., BECK, H. P. & FELGER, I. 2012. Cell biological characterization of the malaria vaccine candidate trophozoite exported protein 1. *PLoS One*, 7, e46112.

KULZER, S., CHARNAUD, S., DAGAN, T., RIEDEL, J., MANDAL, P., PESCE, E. R., BLATCH, G. L., CRABB, B. S., GILSON, P. R. & PRZYBORSKI, J. M. 2012. *Plasmodium falciparum*-encoded exported hsp70/hsp40 chaperone/co-chaperone complexes within the host erythrocyte. *Cell Microbiol*, 14, 1784-95.

KULZER, S., RUG, M., BRINKMANN, K., CANNON, P., COWMAN, A., LINGELBACH, K., BLATCH, G. L., MAIER, A. G. & PRZYBORSKI, J. M. 2010. Parasite-encoded Hsp40 proteins define novel mobile structures in the cytosol of the *P. falciparum*-infected erythrocyte. *Cell Microbiol*, 12, 1398-420.

LADDA, R., ARNOLD, J. & MARTIN, D. 1966. Electron microscopy of *Plasmodium falciparum* . 1. The structure of trophozoites in erythrocytes of human volunteers. *Trans R Soc Trop Med Hyg*, 60, 369-75.

LAMBROS, C. & VANDERBERG, J. P. 1979. Synchronization of *Plasmodium falciparum* erythrocytic stages in culture. *J Parasitol*, 65, 418-20.

LEECH, J. H., BARNWELL, J. W., MILLER, L. H. & HOWARD, R. J. 1984. Identification of a strain-specific malarial antigen exposed on the surface of *Plasmodium falciparum*-infected erythrocytes. *J Exp Med*, 159, 1567-75.

LIU, W., LI, Y., LEARN, G. H., RUDICELL, R. S., ROBERTSON, J. D., KEELE, B. F., NDJANGO, J. B., SANZ, C. M., MORGAN, D. B., LOCATELLI, S., GONDER, M. K., KRANZUSCH, P. J., WALSH, P. D., DELAPORTE, E.,

- MPOUDI-NGOLE, E., GEORGIEV, A. V., MULLER, M. N., SHAW, G. M., PEETERS, M., SHARP, P. M., RAYNER, J. C. & HAHN, B. H. 2010. Origin of the human malaria parasite *Plasmodium falciparum* in gorillas. *Nature*, 467, 420-5.
- MAIER, A. G., COOKE, B. M., COWMAN, A. F. & TILLEY, L. 2009. Malaria parasite proteins that remodel the host erythrocyte. *Nat Rev Microbiol*, 7, 341-54.
- MAIER, A. G., RUG, M., O'NEILL, M. T., BEESON, J. G., MARTI, M., REEDER, J. & COWMAN, A. F. 2007. Skeleton-binding protein 1 functions at the parasitophorous vacuole membrane to traffic PfEMP1 to the *Plasmodium falciparum*-infected erythrocyte surface. *Blood*, 109, 1289-97.
- MAIER, A. G., RUG, M., O'NEILL, M. T., BROWN, M., CHAKRAVORTY, S., SZESTAK, T., CHESSON, J., WU, Y., HUGHES, K., COPPEL, R. L., NEWBOLD, C., BEESON, J. G., CRAIG, A., CRABB, B. S. & COWMAN, A. F. 2008. Exported proteins required for virulence and rigidity of *Plasmodium falciparum*-infected human erythrocytes. *Cell*, 134, 48-61.
- MANTEL, P. Y., HOANG, A. N., GOLDOWITZ, I., POTASHNIKOVA, D., HAMZA, B., VOROBYEV, I., GHIRAN, I., TONER, M., IRIMIA, D., IVANOV, A. R., BARTENEVA, N. & MARTI, M. 2013. Malaria-infected erythrocyte-derived microvesicles mediate cellular communication within the parasite population and with the host immune system. *Cell Host Microbe*, 13, 521-34.
- MARTI, M., GOOD, R. T., RUG, M., KNUEPFER, E. & COWMAN, A. F. 2004. Targeting malaria virulence and remodeling proteins to the host erythrocyte. *Science*, 306, 1930-3.
- MATSUMOTO, Y., AIKAWA, M. & BARNWELL, J. W. 1988. Immunoelectron microscopic localization of vivax malaria antigens to the clefts and caveola-vesicle complexes of infected erythrocytes. *Am J Trop Med Hyg*, 39, 317-22.

- MAURER, G. 1900. Die tüpfelung der wirtszelle des tertianparasiten. *Centralblatt für Bakteriologie Abt. I*, 28, 114-125.
- MAYER, C., SLATER, L., ERAT, M. C., KONRAT, R. & VAKONAKIS, I. 2012. Structural analysis of the *Plasmodium falciparum* erythrocyte membrane protein 1 (PfEMP1) intracellular domain reveals a conserved interaction epitope. *J Biol Chem*, 287, 7182-9.
- MBENGUE, A., AUDIGER, N., VIALLA, E., DUBREMETZ, J. F. & BRAUN-BRETON, C. 2013. Novel *Plasmodium falciparum* Maurer's clefts protein families implicated in the release of infectious merozoites. *Mol Microbiol*, 88, 425-42.
- MBENGUE, A., VIALLA, E., BERRY, L., FALL, G., AUDIGER, N., DEMETTRE-VERCEIL, E., BOTELLER, D. & BRAUN-BRETON, C. 2015. New Export Pathway in *Plasmodium falciparum*-Infected Erythrocytes: Role of the Parasite Group II Chaperonin, PfTRiC. *Traffic*, 16, 461-75.
- MCHUGH, E., BATINOVIC, S., HANSSEN, E., MCMILLAN, P. J., KENNY, S., GRIFFIN, M. D., CRAWFORD, S., TRENHOLME, K. R., GARDINER, D. L., DIXON, M. W. & TILLEY, L. 2015. A repeat sequence domain of the ring-exported protein-1 of *Plasmodium falciparum* controls export machinery architecture and virulence protein trafficking. *Mol Microbiol*.
- MCLEAN, S. A., PHILLIPS, R. S., PEARSON, C. D. & WALLIKER, D. 1987. The effect of mosquito transmission of antigenic variants of *Plasmodium chabaudi*. *Parasitology*, 94 (Pt 3), 443-9.
- MCMILLAN, P. J., MILLET, C., BATINOVIC, S., MAIORCA, M., HANSSEN, E., KENNY, S., MUHLE, R. A., MELCHER, M., FIDOCK, D. A., SMITH, J. D., DIXON, M. W. & TILLEY, L. 2013. Spatial and temporal mapping of the PfEMP1 export pathway in *Plasmodium falciparum*. *Cell Microbiol*, 15, 1401-18.

- MESEN-RAMIREZ, P., REINSCH, F., BLANCKE SOARES, A., BERGMANN, B., ULLRICH, A. K., TENZER, S. & SPIELMANN, T. 2016. Stable Translocation Intermediates Jam Global Protein Export in *Plasmodium falciparum* Parasites and Link the PTEX Component EXP2 with Translocation Activity. *PLoS Pathog*, 12, e1005618.
- MILLS, J. P., DIEZ-SILVA, M., QUINN, D. J., DAO, M., LANG, M. J., TAN, K. S., LIM, C. T., MILON, G., DAVID, P. H., MERCEREAU-PUIJALON, O., BONNEFOY, S. & SURESH, S. 2007. Effect of plasmodial RESA protein on deformability of human red blood cells harboring *Plasmodium falciparum*. *Proc Natl Acad Sci U S A*, 104, 9213-7.
- MOREIRA, C. K., NAISSANT, B., COPPI, A., BENNETT, B. L., AIME, E., FRANKE-FAYARD, B., JANSE, C. J., COPPENS, I., SINNIS, P. & TEMPLETON, T. J. 2016. The Plasmodium PHIST and RESA-Like Protein Families of Human and Rodent Malaria Parasites. *PLoS One*, 11, e0152510.
- MULLOCK, B. M., SMITH, C. W., IHRKE, G., BRIGHT, N. A., LINDSAY, M., PARKINSON, E. J., BROOKS, D. A., PARTON, R. G., JAMES, D. E., LUZIO, J. P. & PIPER, R. C. 2000. Syntaxin 7 is localized to late endosome compartments, associates with Vamp 8, and Is required for late endosome-lysosome fusion. *Mol Biol Cell*, 11, 3137-53.
- MUNDWILER-PACHLATKO, E. & BECK, H. P. 2013. Maurer's clefts, the enigma of *Plasmodium falciparum*. *Proc Natl Acad Sci U S A*, 110, 19987-94.
- MURRAY, C. J. L., ROSENFELD, L. C., LIM, S. S., ANDREWS, K. G., FOREMAN, K. J., HARING, D., FULLMAN, N., NAGHAVI, M., LOZANO, R. & LOPEZ, A. D. 2012. Global malaria mortality between 1980 and 2010: a systematic analysis. *The Lancet*, 379, 413-431.
- NACER, A., CLAES, A., ROBERTS, A., SCHEIDIG-BENATAR, C., SAKAMOTO, H., GHORBAL, M., LOPEZ-RUBIO, J. J. & MATTEI, D. 2015. Discovery of a

novel and conserved *Plasmodium falciparum* exported protein that is important for adhesion of PfEMP1 at the surface of infected erythrocytes. *Cell Microbiol*, 17, 1205-16.

NILSSON, S., ANGELETTI, D., WAHLGREN, M., CHEN, Q. & MOLL, K. 2012. *Plasmodium falciparum* antigen 332 is a resident peripheral membrane protein of Maurer's clefts. *PLoS One*, 7, e46980.

NUNES, M. C., GOLDRING, J. P., DOERIG, C. & SCHERF, A. 2007. A novel protein kinase family in *Plasmodium falciparum* is differentially transcribed and secreted to various cellular compartments of the host cell. *Mol Microbiol*, 63, 391-403.

OBERLI, A., SLATER, L. M., CUTTS, E., BRAND, F., MUNDWILER-PACHLATKO, E., RUSCH, S., MASIK, M. F., ERAT, M. C., BECK, H. P. & VAKONAKIS, I. 2014. A *Plasmodium falciparum* PHIST protein binds the virulence factor PfEMP1 and comigrates to knobs on the host cell surface. *FASEB J*, 28, 4420-33.

OBERLI, A., ZURBRUGG, L., RUSCH, S., BRAND, F., BUTLER, M. E., DAY, J. L., CUTTS, E. E., LAVSTSEN, T., VAKONAKIS, I. & BECK, H. P. 2016. *Plasmodium falciparum* Plasmodium helical interspersed subtelomeric proteins contribute to cytoadherence and anchor P. falciparum erythrocyte membrane protein 1 to the host cell cytoskeleton. *Cell Microbiol*, 18, 1415-28.

OH, S. S., VOIGT, S., FISHER, D., YI, S. J., LEROY, P. J., DERICK, L. H., LIU, S. & CHISHTI, A. H. 2000. *Plasmodium falciparum* erythrocyte membrane protein 1 is anchored to the actin-spectrin junction and knob-associated histidine-rich protein in the erythrocyte skeleton. *Mol Biochem Parasitol*, 108, 237-47.

PACHLATKO, E., RUSCH, S., MULLER, A., HEMPHILL, A., TILLEY, L., HANSEN, E. & BECK, H. P. 2010. MAHRP2, an exported protein of

Plasmodium falciparum, is an essential component of Maurer's cleft tethers. *Mol Microbiol*, 77, 1136-52.

PASINI, E. M., BRAKS, J. A., FONAGER, J., KLOP, O., AIME, E., SPACCAPELO, R., OTTO, T. D., BERRIMAN, M., HISS, J. A., THOMAS, A. W., MANN, M., JANSE, C. J., KOCKEN, C. H. & FRANKE-FAYARD, B. 2013. Proteomic and genetic analyses demonstrate that *Plasmodium berghei* blood stages export a large and diverse repertoire of proteins. *Mol Cell Proteomics*, 12, 426-48.

PASVOL, G., WILSON, R. J., SMALLEY, M. E. & BROWN, J. 1978. Separation of viable schizont-infected red cells of *Plasmodium falciparum* from human blood. *Ann Trop Med Parasitol*, 72, 87-8.

PEI, X., GUO, X., COPPEL, R., MOHANDAS, N. & AN, X. 2007. *Plasmodium falciparum* erythrocyte membrane protein 3 (PfEMP3) destabilizes erythrocyte membrane skeleton. *J Biol Chem*, 282, 26754-8.

PONNUDURAI, T., LEEUWENBERG, A. D. & MEUWISSEN, J. H. 1981. Chloroquine sensitivity of isolates of *Plasmodium falciparum* adapted to in vitro culture. *Trop Geogr Med*, 33, 50-4.

PROMMANA, P., UTHAIPIBULL, C., WONGSOMBAT, C., KAMCHONWONGPAISAN, S., YUTHAVONG, Y., KNUEPFER, E., HOLDER, A. A. & SHAW, P. J. 2013. Inducible knockdown of *Plasmodium* gene expression using the glmS ribozyme. *PLoS One*, 8, e73783.

RALPH, S. A., SCHEIDIG-BENATAR, C. & SCHERF, A. 2005. Antigenic variation in *Plasmodium falciparum* is associated with movement of var loci between subnuclear locations. *Proc Natl Acad Sci U S A*, 102, 5414-9.

RECHSTEINER, M. & ROGERS, S. W. 1996. PEST sequences and regulation by proteolysis. *Trends Biochem Sci*, 21, 267-71.

- REGEV-RUDZKI, N., WILSON, D. W., CARVALHO, T. G., SISQUELLA, X., COLEMAN, B. M., RUG, M., BURSAC, D., ANGRISANO, F., GEE, M., HILL, A. F., BAUM, J. & COWMAN, A. F. 2013. Cell-cell communication between malaria-infected red blood cells via exosome-like vesicles. *Cell*, 153, 1120-33.
- RIGLAR, D. T., ROGERS, K. L., HANSEN, E., TURNBULL, L., BULLEN, H. E., CHARNAUD, S. C., PRZYBORSKI, J., GILSON, P. R., WHITCHURCH, C. B., CRABB, B. S., BAUM, J. & COWMAN, A. F. 2013. Spatial association with PTEX complexes defines regions for effector export into *Plasmodium falciparum*-infected erythrocytes. *Nat Commun*, 4, 1415.
- ROGERSON, S. J., HVIID, L., DUFFY, P. E., LEKE, R. F. & TAYLOR, D. W. 2007. Malaria in pregnancy: pathogenesis and immunity. *Lancet Infect Dis*, 7, 105-17.
- RUG, M., CYRKLAFF, M., MIKKONEN, A., LEMGRUBER, L., KUELZER, S., SANCHEZ, C. P., THOMPSON, J., HANSEN, E., O'NEILL, M., LANGER, C., LANZER, M., FRISCHKNECHT, F., MAIER, A. G. & COWMAN, A. F. 2014. Export of virulence proteins by malaria-infected erythrocytes involves remodeling of host actin cytoskeleton. *Blood*, 124, 3459-68.
- RUG, M., PRESCOTT, S. W., FERNANDEZ, K. M., COOKE, B. M. & COWMAN, A. F. 2006. The role of KAHRP domains in knob formation and cytoadherence of *P falciparum*-infected human erythrocytes. *Blood*, 108, 370-8.
- RUSSO, I., BABBITT, S., MURALIDHARAN, V., BUTLER, T., OKSMAN, A. & GOLDBERG, D. E. 2010. Plasmeprin V licenses Plasmodium proteins for export into the host erythrocyte. *Nature*, 463, 632-6.
- SARGEANT, T. J., MARTI, M., CALER, E., CARLTON, J. M., SIMPSON, K., SPEED, T. P. & COWMAN, A. F. 2006. Lineage-specific expansion of proteins exported to erythrocytes in malaria parasites. *Genome Biol*, 7, R12.

- SARIDAKI, T., SANCHEZ, C. P., PFAHLER, J. & LANZER, M. 2008. A conditional export system provides new insights into protein export in *Plasmodium falciparum*-infected erythrocytes. *Cell Microbiol*, 10, 2483-95.
- SBRISSA, D., IKONOMOV, O. C., FU, Z., IJUIN, T., GRUENBERG, J., TAKENAWA, T. & SHISHEVA, A. 2007. Core protein machinery for mammalian phosphatidylinositol 3,5-bisphosphate synthesis and turnover that regulates the progression of endosomal transport. Novel Sac phosphatase joins the ArPIKfyve-PIKfyve complex. *J Biol Chem*, 282, 23878-91.
- SCHERF, A., LOPEZ-RUBIO, J. J. & RIVIERE, L. 2008. Antigenic variation in *Plasmodium falciparum*. *Annu Rev Microbiol*, 62, 445-70.
- SCHERMELLEH, L., CARLTON, P. M., HAASE, S., SHAO, L., WINOTO, L., KNER, P., BURKE, B., CARDOSO, M. C., AGARD, D. A., GUSTAFSSON, M. G., LEONHARDT, H. & SEDAT, J. W. 2008. Subdiffraction multicolor imaging of the nuclear periphery with 3D structured illumination microscopy. *Science*, 320, 1332-6.
- SCHERMELLEH, L., HEINTZMANN, R. & LEONHARDT, H. 2010. A guide to super-resolution fluorescence microscopy. *J Cell Biol*, 190, 165-75.
- SCHÜFFNER, W. A. P. 1899. Beitrag zur kenntniss der malaria. *Deutsch. Archiv. f. klein. Med*, 64, 428-449.
- SHERLING, E. S., KNUEPFER, E., BRZOSTOWSKI, J. A., MILLER, L. H., BLACKMAN, M. J. & VAN OOIJ, C. 2017. The *Plasmodium falciparum* rhoptry protein RhopH3 plays essential roles in host cell invasion and nutrient uptake. *Elife*, 6.

- SIAU, A., HUANG, X., WENG, M., SZE, S. K. & PREISER, P. R. 2016. Proteome mapping of Plasmodium: identification of the *P. yoelii* remodelome. *Sci Rep*, 6, 31055.
- SILVA, M. D., COOKE, B. M., GUILLOTTE, M., BUCKINGHAM, D. W., SAUZET, J. P., LE SCANF, C., CONTAMIN, H., DAVID, P., MERCEREAU-PUIJALON, O. & BONNEFOY, S. 2005. A role for the *Plasmodium falciparum* RESA protein in resistance against heat shock demonstrated using gene disruption. *Mol Microbiol*, 56, 990-1003.
- SLEEBES, B. E., LOPATICKI, S., MARAPANA, D. S., O'NEILL, M. T., RAJASEKARAN, P., GAZDIK, M., GUNTHER, S., WHITEHEAD, L. W., LOWES, K. N., BARFOD, L., HVIID, L., SHAW, P. J., HODDER, A. N., SMITH, B. J., COWMAN, A. F. & BODDEY, J. A. 2014. Inhibition of Plasmeprin V activity demonstrates its essential role in protein export, PfEMP1 display, and survival of malaria parasites. *PLoS Biol*, 12, e1001897.
- SPIELMANN, T. & GILBERGER, T. W. 2010. Protein export in malaria parasites: do multiple export motifs add up to multiple export pathways? *Trends Parasitol*, 26, 6-10.
- SPIELMANN, T., HAWTHORNE, P. L., DIXON, M. W., HANNEMANN, M., KLOTZ, K., KEMP, D. J., KLONIS, N., TILLEY, L., TRENHOLME, K. R. & GARDINER, D. L. 2006. A cluster of ring stage-specific genes linked to a locus implicated in cytoadherence in *Plasmodium falciparum* codes for PEXEL-negative and PEXEL-positive proteins exported into the host cell. *Mol Biol Cell*, 17, 3613-24.
- SPILLMAN, N. J., BECK, J. R., GANESAN, S. M., NILES, J. C. & GOLDBERG, D. E. 2017. The chaperonin TRiC forms an oligomeric complex in the malaria parasite cytosol. *Cell Microbiol*, 19.

- SPYCHER, C., KLONIS, N., SPIELMANN, T., KUMP, E., STEIGER, S., TILLEY, L. & BECK, H. P. 2003. MAHRP-1, a novel *Plasmodium falciparum* histidine-rich protein, binds ferriprotoporphyrin IX and localizes to the Maurer's clefts. *J Biol Chem*, 278, 35373-83.
- SPYCHER, C., RUG, M., KLONIS, N., FERGUSON, D. J., COWMAN, A. F., BECK, H. P. & TILLEY, L. 2006. Genesis of and trafficking to the Maurer's clefts of *Plasmodium falciparum*-infected erythrocytes. *Mol Cell Biol*, 26, 4074-85.
- SPYCHER, C., RUG, M., PACHLATKO, E., HANSSEN, E., FERGUSON, D., COWMAN, A. F., TILLEY, L. & BECK, H. P. 2008. The Maurer's cleft protein MAHRP1 is essential for trafficking of PfEMP1 to the surface of *Plasmodium falciparum*-infected erythrocytes. *Mol Microbiol*, 68, 1300-14.
- TAYLOR, D. W., PARRA, M., CHAPMAN, G. B., STEARNS, M. E., RENER, J., AIKAWA, M., UNI, S., ALEY, S. B., PANTON, L. J. & HOWARD, R. J. 1987. Localization of *Plasmodium falciparum* histidine-rich protein 1 in the erythrocyte skeleton under knobs. *Mol Biochem Parasitol*, 25, 165-74.
- TAYLOR, S. M. & FAIRHURST, R. M. 2014. Malaria parasites and red cell variants: when a house is not a home. *Curr Opin Hematol*, 21, 193-200.
- THOMPSON, J., FERNANDEZ-REYES, D., SHARLING, L., MOORE, S. G., ELING, W. M., KYES, S. A., NEWBOLD, C. I., KAFATOS, F. C., JANSE, C. J. & WATERS, A. P. 2007. Plasmodium cysteine repeat modular proteins 1-4: complex proteins with roles throughout the malaria parasite life cycle. *Cell Microbiol*, 9, 1466-80.
- TIBURCIO, M., DIXON, M. W., LOOKER, O., YOUNIS, S. Y., TILLEY, L. & ALANO, P. 2015. Specific expression and export of the *Plasmodium falciparum* Gametocyte EXported Protein-5 marks the gametocyte ring stage. *Malar J*, 14, 334.

- TILLEY, L., STRAIMER, J., GNADIG, N. F., RALPH, S. A. & FIDOCK, D. A. 2016. Artemisinin Action and Resistance in *Plasmodium falciparum*. *Trends Parasitol*, 32, 682-96.
- TOMAS, A., FUTTER, C. & MOSS, S. E. 2004. Annexin 11 is required for midbody formation and completion of the terminal phase of cytokinesis. *J Cell Biol*, 165, 813-22.
- TRAGER, W. & JENSEN, J. B. 1976. Human malaria parasites in continuous culture. *Science*, 193, 673-5.
- TRAGER, W., RUDZINSKA, M. A. & BRADBURY, P. C. 1966. The fine structure of *Plasmodium falciparum* and its host erythrocytes in natural malarial infections in man. *Bull World Health Organ*, 35, 883-5.
- TRELKA, D. P., SCHNEIDER, T. G., REEDER, J. C. & TARASCHI, T. F. 2000. Evidence for vesicle-mediated trafficking of parasite proteins to the host cell cytosol and erythrocyte surface membrane in *Plasmodium falciparum* infected erythrocytes. *Mol Biochem Parasitol*, 106, 131-45.
- TURNER, L., LAVSTSEN, T., BERGER, S. S., WANG, C. W., PETERSEN, J. E., AVRIL, M., BRAZIER, A. J., FREETH, J., JESPERSEN, J. S., NIELSEN, M. A., MAGISTRADO, P., LUSINGU, J., SMITH, J. D., HIGGINS, M. K. & THEANDER, T. G. 2013. Severe malaria is associated with parasite binding to endothelial protein C receptor. *Nature*, 498, 502-5.
- UDAGAMA, P. V., ATKINSON, C. T., PEIRIS, J. S., DAVID, P. H., MENDIS, K. N. & AIKAWA, M. 1988. Immunoelectron microscopy of Schuffner's dots in *Plasmodium vivax*-infected human erythrocytes. *Am J Pathol*, 131, 48-52.
- VINCENSINI, L., RICHERT, S., BLISNICK, T., VAN DORSSELAER, A., LEIZEWAGNER, E., RABILLOUD, T. & BRAUN BRETON, C. 2005. Proteomic

analysis identifies novel proteins of the Maurer's clefts, a secretory compartment delivering *Plasmodium falciparum* proteins to the surface of its host cell. *Mol Cell Proteomics*, 4, 582-93.

VOIGT, S., HANSPAL, M., LEROY, P. J., ZHAO, P. S., OH, S. S., CHISHTI, A. H. & LIU, S. C. 2000. The cytoadherence ligand *Plasmodium falciparum* erythrocyte membrane protein 1 (PfEMP1) binds to the P. falciparum knob-associated histidine-rich protein (KAHRP) by electrostatic interactions. *Mol Biochem Parasitol*, 110, 423-8.

VOSS, T. S., HEALER, J., MARTY, A. J., DUFFY, M. F., THOMPSON, J. K., BEESON, J. G., REEDER, J. C., CRABB, B. S. & COWMAN, A. F. 2006. A var gene promoter controls allelic exclusion of virulence genes in *Plasmodium falciparum* malaria. *Nature*, 439, 1004-8.

WATERKEYN, J. G., WICKHAM, M. E., DAVERN, K. M., COOKE, B. M., COPPEL, R. L., REEDER, J. C., CULVENOR, J. G., WALLER, R. F. & COWMAN, A. F. 2000. Targeted mutagenesis of *Plasmodium falciparum* erythrocyte membrane protein 3 (PfEMP3) disrupts cytoadherence of malaria-infected red blood cells. *EMBO J*, 19, 2813-23.

WATERMEYER, J. M., HALE, V. L., HACKETT, F., CLARE, D. K., CUTTS, E. E., VAKONAKIS, I., FLECK, R. A., BLACKMAN, M. J. & SAIBIL, H. R. 2016. A spiral scaffold underlies cytoadherent knobs in *Plasmodium falciparum*-infected erythrocytes. *Blood*, 127, 343-51.

WHITE, N. J., PUKRITTAYAKAMEE, S., HIEN, T. T., FAIZ, M. A., MOKUOLU, O. A. & DONDORP, A. M. 2013. Malaria. *Lancet*.

WHO 2014. World Malaria Report, 2014. WHO Press,.

- WICKERT, H., GOTTLER, W., KROHNE, G. & LANZER, M. 2004. Maurer's cleft organization in the cytoplasm of *Plasmodium falciparum*-infected erythrocytes: new insights from three-dimensional reconstruction of serial ultrathin sections. *Eur J Cell Biol*, 83, 567-82.
- WICKERT, H., ROHRBACH, P., SCHERER, S. J., KROHNE, G. & LANZER, M. 2003a. A putative Sec23 homologue of *Plasmodium falciparum* is located in Maurer's clefts. *Mol Biochem Parasitol*, 129, 209-13.
- WICKERT, H., WISSING, F., ANDREWS, K. T., STICH, A., KROHNE, G. & LANZER, M. 2003b. Evidence for trafficking of PfEMP1 to the surface of *P. falciparum*-infected erythrocytes via a complex membrane network. *Eur J Cell Biol*, 82, 271-84.
- WICKHAM, M. E., RUG, M., RALPH, S. A., KLONIS, N., MCFADDEN, G. I., TILLEY, L. & COWMAN, A. F. 2001. Trafficking and assembly of the cytoadherence complex in *Plasmodium falciparum*-infected human erythrocytes. *EMBO J*, 20, 5636-49.
- ZHANG, Y., HUANG, C., KIM, S., GOLKARAM, M., DIXON, M. W., TILLEY, L., LI, J., ZHANG, S. & SURESH, S. 2015. Multiple stiffening effects of nanoscale knobs on human red blood cells infected with *Plasmodium falciparum* malaria parasite. *Proc Natl Acad Sci U S A*, 112, 6068-73.

